Spin Chemistry

DOI: 10.1002/anie.200602205

Control of Magnetic Properties through External Stimuli

Osamu Sato, Jun Tao, and Yuan-Zhu Zhang*

Keywords:
magnetic properties · photochemistry · radicals · spin crossover · valence isomerization

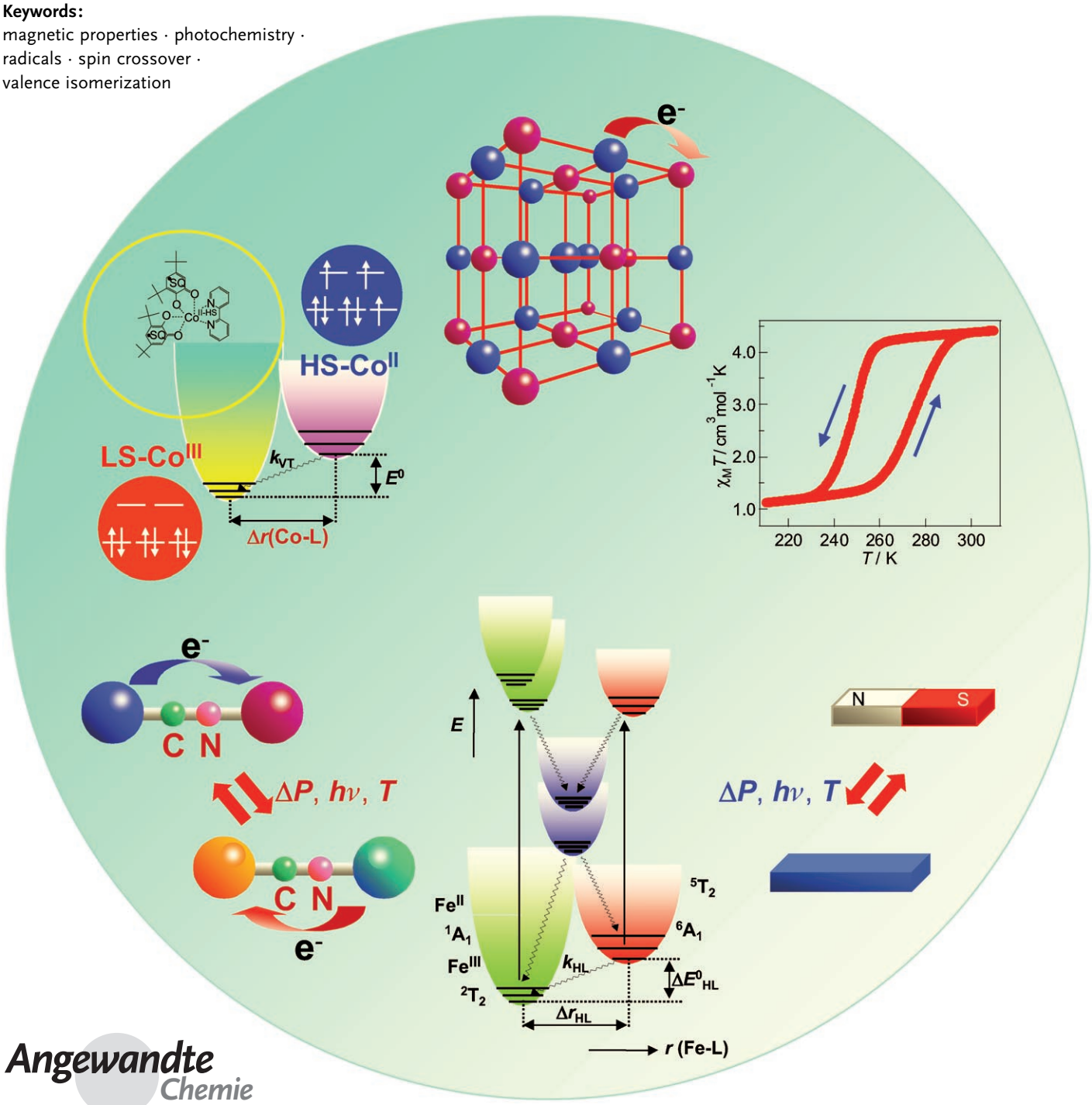

The magnetic properties of many magnetic materials can be controlled by external stimuli. The principal focus here is on the thermal, photochemical, electrochemical, and chemical control of phase transitions that involve changes in magnetization. The molecular compounds described herein range from metal complexes, through pure organic compounds to composite materials. Most of the Review is devoted to the properties of valence-tautomeric compounds, molecular magnets, and spin-crossover complexes, which could find future application in memory devices or optical switches.

From the Contents

1. Introduction

There has recently been great interest in the study of the magnetic properties of molecular compounds. In the last two decades, many molecular magnetic compounds have been developed. In particular, room-temperature magnets were reported in 1991[1] and 1995.[2] Furthermore, molecular magnets consisting of pure organic radicals were first reported in 1991.[3] Additionally, new types of magnets with unusual magnetic properties have also been reported, for example, single-molecule magnets and single-chain magnets.[4–6] These all exhibit a hysteresis loop at the single-molecule level or the single-chain level. Hence, the study of quantum magnets has attracted great attention from the viewpoint of practical applications to high-density recording media as well as for basic science. Indeed, the preparation of molecular magnets with high critical temperatures and high blocking temperatures is still a great challenge in this field.

Another important subject in this field is the preparation of tunable molecular magnetic compounds. Tunable compounds are those in which the magnetic properties can be switched by some external perturbation. This is an important objective, because such tunable compounds can be used for future molecular memory and switching devices. Furthermore, studies of the way in which magnetic properties respond to external perturbations give us some insight into the intrinsic nature of the materials. Indeed, many switchable molecular compounds have already been developed.

Among the possible external perturbations, thermal perturbations are the most widespread. In fact, the number of thermally switchable compounds is already large; spin-crossover complexes and valence-tautomeric compounds are typical extensively studied examples.[7–12] Photoinduced magnetization has recently become an important topic,[13–15] as light is a very useful and powerful tool for controlling the physical properties of molecular compounds. The photocontrol of spin transitions, photoinduced valence tautomerism, and photomagnets has recently been reported.[7,13–15] In addition to light, the application of pressure, electrochemical redox reactions, and chemical treatments can be used to control magnetic properties. Furthermore, combinations of different external perturbations afford novel tunable compounds that exhibit multistate switching owing to their responses to the multiple external perturbations. More recently, the growing interest in porous compounds has led to concept of controlling the magnetic properties of metal–organic open frameworks by guest molecules or ions.

In this Review, we describe recent advances in the development of such switchable molecular magnetic materials. First, we describe the dynamic properties of valence-tautomeric compounds.[10–12,16–20] Cobalt compounds (which are the most common valence-tautomeric materials) are described first, as well as other metal complexes and related systems. Next, we describe the dynamic properties of molecular magnets, which range from pure organic materials to metal complexes and composite materials.[13–15,21–25] Finally, several recent topics such as spin-crossover phenomena are described.[7–9,26–32]

Valence tautomerism, molecular magnets, and spin-crossover are usually reviewed separately, as this enables a concise and comprehensive review of each field. By contrast, in this work we assemble these topics together, as the phenomena that appear in each system resemble each other. For example,

[*] Prof. O. Sato, Dr. Y.-Z. Zhang
Kyushu University
Institute for Materials Chemistry and Engineering
6-1 Kasuga, 816-8580, Fukuoka (Japan)
Fax: (+81) 92-583-7787
E-mail: sato@cm.kyushu-u.ac.jp
Homepage: http://www.cm.kyushu-u.ac.jp/dv14/home_e.html
Prof. J. Tao
Xiamen University
Department of Chemistry
Xiamen 361005 (P.R. China)

spin transitions play an important role in most of the valence-tautomeric compounds and switchable molecular magnets. The concept of entropy-driven phase transitions is a versatile concept for each system. Furthermore, a technique that controls the magnetic properties for a given system is in many cases useful for other systems. Hence, we think that it is valuable to introduce in one article several systems that may seem to be different in appearance but are closely related to each other.

2. Valence Tautomerism

Compounds that exhibit interconversion between redox isomers are known as valence-tautomeric compounds. Valence tautomerism (redox isomerism) has attracted great attention recently because conversion of the redox state involves changes in the magnetic properties as well as changes in the oxidation state. A well-studied, representative example of such compounds are Co complexes with semiquinonate and catecholate ligands.[16]

2.1. Valence-Tautomeric Co Compounds

Buchanan and Pierpont reported that the Co compound $[Co^{II\text{-}HS}(3,5\text{-dbsq})_2(bpy)]$ (HS = high spin; bpy = 2,2′-bipyridine; 3,5-dbsq = 3,5-di-*tert*-butyl-1,2-semiquinonate) shows thermally induced charge transfer between the Co center and the semiquinone ligand in solution.[16,33] The valence tautomerism can be expressed as $[Co^{II\text{-}HS}(3,5\text{-dbsq})_2(bpy)] \rightleftharpoons [Co^{III\text{-}LS}(3,5\text{-dbsq})(3,5\text{-dbcat})(bpy)]$ (LS = low spin; 3,5-dbcat = 3,5-di-*tert*-butyl-1,2-catecholate). The chemical structure of this Co valence-tautomeric complex is shown in Figure 1. The tautomerism involves a distinct change in the magnetic properties as well as the optical properties. After this finding, many valence-tautomeric compounds were developed. For example, in 1993, valence tautomerism in the solid state was reported for $[Co^{II\text{-}HS}(3,5\text{-dbsq})_2(phen)]\cdot CH_3C_6H_5$ (phen = 1,10-phenanthroline; Figure 2).[34] The transitions between the high-temperature and the low-temperature phase are abrupt, which means that cooperative interactions operate in the compound.

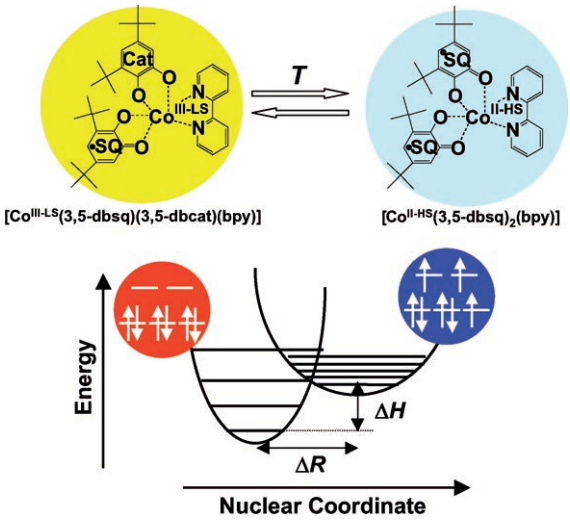

Figure 1. Valence tautomerism of $[Co^{II\text{-}HS}(3,5\text{-dbsq})_2(bpy)]$.

2.1.1. Valence-Tautomeric Co Compounds Exhibiting Hysteresis

A challenging issue is the preparation of Co compounds that exhibit valence tautomerism at around room temperature and also display a hysteresis loop. Such bistable compounds could be used, for example, for switching or memory devices. An example of a compound that exhibits hysteresis is the compound described above, $[Co^{II\text{-}HS}(3,5\text{-dbsq})_2(phen)]\cdot CH_3C_6H_5$, which exhibits hysteresis of as much as 5 K.[34] Pierpont and co-workers reported hysteresis as high as 230 K in $[Co^{III}(3,6\text{-dbcat})(3,6\text{-dbsq})(py_2O)]$ (3,6-dbcat and 3,6-dbsq are the catecholato and semiquinonato forms, respectively, of 3,6-di-*tert*-butyl-*o*-benzoquinone; py_2O = 2,2′-bis(pyridine) ether; Figure 3 and Table 1), although repeated traces show a gradual breakdown in the hysteresis.[10,35] $[Co(cth)(phendiox)]PF_6\cdot 1.5\,CD_2Cl_2$ (cth = *dl*-5,7,7,12,14,14-hexamethyl-1,4,8,11-tetraazacyclotetradecane; phendiox = semiquinonato (phensq) or catecholato (phencat) forms of 9,10-dioxophenantherene) also shows hysteresis. The transition temperatures of the heating and cooling modes are $T_c\uparrow = 244$ K and $T_c\downarrow = 236$ K, respectively ($T_c\uparrow$ and $T_c\downarrow$ are defined as the temperatures at which there is 50% of the high- and 50% of the low-temperature phase in the warming and cooling modes, respectively).[36] It is notable that the non-

Osamu Sato received his PhD in 1994 from the University of Tokyo under Professor Akira Fujishima. His academic career started the same year at the Kanagawa Academy of Science and Technology (KAST), where he became director of the Special Research Laboratory for Optical Science in 1998. Since 2005, he has been a professor of the Institute for Materials Chemistry and Engineering at Kyushu University. He was awarded the CSJ Award for Young Chemists in 1998 and his research interests include the development of molecular photomagnets, phototunable valence-tautomeric compounds, LIESST complexes, and phototunable photonic crystals.

Jun Tao received his PhD in 2001 from Zhongshan University under the supervision of Professor Xiao-Ming Chen. He then joined Xiamen University and became an associate professor in 2003. From 2004 to 2006, he joined Professor Sato's group as a JSPS postdoctoral fellow at KAST and Kyushu University. His current research interests include the development of phototunable valence-tautomeric and spin-crossover complexes, single-molecule magnets, and single-chain magnets.

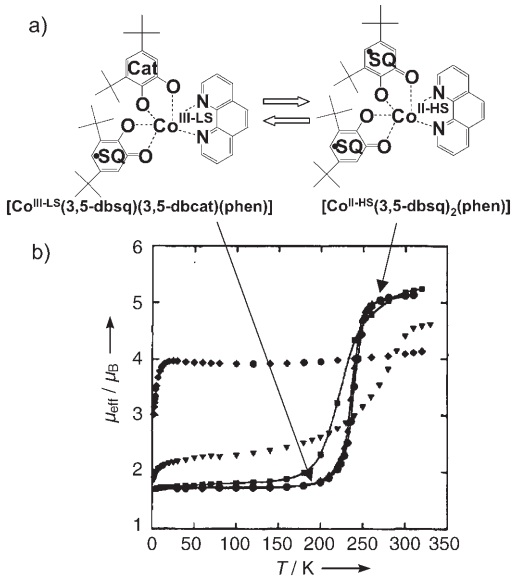

Figure 2. a) Valence tautomerism of $[Co^{II\text{-}HS}(3,5\text{-dbsq})_2(phen)]$. b) Plots of the effective magnetic moment versus T for the following complexes: $[Co(3,5\text{-dbsq})_2(phen)]$ recrystallized from methylcyclohexane (◆); $[Co(3,5\text{-dbsq})_2(phen)]\cdot C_6H_5Cl$ (■); $[Co(3,5\text{-dbsq})_2(phen)]\cdot C_6H_5Cl$ in the heating (●) and cooling (▲) modes; $[Co(3,5\text{-dbsq})_2(phen)]\cdot C_6H_5Cl$ after heating at 70 °C under vacuum for 12 h (▼). Reprinted with permission from reference [34]. Copyright 1993, The American Chemical Society.

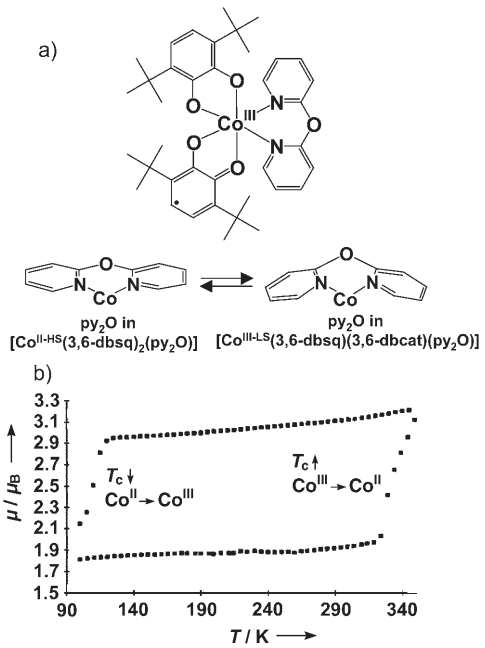

Figure 3. a) Molecular structure of $[Co^{III\text{-}LS}(3,6\text{-dbsq})(3,6\text{-dbcat})(py_2O)]$ and the structural change of py_2O during valence tautomerism. b) Hysteresis of $[Co(3,6\text{-dbsq})_2(py_2O)]$. The hysteresis loop was obtained with a sample of the Co^{III} isomer obtained from acetone by starting at 100 K. Reprinted with permission from reference [35]. Copyright 1997, The American Chemical Society.

deuterated sample $[Co(cth)(phendiox)]PF_6\cdot 1.5\,CH_2Cl_2$ (Scheme 1a) does not show hysteresis and that its transition temperature is 300 K.[37] The X-ray powder diffraction patterns of the deuterated and non-deuterated forms were found to be different from each other.[36] Furthermore, it was reported that $[Co(phen)L]\cdot 0.5\,CH_2Cl_2$ (L = dioxolene ligand 3,5-bis(3′,4′-dihydroxy-5′-*tert*-butylphenyl)-1-*tert*-butylbenzene) shows a hysteresis of 12 K,[38] although the transition is only gradual.

Valence tautomerism observed at around room temperature in toluene was reported for $[Co^{III}(cat\text{-}N\text{-}bq)(cat\text{-}N\text{-}sq)]$ (cat-N-bq = 2-(2-hydroxy-3,5-di-*tert*-butylphenylimino)-4,6-di-*tert*-butylcyclohexa-3,5-dienone; cat-N-sq is the corresponding dianionic semiquinonato analogue of cat-N-bq).[39] The transition can be expressed as $[Co^{III}(cat\text{-}N\text{-}bq)(cat\text{-}N\text{-}sq)] \rightleftharpoons [Co^{II}(cat\text{-}N\text{-}bq)_2]$ (Scheme 1c). However, the transition temperature was higher in the solid state and no hysteresis was observed. Similar behavior was observed in $[Co^{III}(tpy)(cat\text{-}N\text{-}sq)]Y$ (tpy = 2,2′:6′,2″-terpyridine; Y = PF_6, BPh_4; Scheme 1b).[40]

More recently, abrupt and distinct hysteresis was reported for the dinuclear complex $[\{Co(tpa)\}_2(dhbq)]\cdot(PF_6)_3$ (tpa = tris(2-pyridylmethyl)amine, dhbq = deprotonated 2,5-dihydroxy-1,4-benzoquinone; Figure 4).[41] The interconversion can be expressed as $[\{Co^{III\text{-}LS}(tpa)\}_2(dhbq^{3-})]^{3+} \rightleftharpoons [Co^{III\text{-}LS}(tpa)(dhbq^{2-})Co^{II\text{-}HS}(tpa)]^{3+}$. An important characteristic of this material is that the hysteresis is observed at around room temperature, not at low temperature. The hysteresis width is as large as 13 K, and thus this is a valence-tautomeric compound that exhibits a room-temperature transition with hysteresis. However, the hysteresis width is not large enough for practical applications, and hence the preparation of valence-tautomeric compounds with much larger hysteresis at around room temperature is still a challenge in this field.

Valence tautomerism is an entropy-driven process.[42] The variation in entropy ΔS arises from both electronic (ΔS_{el}) and vibrational (ΔS_{vib}) contributions. The interaction of spins in the Co compound $[Co^{II\text{-}HS}(dbsq)_2(N\text{-}N)]$ (dbsq = 3,5-dbsq or 3,6-dbsq; N-N = nitrogen-donor ancillary ligands) gives rise to 16 states, and its electronic degeneracy is 16.[43] In contrast, the electronic degeneracy of $[Co^{III\text{-}LS}(dbcat)(dbsq)(N\text{-}N)]$ (dbcat = 3,5-dbcat or 3,6-dbcat) with mixed-valence dioxolene ligands is only 4.[43] Thus, $\Delta S_{el} = S_{el}(II\text{-}HS) - S_{el}(III\text{-}LS) > 0$ (II-HS = $[Co^{II\text{-}HS}(dbsq)_2(N\text{-}N)]$ and III-LS = $[Co^{III\text{-}LS}(dbcat)(dbsq)(N\text{-}N)]$).[43] Furthermore, the high-temperature

Yuan-Zhu Zhang was born in Shandong, China in 1977. He completed his BS (2000) and PhD (2005, under Professor Song Gao) at the College of Chemistry and Molecular Engineering in Peking University. Then he started his postdoctoral work with Professor Osamu Sato at Kyushu University, Japan. He is interested in rare-earth molecular magnets, single-molecule magnets, and photoinduced magnets.

Table 1: Selected compounds that exhibit large hysteresis or hysteresis at room temperature.[a]

Compound	$T_c\downarrow$ [K]	$T_c\uparrow$ [K]	ΔT [K]	Ref.
$[Co^{III}(3,6\text{-dbcat})(3,6\text{-dbsq})(py_2O)]$	100	330	230	[35]
$[Co^{III}(cth)(phencat)]PF_6\cdot 1.5\,CD_2Cl_2$	236	244	8	[36]
$[\{Co^{II}(tpa)\}_2(dhbq)]\cdot(PF_6)_3$	297	310	13	[41]
TTTA	230	305	75	[158]
PDTA	297	343	46	[159]
TDP-DTA	120	185	65	[161]
neutral spirobiphenalenyl radical	325	348	23	[172]
$Na_{0.68}[Co_{1.20}Fe(CN)_6]\cdot 3.7\,H_2O$[b]	275	305	30	[269]
$Rb_{0.73}[Mn\{Fe(CN)_6\}_{0.91}]\cdot z\,H_2O$[b]	147	263	116	[198]
$Cs[\{Co^{II}(3\text{-cyanopyridine})_2\}\{W^V(CN)_8\}]\cdot H_2O$	167	216	49	[205]
$[\{Co^{II}(pmd)(H_2O)\}_2\{Co^{II}(H_2O)_2\}\{W^V(CN)_8\}_2(pmd)_2]\cdot 2\,H_2O$	208	298	90	[212]
$Cs^I[\{Fe^{II\text{-}HS}Cr^{III}(CN)_6\}_{0.94}\{Fe^{II\text{-}LS}Cr^{III}(NC)_6\}_{0.06}]\cdot 1.3\,H_2O$	211	238	27	[219]
$[Fe^{II}(pm\text{-}pea)(NCS)_2]$	194	231	37	[248]
$[Fe^{II}_{0.75}Zn^{II}_{0.25}(pm\text{-}pea)(NCS)_2]$	140	230	90	[249]
$[Fe^{II}_{0.8}Ni^{II}_{0.2}(pm\text{-}pea)(NCS)_2]$	176	268	92	[249]
$[Fe^{II}(dpp)_2(NCS)_2]\cdot py$	123	163	40	[251]
$[Fe^{II}(paptH)_2](NO_3)_2$	229	263	34	[253]
$[Fe^{II}(2\text{-pic})_3]Cl_2\cdot H_2O$[c]	199	290	91	[254]
$[\{Fe^{II}(Htrz)_3\}_{2.85}\{Fe^{II}(4\text{-}NH_2\text{-}trz)_3\}_{0.15}](ClO_4)_2\cdot n\,H_2O$	288	304	16	[256]
$[Fe^{II}(4\text{-}NH_2\text{-}trz)_3](NO_3)_{1.7}(BF_4)_{0.3}$	277	337	60	[257]
$[Fe^{II}(hyptrz)_3](4\text{-chloro-3-nitrophenylsulfonate})_2\cdot 2\,H_2O$	120	168	48	[258]
$[Fe^{II}(pyz)\{Pt(CN)_4\}]$	284	308	24	[260]
$[Fe^{III}(qsal)_2]NCSe$[d]	212	282	70	[252]
$Li[Fe^{III}(5\text{-Br-thsa})_2]H_2O$	294	333	39	[261]
$[Co^{II}(C_{14}\text{-tpy})_2](BF_4)_2$	250	306	56	[44]

[a] A list with frequently used abbreviations can be found at the end of the Review. [b] Hysteresis width and temperature depend strongly on the composition of the compounds. [c] Apparent phase transition; see text. [d] Two-step transition.

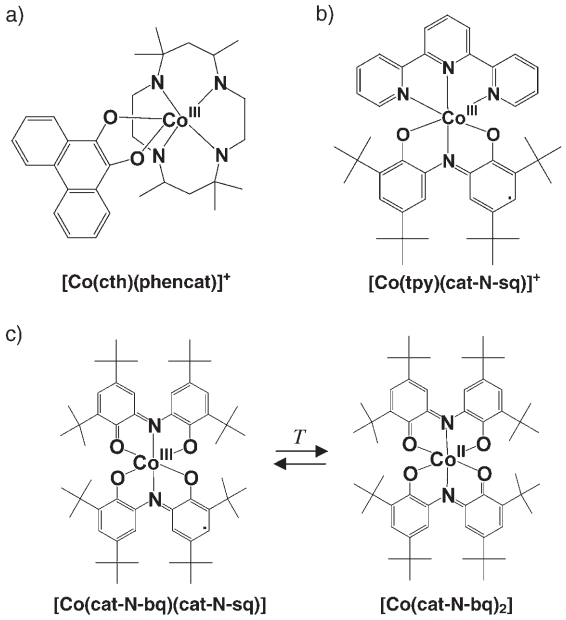

Scheme 1. Molecular structures of a) $[Co(cth)(phencat)]^+$[37] and b) $[Co(tpy)(cat\text{-}N\text{-}sq)]^+$.[40] c) Valence tautomerism $[Co^{III}(cat\text{-}N\text{-}bq)(cat\text{-}N\text{-}sq)]\rightleftharpoons[Co^{II}(cat\text{-}N\text{-}bq)_2]$.[66]

phase has a relatively longer ligand-to-metal bond length than that of the low-temperature phase, because two electrons in the d orbital of the high-temperature phase occupy an e_g orbital, which has antibonding character. This weakens the chemical bond and hence results in a longer bond length. The weaker metal-to-ligand bonding leads to a shallower potential well and closer spacing of the vibrational levels.[43] Hence, the density of the vibration between Co and its ligands in the high-temperature phase $[Co^{II\text{-}HS}(dbsq)_2(N\text{-}N)]$ is larger than that in the $[Co^{III\text{-}LS}(dbcat)(dbsq)(N\text{-}N)]$ structure. Thus, the term $\Delta S_{vib}=S_{vib}(\text{II-HS})-S_{vib}(\text{III-LS})$ is positive, and $\Delta S=S(\text{II-HS})-S(\text{III-LS})=\Delta S_{el}+\Delta S_{vib}>0$. If the difference in the enthalpy $\Delta H=H(\text{II-HS})-H(\text{III-LS})$ is positive in that situation, then $[Co^{III\text{-}LS}(dbcat)(dbsq)(N\text{-}N)]$ is the ground state. However, on warming, the entropy factor dominates and hence the $[Co^{II\text{-}HS}(dbsq)_2(N\text{-}N)]$ state can be the most stable form. Thus, valence-tautomeric transitions can be expected when the value of $\Delta H=H(\text{II-HS})-H(\text{III-LS})$ is positive but small enough to be overcome by virtue of its entropy term, so that the sign of ΔG ($\Delta G=\Delta H-T\Delta S$) changes for a given temperature.

Hysteresis effects are observed when intermolecular interactions are strong and cooperative effects are operative in the compound. A possibility of enhancing the intermolecular interactions is to construct a polymer structure in which the molecules are bound to each other by hydrogen bonds,

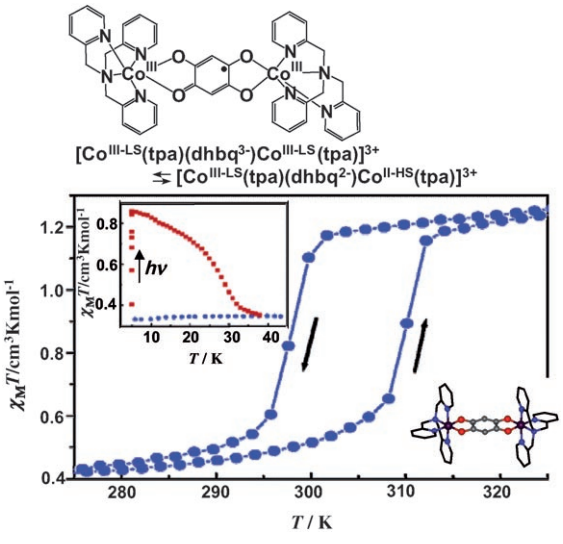

Figure 4. Temperature dependence of $\chi_M T$ value of $[\{Co(tpa)\}_2(dhbq)](PF_6)_3$ (χ_M is the molar magnetic susceptibility) and photoinduced changes in magnetization by irradiation at 532 nm (inset).[41] Reprinted with permission from reference [41]. Copyright 2006, The American Chemical Society.

coordinate bonds, or π–π interactions. Indeed, π–π interactions operate in the compound $[\{Co(tpa)\}_2(dhbq)](PF_6)_3$ mentioned above, which exhibits room-temperature hysteresis.[41]

Owing to the reasons given above, the reverse transition (with $Co^{III\text{-}LS}$ as the high-temperature phase and $Co^{II\text{-}HS}$ as the low-temperature phase) cannot generally be expected in valence-tautomeric systems. There can however be exceptions, as in the case of reverse spin-crossover, which was reported recently.[44]

2.2. Photoinduced Valence Tautomerism

2.2.1. Transient Effects; Fast Relaxation

Photoirradiation effects have been reported for some Co valence-tautomeric compounds. Transient photoinduced valence tautomerism was observed in $[Co^{III\text{-}LS}$(3,5-dbsq)(3,5-dbcat)(phen)] (Figure 5).[45,46] Excitation of the ligand-to-metal charge-transfer (LMCT) band by 532-nm light from a

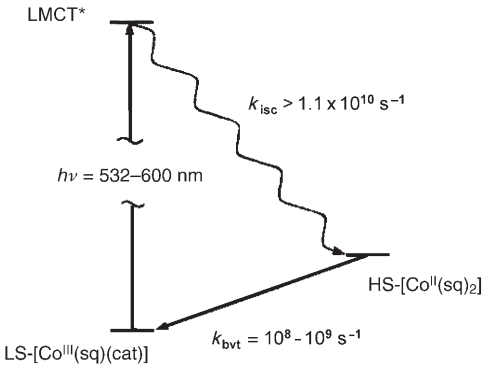

Figure 5. Jablonski diagram for the photoinduced valence tautomerism. A laser pulse in the charge-transfer absorption band of the $Co^{III\text{-}LS}$ tautomer at 532–600 nm leads to population of a LMCT excited state. Rapid intersystem crossing produces the $Co^{II\text{-}HS}$ state followed by a slower back valence tautomerization. Reprinted with permission from reference [46]. Copyright 1996, The American Chemical Society.

picosecond Nd-YAG laser induced charge transfer from 3,5-dbcat to $Co^{III\text{-}LS}$ to form the LMCT excited state, which then relaxed to the $[Co^{II\text{-}HS}$(3,5-dbsq)$_2$(phen)] state. The lifetime of the metastable $[Co^{II\text{-}HS}$(3,5-dbsq)$_2$(phen)] state at 190.4 K was approximately 600 ns.

By using femtosecond pulsed lasers, a much faster process in $[Co^{II\text{-}HS}(Me_4cyclam)(phensq)]PF_6$ (Me_4cyclam = 1,4,8,11-tetramethyl-1,4,8,11-tetraazacyclotetradecane) could be studied.[47] Valence tautomerism was induced upon excitation of the metal-to-ligand charge-transfer (MLCT) band at 400 nm. The photoinduction proceeds in two separate steps lasting 150 fs and 7 ps. The subsequent conversion of [Co^{III}(cat)] into [Co^{II}(sq)] took 170 ns.

$[Co^{III\text{-}LS}$(cat-N-bq)(cat-N-sq)] was recently studied by a UV/Vis pump–probe technique.[48] The LMCT excited state was first created by irradiation at 480 nm, with subsequent relaxation to the $[Co^{II\text{-}HS}$(cat-N-bq)$_2$] state, and finally reversion to the original $[Co^{III\text{-}LS}$(cat-N-bq)(cat-N-sq)] state. The lifetime of the LMCT excited state was 180 fs, and that of the $[Co^{II\text{-}HS}$(cat-N-bq)$_2$] state was 410 ps (in $CHCl_3$). The fast back valence tautomerism can be explained by the strong electronic coupling between $[Co^{II\text{-}HS}$(cat-N-bq)$_2$] and $[Co^{III\text{-}LS}$(cat-N-bq)(cat-N-sq)].

2.2.2. Photoinduced Valence Tautomerism with Long Lifetime

As in the case of the LIESST (light-induced excited spin-state trapping) effects observed for Fe^{II} and Fe^{III} spin-crossover complexes,[49,50] photoinduced valence tautomerism with extremely long lifetime has been discovered in some valence-tautomeric compounds (Scheme 2).[51–58] These

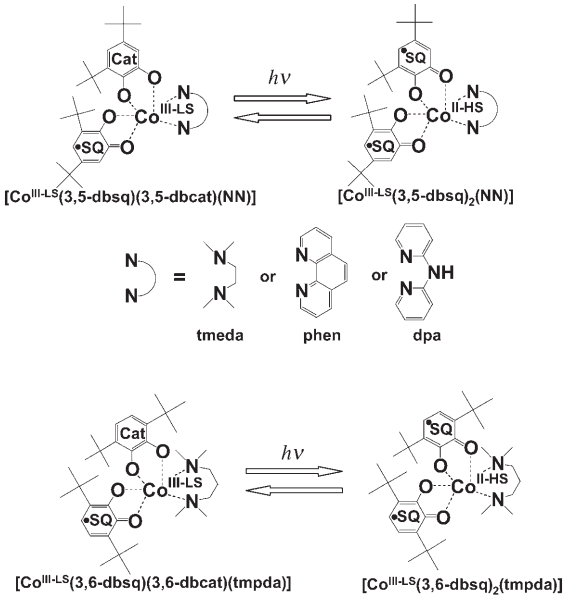

Scheme 2. Co compounds that show photoinduced valence tautomerism with long lifetimes.[51–58] This phenomenon is similar to the LIESST effect in Fe spin-crossover complexes.[7,49,50]

include $[Co^{III\text{-}LS}$(3,5-dbsq)(3,5-dbcat)(phen)]·$CH_3C_6H_5$,[52,56] $[Co^{III\text{-}LS}$(3,5-dbsq)(3,5-dbcat)(tmeda)] (tmeda = *N*,*N*,*N*′,*N*′-tetramethylethylenediamine),[53,54] $[Co^{III\text{-}LS}$(3,6-dbsq)(3,6-dbcat)(tmpda)] (tmpda = *N*,*N*,*N*′,*N*′-tetramethylpropylenediamine),[55] $[Co^{III\text{-}LS}$(3,5-dbsq)(3,5-dbcat)(dpa)] (dpa = 2,2′-dipyridylamine),[57] and $[Co^{III\text{-}LS}$(3,5-dbsq)(3,5-dbcat)-(phen)]·C_6H_5Cl.[58] The lifetime at 5 K of $[Co^{II\text{-}HS}$(3,5-dbsq)$_2$-(tmeda)] is 175 min.[54] The induction of photoinduced valence tautomerism was confirmed by X-ray absorption spectroscopy as well as by IR and UV/Vis spectra.[59]

The relaxation rate constant k_{bvt} plotted as $\ln(k_{bvt})$ versus $1/T$ for $[Co^{II\text{-}HS}$(3,5-dbsq)$_2$(phen)]·C_6H_5Cl shows that the interconversion from metastable $[Co^{II\text{-}HS}$(3,5-dbsq)$_2$(phen)] into $[Co^{III\text{-}LS}$(3,5-dbsq)(3,5-dbcat)(phen)] follows Arrhenius behavior at temperatures above 25 K, which indicates that relaxation is a thermally activated process. However, at temperatures below 25 K, deviations from linearity are observed. The relaxation rate finally becomes temperature-

independent, which suggests the appearance of tunneling effects.

More recently, photoinduced valence tautomerism was reported in the dinuclear Co complex [{Co(cth)}$_2$(dhbq)]-

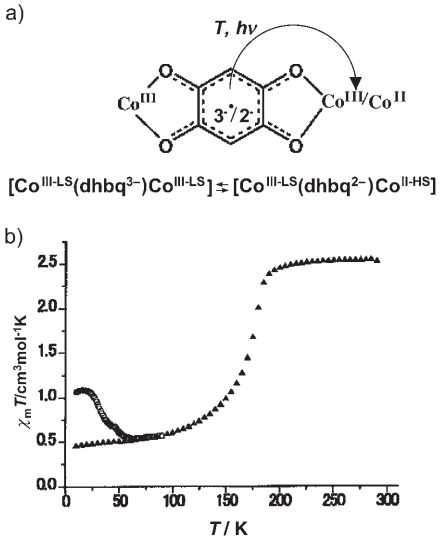

Figure 6. a) The cation of the Co complex [{Co(cth)}$_2$(dhbq)](PF$_6$)$_3$.[60] b) Plot of $\chi_M T$ versus T for [{Co(cth)}$_2$(dhbq)](PF$_6$)$_3$ measured before (▲) and after (□) irradiation at 647 nm.[60] Reprinted from reference [60].

(PF$_6$)$_3$ (Figure 6).[60] The magnetization value increases at 5 K after irradiation (647.1–676.4 nm). The photoprocess was [Co$^{III\text{-}LS}$(dhbq^{3-})Co$^{III\text{-}LS}$]→[Co$^{III\text{-}LS}$(dhbq^{2-})Co$^{II\text{-}HS}$]. The metastable state [Co$^{III\text{-}LS}$(dhbq^{2-})Co$^{II\text{-}HS}$] relaxed back to the original state at around 40 K. The dinuclear compound [{Co(tpa)}$_2$(dhbq)](PF$_6$)$_3$, which shows room-temperature hysteresis as described above, also exhibits photoinduced valence tautomerism (Figure 4).[41]

2.2.3. Photomechanical Effects

Another important property reported thus far is the photomechanical effect.[61] Crystalline [Co$^{III\text{-}LS}$(3,6-dbsq)(3,6-dbcat)(pyz)] has a one-dimensional chain structure bridged by pyrazine (pyz) (Figure 7). When the crystals are illuminated on one side by a tungsten lamp, they bend reversibly in response to the light. It is thought that ligand-to-metal charge transfer is induced by the irradiation, which results in the elongation of the metal–ligand bond. The metal-to-ligand bonds of the Co$^{II\text{-}HS}$ species are known to be longer than those of the Co$^{III\text{-}LS}$ species by about 0.2 Å. As a result, the size of the crystals in the irradiated region expands, which results in the induction of photomechanical effects.

Prior to this work, quite distinct photomechanical effects were reported in [Rh^{I}(3,6-dbsq)(CO)$_2$] (Figure 8).[62–64] Irradiation at 2000 nm induces bending in these crystals. The photomechanical effect in this case is much greater than that in the Co complexes described above.

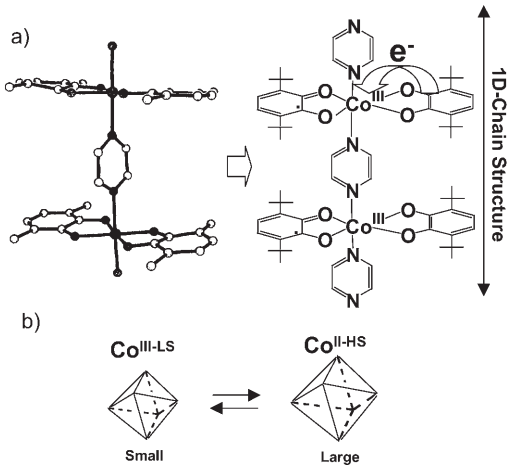

Figure 7. a) Complex unit of [{Co$^{III\text{-}LS}$(3,6-dbsq)(3,6-dbcat)(pyz)}$_n$]. Reprinted with permission from reference [61]. Copyright 1994, The American Chemical Society. b) Change in the molecular volume upon valence tautomerism.

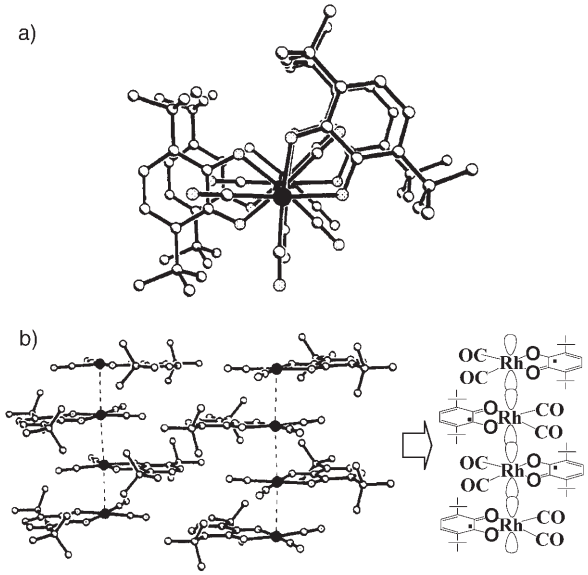

Figure 8. a) View of [Rh(3,6-dbsq)(CO)$_2$] down to the crystallographic *a* axis.[63] b) Alignment of molecular columns within the unit cell.[63,64] Reprinted with permission from reference [63]. Copyright 1992, The American Chemical Society.

2.2.4. Coupling of Valence Tautomerism and Electrochemistry

The coupling of valence tautomerism and electrochemistry gives rise to multistate switching systems.[65–67] For example, four-state switching has been reported for [Co$^{III\text{-}LS}$(3,5-dbcat)(3,5-dbsq)(bpy)] by Ruiz et al.[65] More recently, the same group reported similar redox-tunable valence tautomerism for [Co^{III}(cat-N-bq)(cat-N-sq)] (Scheme 3).[67]

2.3. Valence-Tautomeric Mn Compounds

Other than Co complexes, complexes of some other metals such as manganese also exhibit valence tautomerism.

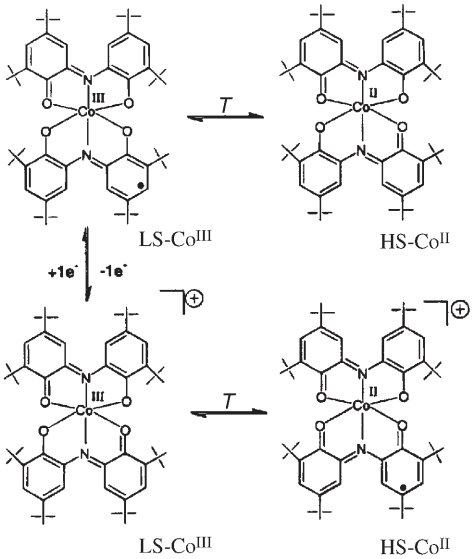

Scheme 3. Redox-tunable valence tautomerism of [Co^III(cat-N-bq)(cat-N-sq)].[66] Reprinted with permission from reference [66]. Copyright 2000, The American Chemical Society.

An important example is $[Mn^{IV}(py)_2(3,5\text{-dbcat})_2]$ (py = pyridine; Scheme 4), which can exist in three possible states: $[Mn^{IV}(py)_2(3,5\text{-dbcat})_2] \rightleftharpoons [Mn^{III}(py)_2(3,5\text{-dbsq})(3,5\text{-dbcat})] \rightleftharpoons [Mn^{II}(py)_2(3,5\text{-dbsq})_2]$. The electron configurations

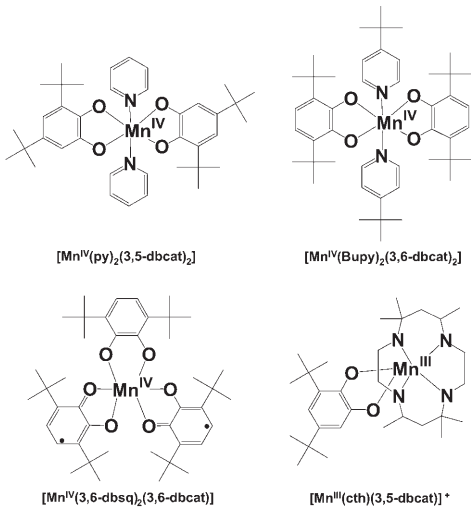

Scheme 4. Molecular structure of valence-tautomeric Mn complexes.[68, 69, 72, 73]

of the d orbitals of Mn^{II}, Mn^{III}, and Mn^{IV} are $t_{2g}^3e_g^2$, $t_{2g}^3e_g^1$, and $t_{2g}^3e_g^0$, respectively. Indeed, $[Mn^{IV}(py)_2(3,5\text{-dbcat})_2]$ in toluene undergoes valence tautomerism between $[Mn^{IV}(py)_2(3,5\text{-dbcat})_2]$ and $[Mn^{II}(py)_2(3,5\text{-dbsq})_2]$.[68] The transitions are accompanied by changes in the ligand-to-metal bond lengths: the transition from Mn^{IV} to Mn^{III} induces a change in axial bond length, and the transition from Mn^{III} to Mn^{II} involves a change in the equatorial Mn–O bond lengths (Figure 9). The average ligand-to-metal bond lengths of the Mn^{II} species are greater than those of the Mn^{III} species, and these are greater

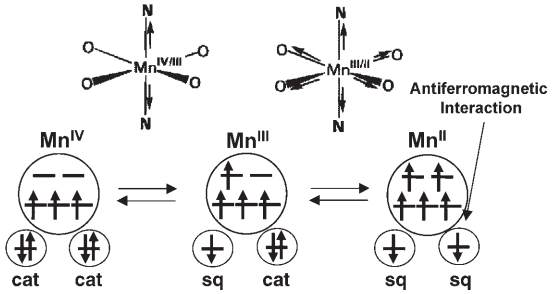

Figure 9. Change in the structure and electronic states in valence-tautomeric Mn compounds. Reprinted with permission from reference [71]. Copyright 1997, The American Chemical Society.

than those of Mn^{IV} species. This difference is because two and one electrons occupy the antibonding e_g orbital of the Mn^{II} and Mn^{III} complexes, respectively. The longer ligand-to-metal bonds suggest the presence of a high density of vibrational states, which contributes to the entropy gain. Hence, if the valence-tautomeric transition occurs in two steps, then $[Mn^{II}(py)_2(3,5\text{-dbsq})_2]$ should be the high-temperature phase, $[Mn^{III}(py)_2(3,5\text{-dbsq})(3,5\text{-dbcat})]$ should be the intermediate phase, and $[Mn^{IV}(py)_2(3,5\text{-dbcat})_2]$ should be the low-temperature phase. Furthermore, the spins on the Mn center and the spins on the 3,5-dbsq ligands interact antiferromagnetically. Hence, the spin ground state of the Mn complexes is always $S = 3/2$. Therefore, in contrast to the Co valence-tautomeric compounds, the change in the magnetization with valence tautomerism is not so distinct. However, large differences are observed in the charge-transfer bands in the near-IR region. $[Mn^{III}(py)_2(3,5\text{-dbsq})(3,5\text{-dbcat})]$ shows an intense ligand-to-ligand charge-transfer (LLCT) band, whereas there are no LLCT bands for $[Mn^{IV}(py)_2(3,5\text{-dbcat})_2]$ or $[Mn^{II}(py)_2(3,5\text{-dbsq})_2]$. Hence, the valence tautomerism paths can be followed by monitoring this band.

Another example of a compound that exhibits valence tautomerism is $[Mn^{IV}(bupy)_2(3,6\text{-dbcat})_2]$ (bupy = 4-*tert*-butylpyridine; Scheme 4).[69] Figure 10 shows its near-IR absorption spectra and magnetic properties. Although no distinct change in magnetization can be observed, the LLCT band at around 2100 nm increases with increasing temperature. The spectral change shows the transition from the room-temperature form $[Mn^{IV}(bupy)_2(3,6\text{-dbcat})_2]$ to the high-temperature form $[Mn^{III}(bupy)_2(3,6\text{-dbcat})(3,6\text{-dbsq})]$. Furthermore, an additional transition to $[Mn^{II}(bupy)_2(3,6\text{-dbsq})_2]$ in toluene is suspected.

Similarly, several other Mn complexes exhibit valence tautomerism.[70–73] Among these, $[Mn^{IV}(3,6\text{-dbsq})_2(3,6\text{-dbcat})]$ (Scheme 4) is the first example of valence-tautomeric interconversion of a transition-metal complex that does not have $M(N\text{-}N)(dbq)_2$ structure (M = Co or Mn; dbq = 3,5-dbsq, 3,5-dbcat, 3,6-dbsq, or 3,6-dbcat).[72] Another example is the charged valence-tautomeric compound $[Mn^{III}(cth)(3,5\text{-dbcat})]^+$ (Scheme 4), whose transition temperature can be modified by changing the counter anion.[73] More recently, it was reported that the isomers of Mn complexes with polymeric structures of composition $[\{Mn_2^{III}(H_2L^1)(Cl_4cat)_4{\cdot}2H_2O\}_\infty]$ [L^1 = *N*,*N*′-bis(2-pyridylmethyl)-1,2-eth-

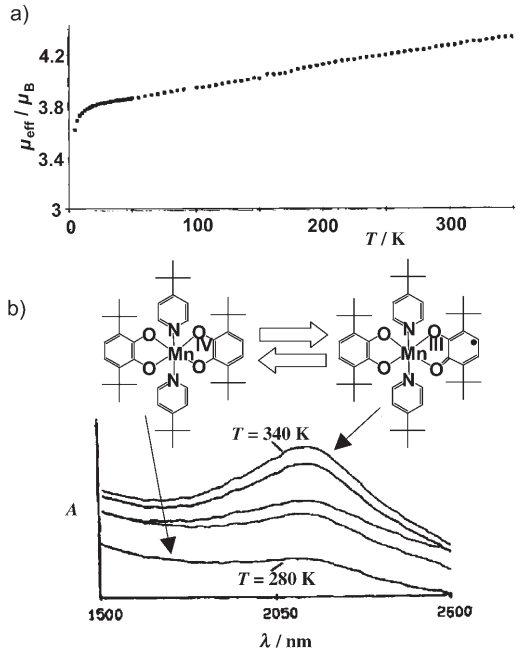

Figure 10. a) Plot of magnetic moment versus *T* for *trans*-[Mn^{III}(bupy)$_2$-(3,6-dbsq)(3,6-dbcat)]. b) Temperature-dependent changes in the transition at 2100 nm of *trans*-[Mn^{III}(bupy)$_2$(3,6-dbsq)(3,6-dbcat)] in the solid state. Reprinted with permission from reference [69]. Copyright 1994, Elsevier.

anediamine, Cl_4cat = tetrachlorocatecholate dianion] and [{$Mn_2^{III}(H_2L^2)(Cl_4cat)_4 \cdot 2CH_3CN \cdot 2H_2O\}_\infty$] [$L^2$ = *N*,*N*′-bis(2-pyridylmethyl)-1,3-propanediamine] also exhibit valence tautomerism: $[Mn_2^{III}(Cl_4cat)_2(Cl_4sq)_2] \rightleftharpoons [Mn_2^{II}(Cl_4sq)_4]$ (Cl_4sq = tetrachlorosemiquinonate anion).[74] As in the case of the Co complexes, electrochemically switchable molecular arrays have also been reported for Mn complexes.[67]

2.4. Valence-Tautomeric Cu Compounds

Cu complexes also exhibit thermally induced valence tautomerism (Scheme 5).[75] An example of a Cu valence-tautomeric compound is [$Cu^I(py)_2$(phensq)].[75] The EPR signal in a 1:10 mixture of pyridine and toluene shows that the complex is in the [$Cu^I(py)_2$(phensq)] state at 300 K, but in the form [$Cu^{II}(py)_2$(phencat)] at 77 K. Another example is observed in [Cu^I(mmb)(3,5-dbsq)] (mmb = 1-methyl-2-(methylthiomethyl)-1*H*-benzimidazole).[76] The EPR spectra showed that it takes the [Cu^{II}(mmb)(3,5-dbcat)] form at low temperature in THF. In contrast, above 250 K, the EPR signal of [Cu^I(mmb)(3,5-dbsq)] starts to appear, and it dominates above 350 K. The compounds [Cu^I(dde)(3,5-dbsq)]/[Cu^{II}-(dde)(3,5-dbcat)] (dde = 1-diphenylphosphino-2-dimethylaminoethane) and [Cu^I(mtq)(3,5-dbsq)]/[Cu^{II}(mtq)(3,5-dbcat)] (mtq = 8-methylthioquinoline) also exhibit valence tautomerism.[77,78] Valence tautomerism of copper can also be observed in enzymes that play an important role in the oxidation of amines.[79] Hence, the study of Cu valence-tautomeric systems is important from biological and biomimetic viewpoints, as well as for basic science.

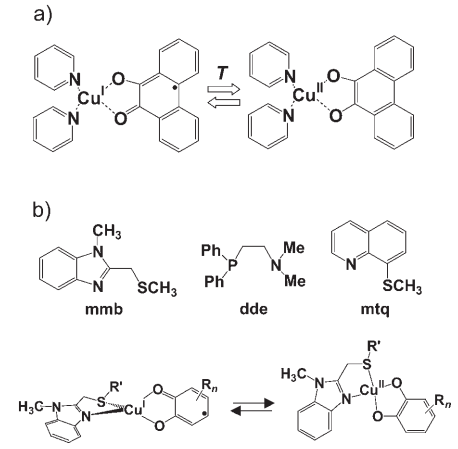

Scheme 5. a) Valence tautomerism between [$Cu^I(py)_2$(phensq)] and [$Cu^{II}(py)_2$(phencat)].[75] b) Structures of mmb, dde, and mtq. Note that Cu^I favors tetrahedral geometry, whereas Cu^{II} favors a planar structure.[76]

The ligand-to-metal bond lengths of Cu^I complexes have been reported to be longer than those of Cu^{II} complexes; Cu–O bond lengths differ by about 0.15 Å.[10] This difference suggests that the density of vibrations of the Cu^I state is larger than that of Cu^{II}, which contributes to changes in the entropy term of Cu valence-tautomeric systems, as in the case of Co valence-tautomeric compounds.

2.5. Valence-Tautomeric Fe Compounds

An example of an Fe valence-tautomeric compound has recently been reported, namely, the mixed-valence tetrachlorosemiquinone/tetrachlorocatecholate compound [Fe^{III}-(bispicen)(Cl_4cat)(Cl_4sq)]·DMF (bispicen = *N*,*N*′-bis(2-pyridylmethyl)-1,2-ethanediamine) (Scheme 6a).[80] The [Fe^{III}-

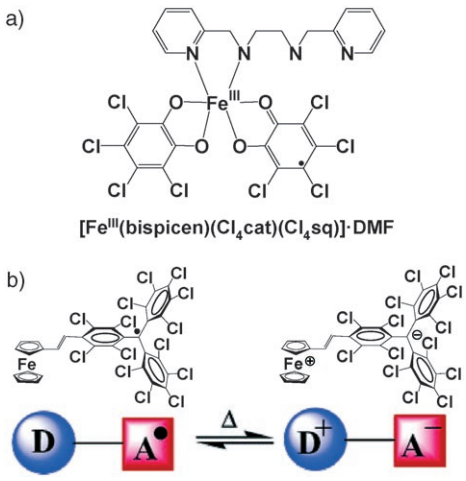

Scheme 6. a) [Fe^{III}(bispicen)(Cl_4cat)(Cl_4sq)]·DMF.[80] b) Valence tautomerism of an electroactive ferrocene-substituted triphenylmethyl radical. Reprinted with permission from reference [81]. Copyright 2003, The American Chemical Society.

(bispicen)(Cl_4cat)(Cl_4sq)]·DMF form has a charge-transfer band (Cl_4cat→Fe^{III}) at around 570 nm. Upon heating the complex, the absorbance at 570 nm decreased with a clear isosbestic point at 650 nm, and the band of the semiquinone–catecholate transition at 1932 nm also decreased with an isosbestic point at around 1880 nm. Thus, the redox state at low temperature is [Fe^{III}(bispicen)(Cl_4cat)(Cl_4sq)], and at high temperature [Fe^{II}(bispicen)(Cl_4sq)$_2$] is favored.

Another valence-tautomeric compound containing Fe ions is an electroactive ferrocene-substituted triphenylmethyl radical (Scheme 6b).[81] Electron transfer from the ferrocene center to the triphenylmethyl radical with increasing temperature was demonstrated by Mössbauer and magnetic measurements. Notably, its transition temperature T_c, at which there are equal amounts of both isomers, occurs at around room temperature.

2.6. Valence-Tautomeric Ni Compounds

Ni complexes also show valence tautomerism. For example, the radical cation of a nickel(II)–porphyrin complex exhibits tautomerism between the Ni^{III}–porphyrin and Ni^{II}–porphyrin π-cation radical states.[82,83] Similarly, the one-electron oxidized Ni^{II}–(disalicylidene)diamine complex [Ni(*t*bu-salcn)] (H_2*t*bu-salcn = *N*,*N*′-bis(3′,5′-di-*tert*-butylsalicylidene)-1,2-cyclohexanediamine) is in the Ni^{II}–phenoxyl radical state at room temperature and the Ni^{III}–phenolate state below −120 °C (Scheme 7a).[84] Chemical control of the valence state of Ni complexes has also been reported recently.[85] [Ni^{II}(Py(Bn)$_2$)(3,5-dbsq)]PF_6 (Py(Bn)$_2$ = *N*,*N*-bis-(benzyl)-*N*-[(2-pyridyl)methyl]amine) in CH_2Cl_2 takes the Ni^{II}–sq state, whereas [Ni^{III}(MePy(Bn)$_2$)(3,5-dbcat)]PF_6 (MePy(Bn)$_2$ = *N*,*N*-bis(benzyl)-*N*-[(6-methyl-2-pyridyl)methyl]amine) in CH_2Cl_2 takes the Ni^{III}–cat state. Subtle differences in the donor ability of the bidentate nitrogen ligands induce drastic changes in the valence state. Furthermore, as shown in Scheme 7b, [Ni^{II}(Py(Bn)$_2$)(3,5-dbsq)]$^+$ in CH_2Cl_2 with 2.5 equivalents of dmf exhibits a transition between the square-planar room-temperature form [Ni^{II}(Py(Bn)$_2$)(3,5-dbsq)]$^+$ and the octahedral form [Ni^{II}(Py(Bn)$_2$)(3,5-dbsq)(dmf)$_2$]$^+$ at low temperature.[86] In contrast, [Ni^{III}(MePy(Bn)$_2$)(3,5-dbcat)]$^+$ in CH_2Cl_2 shows a transition between the square-planar form [Ni^{III}(MePy(Bn)$_2$)(3,5-dbcat)]$^+$ and the octahedral form [Ni^{II}(MePy(Bn)$_2$)(3,5-dbsq)(dmf)$_2$]$^+$ in the presence of 200 equivalents of dmf.[86]

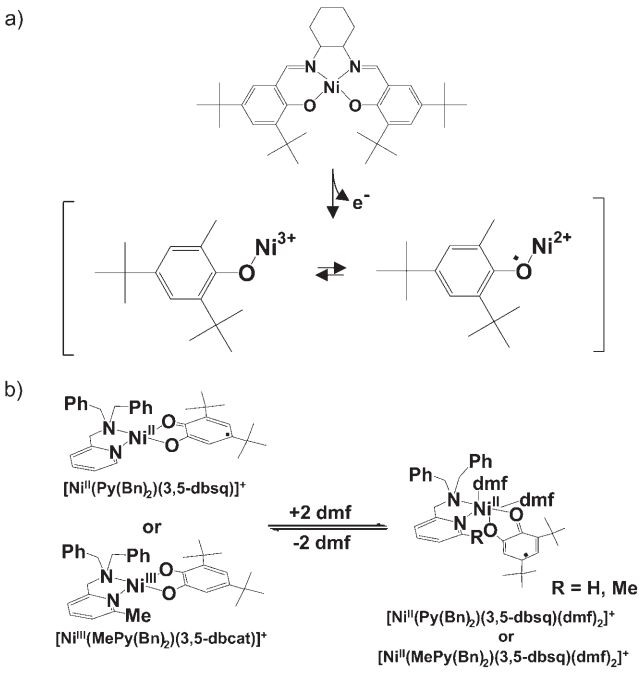

Scheme 7. a) Tautomeric states of an oxidized Ni^{II}–(disalicylidene)diamine complex.[84] b) Transition between square-planar Ni^{II} and octahedral Ni^{II} (top), and between square-planar Ni^{III} and octahedral Ni^{II} (bottom) in DMF/CH_2Cl_2.[86]

2.7. Valence-Tautomeric Rh Compounds

Abakumov et al. reported the reversible intramolecular electron transfer between the metal center and the ligand in a series of Rh–quinone complexes.[87,88] In more recent studies, the valence states of linear-chain Rh complexes could be chemically controlled. The metal center in the linear-chain complex [{Rh(3,6-dbsq)(CO)$_2$}$_\infty$] has the oxidation state Rh^I (Scheme 8a).[63]

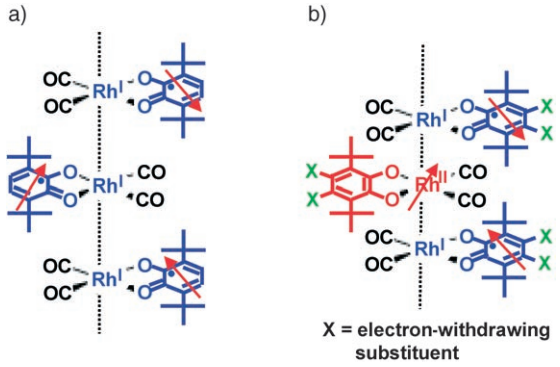

Scheme 8. a) Structure of [{Rh(3,6-dbsq)(CO)$_2$}$_\infty$].[63] b) Structure of [{Rh(3,6-dbdiox-4,5-Cl_2)(CO)$_2$}$_\infty$].[89] Reprinted from reference [89].

Mitsumi et al. prepared the linear-chain mixed-valence rhodium(I,II) semiquinonato/catecholato complex [{Rh(3,6-dbdiox-4,5-Cl_2)(CO)$_2$}$_\infty$] (3,6-dbdiox-4,5-Cl_2 indicates the 3,6-di-*tert*-butyl-4,5-dichloro-1,2-benzosemiquinonate (3,6-dbsq-4,5-Cl_2^-) or the 3,6-di-*tert*-butyl-4,5-dichlorocatecholate (3,6-dbcat-4,5-Cl_2^{2-}); Scheme 8b).[89] The mixed-valence state is formed by electron transfer between the metal d orbitals and the ligand π* orbitals. X-ray crystal structural analysis at 302 K showed that the [Rh(3,6-dbdiox-4,5-Cl_2)(CO)$_2$] molecules form trimeric units in a linear chain. At low temperature, the trimers in the linear chain dimerized as a result of Peierls distortion to form hexameric units, which induced the pairing of unpaired electrons in the d_{z^2} orbitals of the Rh^{II} ions. Notably, the magnetization value shows a rounded hump at 172–208 K.

2.8. Challenges in the Field of Valence-Tautomeric Compounds

With the exception of the mono- and dinuclear Co compounds described above, there are no reports of compounds that exhibit abrupt transitions with hysteresis. Furthermore, trapping of the light-induced excited valence states of Mn, Cu, Fe, Ni, and Rh valence-tautomeric compounds has been unsuccessful. Hence, the preparation of valence-tautomeric compounds that exhibit abrupt transitions with hysteresis and photoinduced valence tautomerism represents one of the central challenges in this field.

3. Other Charge-Transfer Systems

3.1. Metal-to-Metal Charge Transfer in FeCo Heptanuclear Compounds

Other than the general valence-tautomeric compounds in which metal-to-ligand charge transfer is induced, some new types of charge-transfer compounds that exhibit changes in their magnetic properties have recently been reported. A typical example is the FeCo cluster $[\{Co(tmphen)_2\}_3\{Fe(CN)_6\}_2]$ (tmphen = 3,4,7,8-tetramethyl-1,10-phenanthroline; Figure 11),[90,91] which exhibits a charge-transfer-induced spin transition (CTIST). The oxidation state of the compound at room temperature is expressed by $[\{Co^{II\text{-}HS}(tmphen)_2\}_3\{Fe^{III}(CN)_6\}_2]$. The magnetic properties show that a phase transition with CTIST takes place at around 200 K. High-spin Co^{II} ions are oxidized to low-spin Co^{III}, and, concomitantly, Fe^{III} ions are reduced to Fe^{II}. In contrast to the valence-tautomeric Co compounds described in Section 2, the charge transfer occurs between two metal centers, not between a metal center and an organic ligand. Crystal structure analysis shows that large changes in the Co–ligand bond lengths are induced during the phase transition, which suggests that the entropy change originating from the lattice vibration term should contribute greatly to the induction of the CTIST phase transition. A FeCo Prussian Blue analogue with a three-dimensional network structure of Fe and Co centers also exhibits thermally and photochemically induced charge-transfer and photomagnetic effects (see Section 8).[21,92,93]

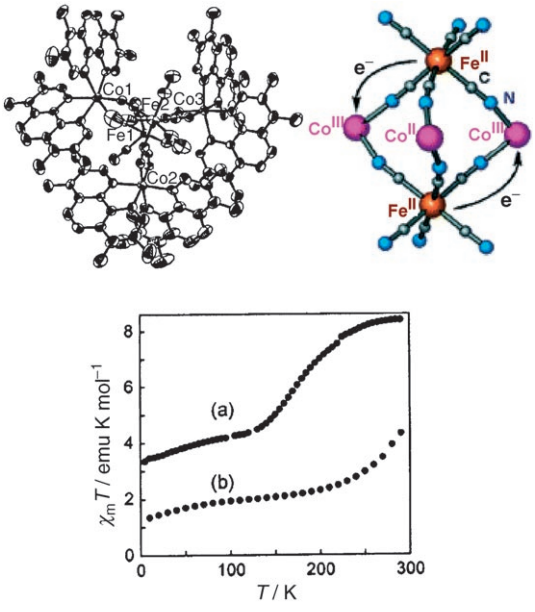

Figure 11. Top: Structure of $[\{Co(tmphen)_2\}_3\{Fe(CN)_6\}_2]$ (ORTEP plot (left) drawn at the 50% probability level; $T = 110$ K).[90,91] Bottom: Plot of $\chi_m T$ versus T for a) red crystals of $[\{Co(tmphen)_2\}_3\{Fe(CN)_6\}_2]$ and b) the blue solid that results when the red crystals are exposed to humid air ($H = 1000$ G). The red crystals exhibit a CTIST.[90,91] Reprinted with permission from reference [90]. Copyright 2004, The American Chemical Society.

3.2. Charge Transfer Coupled with Bond Formation

The recently reported complex $[(bdta)_2\{Co(mnt)_2\}]$ (bdta = 1,3,2-benzodithiazolyl; mnt = maleonitriledithiolate) belongs to a new type of charge-transfer system (Figure 12)[94]

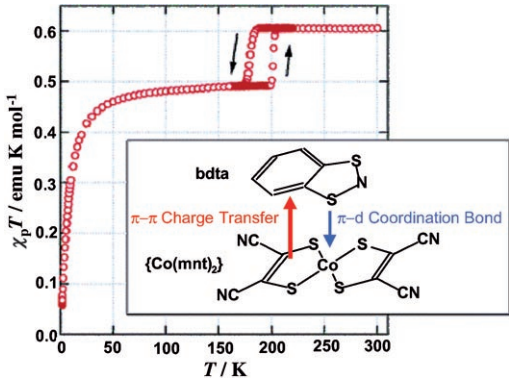

Figure 12. Temperature dependence of $\chi_p T$ for $[(bdta)_2\{Co(mnt)_2\}]$. The inset shows a possible mechanism for coordinate-bond formation during the phase transition at 190 K. Reprinted with permission from reference [94]. Copyright 2006, The American Chemical Society.

and shows an abrupt phase transition at around 190 K with a hysteresis width of 20 K. The phase transition can be expressed as $[(bdta^{0.9+})_2\{Co(mnt)_2\}^{1.8-}] \rightleftharpoons [(bdta^{0.9+})(bdta^{0.5+})\{Co(mnt)_2\}^{1.4-}]$. An important characteristic of this system is that switching between bonding and dissociation of the coordination bond of bdta occurs at the transition temperature. Furthermore, the change in the degree of charge transfer is small, which the authors explain as follows: The electron transfer from $\{Co(mnt)_2\}^{2-}$ to $bdta^+$ through the π overlap decreases the positive charge on the $bdta^+$ ion and enhances its ability to act as a ligand. Thus, bdta forms a coordination bond and partially returns the obtained electron to the vacant d orbitals of the cobalt ion in $\{Co(mnt)_2\}$.

3.3. Transitions between Neutral and Ionic States and Related Phenomena

Compounds that exhibit transitions between neutral and ionic states constitute another intriguing charge-transfer

system (Figure 13).[95–101] A typical example of such a compound is the complex of tetrathiafulvalene (TTF) with *p*-chloranil (CA).[95] Upon cooling, the neutral state is transformed into the ionic state at 80 K. Spectroscopic measurements show that the redox state changes from $TTF^{0.3+}$–$CA^{0.3-}$ (neutral) to $TTF^{0.6+}$–$CA^{0.6-}$ (ionic). The TTF and CA molecules form heterodimers. Hence, both the neutral and ionic phases are diamagnetic. However, an ESR (Electron Spin Resonance) signal appears below T_c (Figure 13b).[102] This signal arises from the spin solitons (defects) formed at the boundaries of the ionic domains. These domains in the crystal can be expressed by $(A^{\rho-}D^{\rho+})(A^{\rho-}D^{\rho+})$-$(A^{\rho-}D^{\rho+})\mathbf{A}^{\rho-}(D^{\rho+}A^{\rho-})(D^{\rho+}A^{\rho-})(D^{\rho+}A^{\rho-})$, where $\mathbf{A}^{\rho-}$ is a defect, or $(D^{\rho+}A^{\rho-})(D^{\rho+}A^{\rho-})(D^{\rho+}A^{\rho-})\mathbf{D}^{\rho+}(A^{\rho-}D^{\rho+})$-$(A^{\rho-}D^{\rho+})(A^{\rho-}D^{\rho+})$, where $\mathbf{D}^{\rho+}$ is a defect. The isolated $TTF(D^{\rho+})$ and $CA(A^{\rho-})$ at the domain walls have unpaired spins, which are responsible for the ESR signals. Similar neutral–ionic transitions are reported for DMTTF–CA (DMTTF = dimethyltetrathiafulvalene).[97] As both the neutral and ionic phases are diamagnetic, TTF–CA and its related compounds are more attractive from the viewpoint of their dielectric properties rather than their magnetic properties.[103]

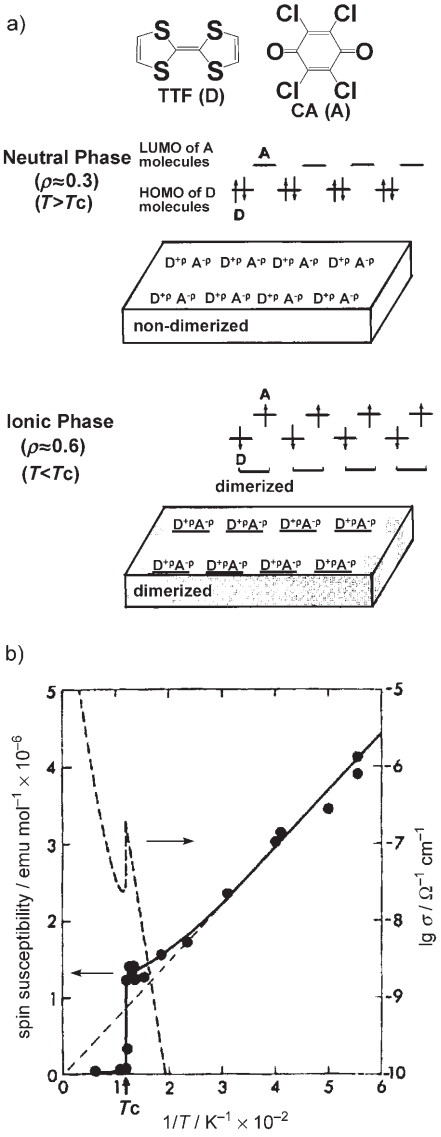

Figure 13. a) Neutral-to-ionic phase transition of TTF-CA. Reprinted with permission from reference [99]. Copyright 1999, The American Chemical Society. b) The total spin susceptibility (solid line) and dc electric conductivity (dashed curve) versus T^{-1} of a single crystal of TTF-CA. The dashed straight line represents paramagnetic Curie behavior. Reprinted with permission from reference [102]. Copyright 2003, The American Physical Society.

More recently, a transformation between the monovalent state $D^+A_3^-$ and the divalent state $D^{2+}A_3^{2-}$ was observed in $[(npbifc)(F_1\text{-}tcnq)_3]$ (npbifc = dineopentylbisferrocene; F_1-tcnq = fluorotetracyanoquinodimethane).[104,105] At room temperature, this compound is a monovalent solid with the monocation $npbifc^+$ and the trimer monoanion $(F_1\text{-}tcnq)_3^-$. Upon cooling to around 120 K, charge transfer from $npbifc^+$ to $(F_1\text{-}tcnq)_3^-$ is induced to form $npbifc^{2+}$ and $(F_1\text{-}tcnq)_3^{2-}$. The change in the redox state is illustrated in Figure 14a.[104] Calorimetric studies revealed that the transition entropy is $20 \pm 2\ J\,mol^{-1}\,K^{-1}$. As the entropies of the electronic terms are comparable between the high- and low-temperature phases, the observed change must arise from the contribution of the lattice term. The change in the frequencies of the lattice vibration might contribute greatly to the entropy term. Notably, the related compound $[(npbifc)(tcnq)_3]$ (tcnq = tet-

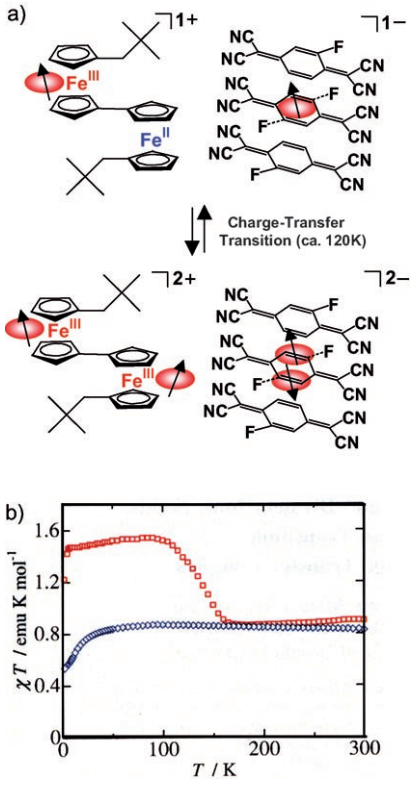

Figure 14. a) Transformation between the monovalent state $D^+A_3^-$ and the divalent state $D^{2+}A_3^{2-}$ in $[(npbifc)(F_1\text{-}tcnq)_3]$. b) Magnetic properties of $[(npbifc)(F_1\text{-}tcnq)_3]$ (red) and $[(npbifc)(tcnq)_3]$ (blue). Reprinted with permission from reference [104]. Copyright 2005, The Physical Society of Japan.

racyanoquinodimethane) does not exhibit such a transformation (Figure 14b).

A purely organic compound that displays intramolecular charge transfer is shown in Figure 15.[106] The complex consists

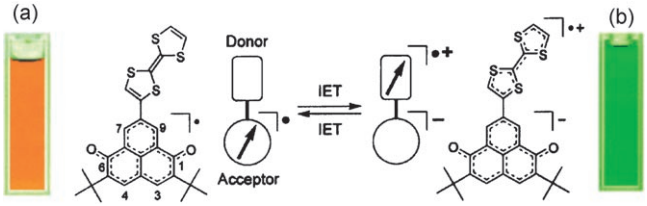

Figure 15. Color of 6OP-TTF in a) CH_2Cl_2 (1.2×10^{-4} M) and b) CF_3CH_2OH (7.6×10^{-5} M) at 293 K. Reprinted from reference [106].

of 2,5-di-*tert*-butyl-6-oxophenalenoxyl (6OP), a stable neutral radical with high electron-accepting ability, and a tetrathiafulvalene (TTF) molecule as an electron donor. The UV/Vis spectrum shows that 6OP-TTF is a neutral radical in CH_2Cl_2, whereas it has a zwitterionic structure with a TTF radical cation moiety and a 6OP anion moiety in CF_3CH_2OH. When it is dissolved in a mixture of CH_2Cl_2/CF_3CH_2OH (199:1), a thermally induced transition between the two states can be observed: the compound exists in the neutral radical form at room temperature and is transformed into the zwitterionic structure upon cooling. These spin-transfer phenomena accompany solvato- and thermochromic effects in organic open-shell systems.

3.4. Two-Step Charge Transfer

Zhang et al. synthesized the heterospin compound $CuCl_4$-bpyp (bpyp = 3,6-bis(4′-(4″-pyridyl)-1′-pyridinyl)pyridazine), which includes an organic radical and a 3d spin component.[107] Irradiation of $CuCl_4$-bpyp with light changed its magnetization value significantly, because electron transfer from the Cl^- ion to the bpyp moiety takes place upon exposure to light. An important characteristic is that the charge transfer occurs in a two-step rather than a one-step process, which makes it distinct from other systems.

3.5. Photoinduced High-Spin Clusters in Metal Complexes

3.5.1. Heptanuclear MoCu Complex

The heptanuclear complex $[Mo^{IV}(CN)_2(CNCu^{II}L)_6]^{8+}$ (L = tris(2-aminoethyl)amine) is a novel charge-transfer system (Figure 16a)[108] consisting of a diamagnetic Mo^{IV} center and six paramagnetic Cu^{II} cations. It has a charge-transfer band (Mo^{IV} to Cu^{II}) at around 440 nm. Irradiation at 10 K into the charge-transfer band causes a progressive increase in its magnetic susceptibility up to a $\chi_M T$ value of 4.8 $cm^3 mol^{-1} K$ (Figure 16b). This increase results from electron transfer from Mo^{IV} to Cu^{II} and trapping of the metastable state. The photoreaction can be expressed as $[Mo^{IV}(CN)_2(CNCu^{II}L)_6]^{8+} \rightarrow [Mo^{V}(CN)_2(CNCu^{I}L)(CNCu^{II}L)_5]^{8+}$. The generated paramagnetic Mo^V center interacts

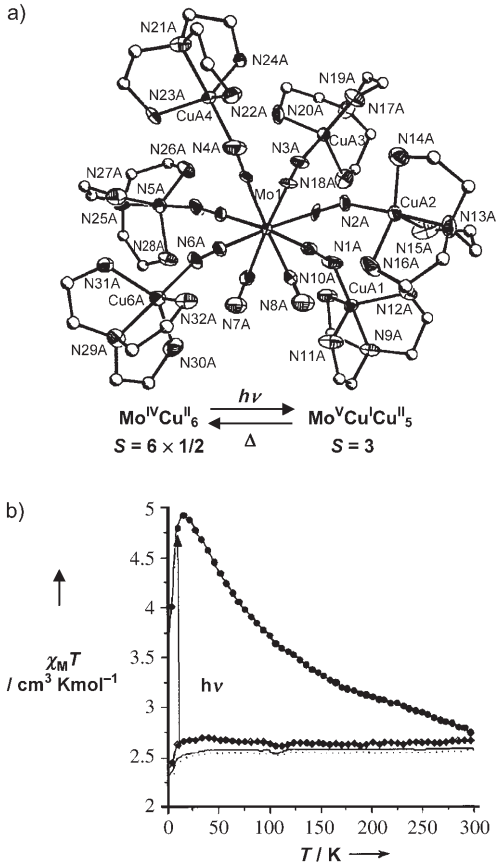

Figure 16. a) Structure of $[Mo(CN)_2\{(CN)CuL\}_6]^{8+}$.[108] b) Temperature dependence of $\chi_M T$: (•••••) before irradiation, (●) after irradiation, (◆) after irradiation and $T > 300$ K.[108] Reprinted from reference [108].

ferromagnetically with five Cu^{II} ions to form a high-spin cluster with $S = 3$. The metastable state could be trapped up to 300 K, which is quite a high temperature in comparison with those of the valence-tautomeric compounds described above. Furthermore, the photoinduced magnetization effect is thermally reversible. It has been suggested that significant local reorganization, such as a structural change between tetrahedral Cu^I and trigonal-bipyramidal Cu^{II}, might be responsible for the relatively high relaxation temperature.[108]

3.5.2. Nitroprusside

Sodium nitroprusside dihydrate ($Na_2[Fe(CN)_5(NO)]\cdot 2H_2O$) is known to be a photochromic molecule.[109–111] Irradiation of the charge-transfer band creates metastable states with different colors. It is believed that the photoirradiation induces structural changes in the Fe–NO bond, which can be trapped at low temperature.[111] If this molecule $[Fe(CN)_5(NO)]^{2-}$ were introduced into the framework of various Prussian blue analogues, their magnetic properties might be modulated. Indeed, changes in the magnetic properties induced by photoirradiation were observed in $Ni[Fe(CN)_5(NO)]\cdot 5.3H_2O$.[112,113] These changes were ascribed to modification of the magnetic coupling between the Ni^{II}(S=1) centers by the nitroprusside. The

increased magnetization value induced by the irradiation returned to its original value after thermal treatment, which indicates that this phenomenon is reversible.

4. Control of Magnetic Properties by Photolysis

4.1. High-Spin Molecules Created by Photolysis

The photomagnetic effects of organic radicals have been studied since the early stages of research into molecular magnetism. Itoh and Wassermann provided experimental evidence for the existence of an aromatic hydrocarbon with quintet spin multiplicity (Figure 17a, top).[114,115] The hydrocarbon involved was *m*-phenylene-bis-phenylmethylene,

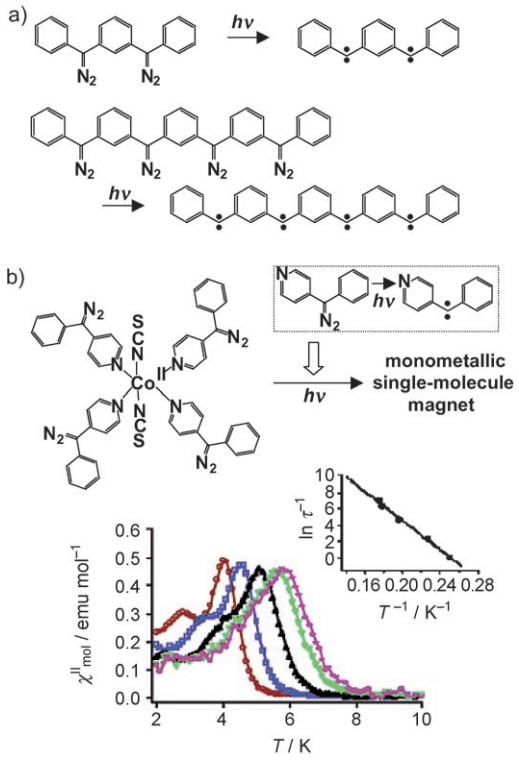

Figure 17. a) Production of high-spin molecules by photolysis.[114,115,122] b) Top: Structure of $[Co(SCN)_2\{4\text{-}(\alpha\text{-diazobenzyl})pyridine\}_4]$.[127] Bottom: Plots of χ'' versus T after irradiation of a 1:4 mixture (10 mM) of $Co(SCN)_2$ and 4-(α-diazobenzyl)pyridine in frozen methyltetrahydrofolate-EtOH with a 5-Oe ac field oscillating at 1000 (♦), 500 (▽), 100 (△), 10 (□), and 1 Hz (○). The inset is an Arrhenius plot.[127] Reprinted with permission from reference [127]. Copyright 2003, The American Chemical Society.

which was formed by the photolysis of 1,3-bis(α-diazobenzyl)benzene. Although this reaction is not reversible, it is a type of photomagnetic effect in the sense that the high-spin molecules are created by photoirradiation. Subsequently, pure organic radicals with large S values have been synthesized through photochemical processes.[116–121] For example, an aromatic hydrocarbon with eight parallel spins was created by photolysis as shown in Figure 17a (bottom).[122]

4.2. Single-Molecule Magnets Created by Photolysis

Heterospin molecule-based magnets have been prepared by combining an organic radical (in this case a carbene) with the 3d spins of a metal ion.[123–128] For example, one-dimensional ferri- and ferromagnetic chains,[124,128] a heterospin system with spin-glasslike behavior,[126] and a single-molecule magnet[127] were prepared by photolysis. Figure 17b shows the molecular structure of $[Co(SCN)_2\cdot\{4\text{-}(\alpha\text{-diazobenzyl})pyridine\}_4]$, in which the cobalt ion is coordinated by six nitrogen atoms from four pyridine rings and two SCN ions in a *trans* configuration. The magnetic properties of the Co complex in frozen solution after irradiation are shown in Figure 17b. It can be seen that the ac susceptibility shows frequency dependence. Furthermore, a hysteresis loop is observed at 2 K. These observations suggest that the Co complex prepared by photolysis is a single-molecule magnet.[127]

5. Changes in Magnetic Properties Accompanying Photochromic Reactions

5.1. Photochemical Generation of Organic Radicals

The reversible control of the magnetic properties of pure organic radicals has been reported.[129] In particular, some of the photochromic reactions involve the formation of radicals, which results in modification of their magnetic properties. Indeed, *trans-syn*-3,3′-diaryl-2,2′-biindenylidene-1,1′-diones exhibit photochromism between yellow and reddish-purple when exposed to sunlight. The reddish-purple crystals showed typical EPR signals for triplet biradicals in the solid state.[130] Xu et al. reported that (2,2′-bis-1*H*-indene)-1,1′-dione-3,3′-dihydroxy-3,3′-dipropyl exhibits photochromism by irradiation in the UV or with sunlight.[131] The biradicals created by irradiation have singlet ground states according to the spin-polarization rule. Furthermore, hexaarylbiimidazole (HABI) derivatives can be cleaved into a pair of triphenylimidazolyl (TPI) radicals by photoirradiation (Figure 18a).[132–134] These compounds also can be considered photomagnetic molecules.

The transformation of quinines into diradicals is another example of the photomagnetization of organic compounds. Irradiation of dibenzoannulated 3,5,3″,5″-tetra(*t*-butyl)-*p*-terphenoquinone with a Xenon lamp produces a diradical (Figure 18b). The change could be repeatedly observed.[135] Similar photochemical formation of diradicals was observed with dibenzo-*ortho*-terphenoquinone.[136]

5.2. Photocontrol of Magnetic Interactions between Organic Radicals

The reversible control of the magnetic interactions of pure organic radicals through a photochromic coupler has also been reported (Scheme 9). An example of this reaction involves an azobenzene derivative with the nitronylnitroxide radical 3,4′-bis(4,5-dihydro-4,4,5,5-tetramethyl-3-oxido-1-oxyl-3-imidazolyl-2-yl)azobenzene (Scheme 9a).[137] The azobenzene undergoes *cis–trans* photoisomerization, which leads

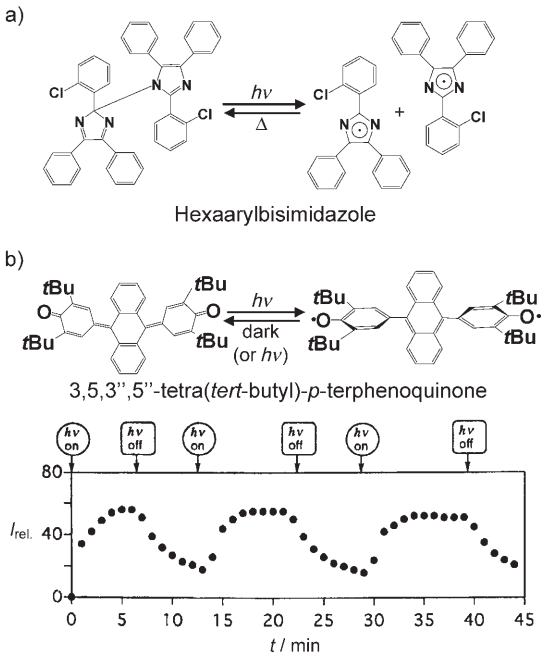

Figure 18. a) Photochemical generation of organic radicals,[132–135] and b) changes in ESR signal intensity.[135] Reprinted with permission from reference [135]. Copyright 1999, The Chemical Society of Japan.

to a change in the EPR signal. In another compound, diarylethene is used as the photoresponsive coupler instead of azobenzene.[138–144] This compound consists of two nitronylnitroxides connected by the diarylethene. Photoirradiation induces photoisomerization between the open and the closed forms. The isomerization switches the magnetic interaction between the radicals, as the closed form can mediate the antiferromagnetic interaction through the π-electron system. More recently, reversible photoswitching of an intramolecular magnetic interaction in diarylethenes with a 2,5-bis(arylethynyl)-4-methyl-3-thienyl side group was reported (Scheme 9b).[144]

Also interesting is the photoinduced self-assembly of radicals exhibited by a ferrocenyl-substituted Schiff base with a polychlorotriphenylmethyl radical (PTM) group (Scheme 9c). Upon *trans–cis* photoisomerization, a dimer structure of the PTM forms through hydrogen bonding. The magnetic interaction between the radicals in the dimer is antiferromagnetic. Hence, a phototransformation from a paramagnetic to a diamagnetic form is observed.[145]

Ito et al. recently reported that a delocalized spin created by chemical oxidation induces parallel spin alignment between two localized nitroxide groups in a *para*-phenylenediamine (pda) derivative (Scheme 10).[146]

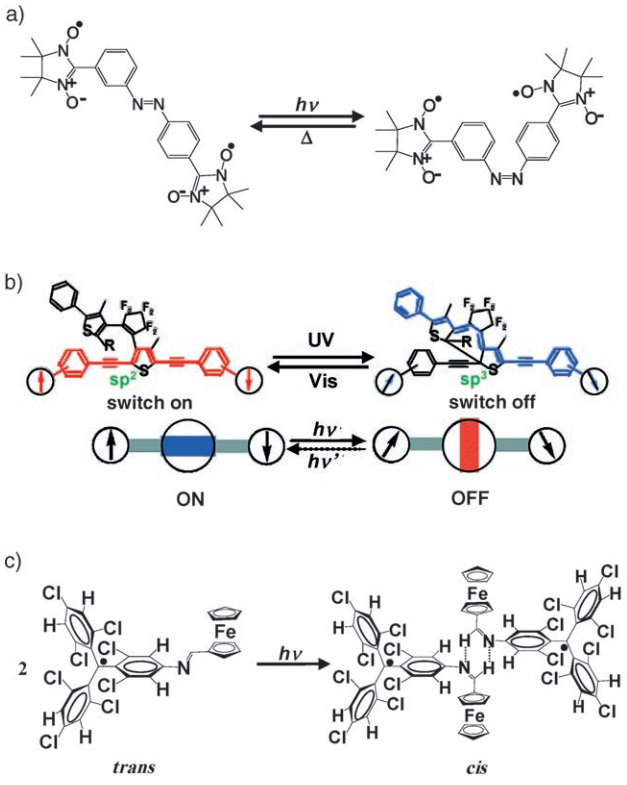

Scheme 9. Photoswitching of an intramolecular magnetic interaction. a) Photoinduced *trans–cis* isomerization of an azobenzene derivative with two nitronylnitroxide radical groups.[137] b) Photochromism of a diarylethene containing a 2,5-arylethynyl-3-thienyl unit.[144] Reprinted with permission from reference [144]. Copyright 2005, The American Chemical Society. c) Photoinduced self-assembly of the PTM radicals.[145]

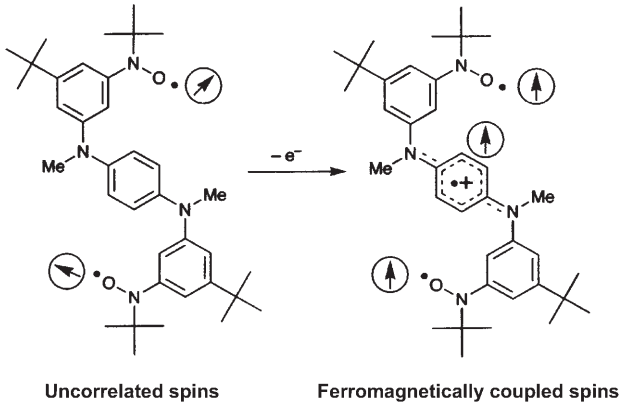

Scheme 10. Spin alignment mediated by an intervalence state in a pda derivative. Reprinted with permission from reference [146]. Copyright 2006, The American Chemical Society.

6. Fast Photoswitching of Spin Multiplicity

6.1. Spin Multiplicity in the Excited State

The fast photoswitching of spin multiplicity and magnetic interactions between organic radicals has been reported by several groups over the past ten years. It was reported that a transient interconversion between a doublet ($S=1/2$) and a quartet ($S=3/2$) state was observed when a fullerenemononitroxide radical and tetraphenylporphinatozinc(II) complex with a *p*-pyridylnitronylnitroxide ligand were excited by a pulsed laser in solution and in the solid state.[147,148] Also, an excited quintet state ($S=2$) was detected when a fullerene

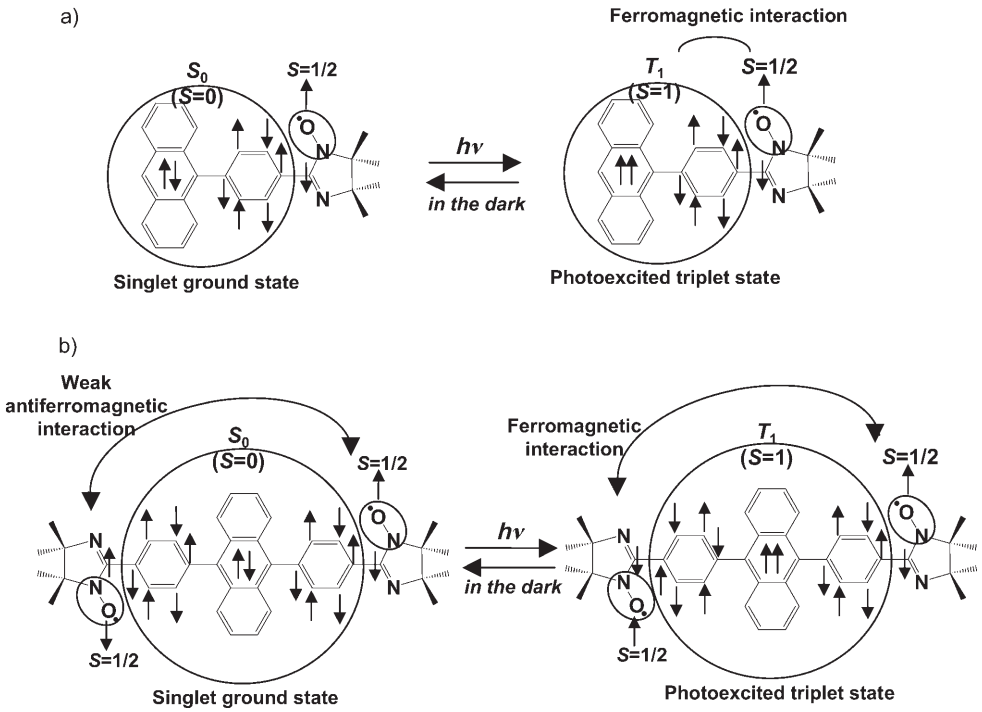

Scheme 11. a) Spin alignment in the doublet ground state and the quartet excited state. In the ground state, the radical spin couples with the closed-shell singlet state of the phenylanthracene moiety. In the photoexcited state, the radical spins couple ferromagnetically with the triplet excited state of the phenylanthracene moiety by spin polarization through π conjugation.[150,151,154] b) Spin alignment through the molecular field of the triplet excited state. In the ground state, the spin-polarization mechanism is dominant and leads to antiferromagnetic coupling between the two radical groups, as the diphenylanthracene spin coupler is a closed shell. In the photoexcited state, the spin-delocalization mechanism overcomes the spin-polarization effect in the anthracene moiety, as the spin coupler becomes an open-shell triplet excited state, which leads to ferromagnetic coupling between the two radical groups in the photoexcited state.[150,151,154]

coordinated by two nitronylnitroxide groups was excited by a pulsed laser;[149] the photoexcited triplet ($S=1$) fullerene interacted ferromagnetically with the two nitroxide ($S=1/2$) radicals to form the quintet state ($S=2$).

In the compounds described above, the nitroxide radical is linked to the fullerene or the tetraphenylporphinatozinc(II) complex through a σ bond. In contrast, the photoswitching of spin multiplicity in purely organic π-conjugated spin systems has recently been reported. For example, Teki et al. studied the photoirradiation effects of π-conjugated compounds with phenylanthracene derivatives as the spin coupler and iminonitroxide radicals as the terminal spin components (Scheme 11).[150,151] The phenylanthracene moiety is a suitable photocoupler, which enables ferro- and antiferromagnetic exchange with the iminonitroxide radicals. Scheme 11 shows the compounds 9-[4-(4,4,5,5-tetramethyl-1-yloxyimidazolin-2-yl)phenyl]anthracene and 9,10-bis[4-(4,4,5,5-tetramethyl-1-yloxyimidazolin-2-yl)phenyl]anthracene, in which a ferromagnetic interaction operates between the radical centers and the photoexcited triplet state in the phenylanthracene derivative. Hence, these compounds exist in the excited state as a quartet ($S=3/2$) and a quintet ($S=2$), respectively.

6.2. Spin Polarization in the Excited State

It is well known that spin polarization effects that depend on the topology of the π-electron system play an important role in the spin alignment of the ground state.[152] To clarify the spin polarization effect in the excited state, Teki et al. investigated photoexcited states with different π topologies.[150,153,154] Scheme 12a shows the lowest excited states of two phenylanthracene derivatives with an iminonitroxide as the terminal radical group. As described above, compound a1 exists in a quartet excited state owing to ferromagnetic coupling, whereas compound a2 is in a doublet excited state because of antiferromagnetic coupling. Scheme 12b shows the lowest excited states of three phenylanthracene derivatives with two iminonitroxide radical groups. Compound b1 shows ferromagnetic coupling to give a quintet excited state, whereas compound b2 has a singlet excited state as a result of antiferromagnetic coupling between the

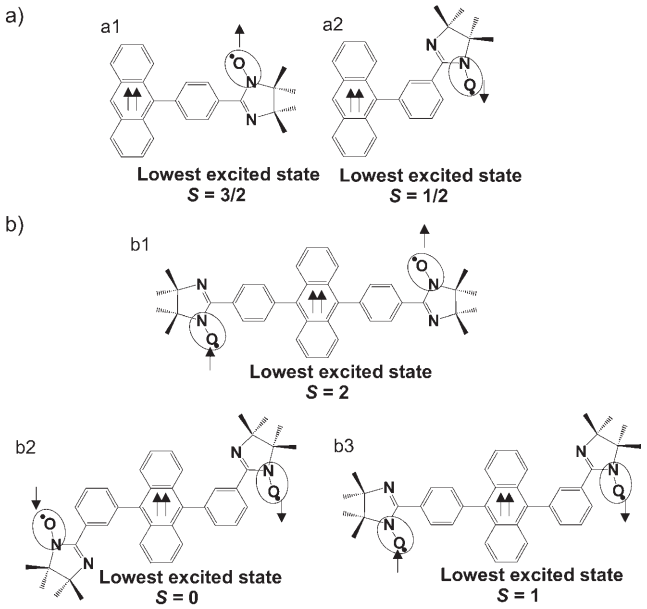

Scheme 12. Spin alignment of the photoexcited state.[150,151,153,154]

spin of the terminal radical and the triplet excited state of the anthracene moiety. Compound b3 gives a triplet excited state as a result of both antiferromagnetic and ferromagnetic coupling. These results clearly show that the sign of the intramolecular exchange interaction and the spin multiplicity of the lowest photoexcited spin state change drastically depending on the topological nature of the π-electron network. In other words, it was found that π-topology also plays an important role in determining the spin alignment of the excited state. These studies on spin alignments provide important information and could lead to new strategies for the development of phototunable spin systems.

7. Magnetic Bistability with Large Hysteresis in Molecular Materials

Some organic radicals undergo phase transitions that are accompanied by lattice dimerization.[155–157] Among them, compounds that show phase transitions involving hysteresis loops have attracted great attention because of their possible application to molecular switches and memory. Indeed, it is reported that some organic radicals exhibit large hysteresis as a result of dimerization of the radicals (Scheme 13).[158–164]

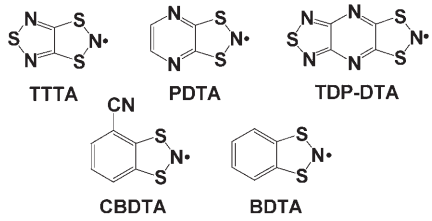

Scheme 13. Molecular structures of TTTA, PDTA, TDP-DTA, CBDTA, and BDTA.

7.1. Magnetic Bistability in Organic Radicals

The organic radical 1,3,5-trithia-2,4,6-triazapentalenyl (TTTA) shows a first-order phase transition with large hysteresis at around room temperature (Figure 19).[158] The high-temperature phase is paramagnetic and the low-temperature phase is diamagnetic. The hysteresis width is as large as 75 K ($T_C\downarrow = 230$ K, $T_c\uparrow = 305$ K). The magnetization changes as a result of dimerization of the organic radicals. The phase interconversion involves the cooperative breaking and making of strong intermolecular S···N′ interactions and a domino-like rotation of molecules within the π-stacked structure, which plays an important role in the induction of large hysteresis.[159] Brusso et al. call this the "domino mechanism".[159] Furthermore, illumination of the radical with a nanosecond pulsed laser within the hysteresis loop induced a phase transition from the diamagnetic to the paramagnetic state.[165,166]

The molecular radical 1,3,2-dithiazolo[4,5-*b*]pyrazin-2-yl (PDTA) also exhibits magnetic bistability just above room

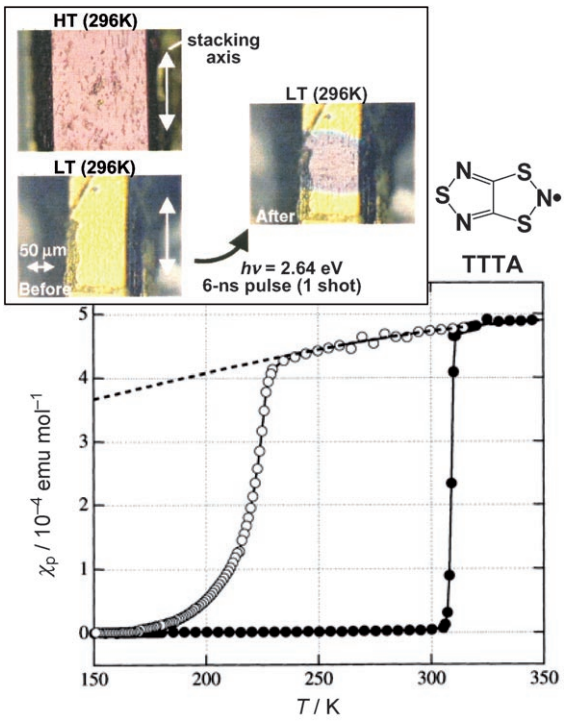

Figure 19. Temperature dependence of the paramagnetic susceptibility χ_p of a polycrystalline sample of TTTA upon cooling (○) and heating (●). Reprinted with permission from reference [158]. Copyright 1999, American Association for the Advancement of Science. Inset: Color change induced by photoirradiation. Reprinted with permission from reference [165]. Copyright 2002, The American Physical Society.

temperature.[159,160] The phase transition temperatures in cooling and warming modes are $T_c\downarrow = 297$ K and $T_c\uparrow = 343$ K, respectively (Figure 20). The diamagnetic low-temperature phase with superimposed stacks of π dimers transformed into the high-temperature phase, which comprises slipped stacks of π radicals ($S = 1/2$). It is thought that the domino mechanism can also be applied in this system.[159]

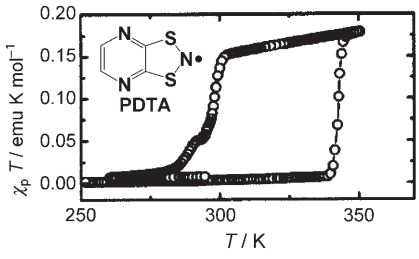

Figure 20. Plot of χ_pT as a function of T for PDTA.[159,160] Reprinted with permission from reference [159]. Copyright 2004, The American Chemical Society.

Another example is the heterocyclic radical 1,2,5-thiadiazolo[3,4-*b*]-1,3,2-dithiazolo[3,4-*b*]pyrazin-2-yl (TDP-DTA),[161] which has a phase transition involving hysteresis

at around 150 K. At high temperature, the structure consists of ribbons of TDP-DTA radicals packed into a slipped π-stack arrangement. Upon cooling, alternate layers of ribbons are shifted laterally to produce arrays of dimers. A multiple tectonic plate slippage is proposed as the mechanism for the phase transition.[161]

More recently, a two-step phase transition in the cyano-functionalized benzodithiazolyl radical (CBDTA) was reported.[162] Upon cooling, CBDTA undergoes a structural change from a paramagnetic regular π stack of radicals into a diamagnetic distorted π stack. No hysteresis was observed. Further cooling causes a change from diamagnetic to paramagnetic behavior below 50 K. This transition exhibits a thermal hysteresis of 13 K. The transition temperatures are $T_c\downarrow = 39$ K and $T_c\uparrow = 26$ K.

7.2. Magnetic Bistability in Ion-Pair Complexes

Some ion-pair complexes that contain $[Ni(mnt)_2]$ also show phase transitions. These include $[RBnPy][Ni(mnt)_2]$ ($[RBnPy]^+ = 1$-(4′-R-benzyl)pyridinium; R = F, Br, Cl, and NO_2),[167,168] $[R'BnPyNH_2][Ni(mnt)_2]$ ($[R'BnPyNH_2]^+ = 1$-(4′-R′-benzyl)-4-aminopyridinium; R′ = Cl and CN),[169,170] and $[H_2dabco][Ni(mnt)_2]_2$ ($[H_2dabco]^{2+}$ = diprotonated 1,4-diazabicyclo[2.2.2]octane).[171] Among them, the complex $[H_2dabco][Ni(mnt)_2]_2$ exhibits a hysteresis loop.[171] The $[H_2dabco][Ni(mnt)_2]_2$ complex has two different structures, an α and a β phase. Both show bistability in their magnetic properties. The transition occurs at around 120 K for the α phase and at 112 K for the β phase. Their hysteresis widths are 1 K and 10 K, respectively. The magnetic behavior above the transition temperature can be interpreted as a singlet–triplet model of an antiferromagnetically coupled ($S = 1/2$) dimer.

7.3. Magnetic, Optical, and Electronic Bistability in a Neutral Spirobiphenalenyl Radical

The conductivities of the bistable molecular compounds mentioned above are generally low. In contrast, a recently reported organic semiconductor containing a neutral spirobiphenalenyl radical shows high conductivity.[172,173] This compound exhibits a phase transition with hysteresis just above room temperature (Figure 21). Interestingly, the unpaired electrons are located in the exterior phenalenyl units of the dimer in the high-temperature phase, whereas the electrons migrate to the interior phenalenyl units and form spin pairs as π dimers in the low-temperature phase. The magnetic properties change from paramagnetic to diamagnetic with the transition from the high- to the low-temperature phase. The conductivity increases by two orders of magnitude in the diamagnetic state, and the IR transmission changes with the phase transition. Thus, this compound is a multifunctional system in which three physical properties, namely, the magnetic, conducting, and optical behavior, change simultaneously with the phase transition.

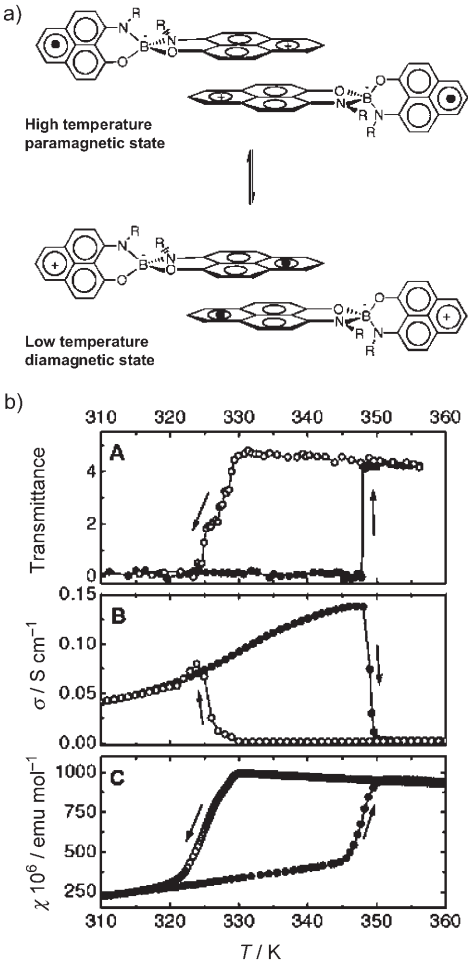

Figure 21. a) Interconversion between the diamagnetic π dimer (low-temperature form) and the paramagnetic π dimer (high-temperature form) of a biphenalenyl radical ($R = C_2H_5$).[172] b) Bistability in IR transmittance at 3.85 μm (A), conductivity (B), and magnetic susceptibility (C) arising from the hysteretic phase transition of a biphenalenyl radical ($R = C_4H_9$). Reprinted with permission from reference [172]. Copyright 2002, American Association for the Advancement of Science.

8. Molecular Magnets

Switchable magnetic properties have been reported in many CN-bridged molecular systems (Table 2). Prussian blue analogues are an important example. Prussian blue ($[Fe^{III}_4\{Fe^{II}(CN)_6\}_3]$) is well known as a pigment and has attracted renewed attention since the middle of the 1980s because of its electrochromic properties. More recently it has attracted attention as a basis for molecule-based magnets.

The magnetic properties of these compounds have been studied since the 1950s,[174,175] but more extensively over the last 15 years. In particular, CrV analogues of Prussian blue have high T_c values, for example, $T_c = 376$ K for $KV^{II}[Cr^{III}(CN)_6]$[176] and $T_c = 375$ K for $K_{0.058}V^{II/III}[Cr^{III}(CN)_6](SO_4)_{0.058}\cdot 0.93\,H_2O$.[177] The discovery of the high-T_c magnets has stimulated studies of the magnetic properties of Prussian blue analogues. It was also found that the magnetic properties in some Prussian blue analogues are switchable.[15,21–23]

Table 2: Selected compounds that exhibit photoinduced magnetization.

Compound	T_c(B) [K][a]	T_c(A) [K][b]	Ref.
$K_{0.4}[Co_{1.3}Fe(CN)_6]\cdot 4.5\,H_2O$	N	26	[21,178]
$Rb_{0.91}[Mn_{1.05}Fe(CN)_6]\cdot 0.6\,H_2O$	12	N	[196]
$[Fe^{II\text{-}HS}{}_{1.5}Cr^{III}(CN)_6]$	21	21	[220]
$Cs[Co^{II}(3\text{-cyanopyridine})_2W^{V}(CN)_8]\cdot H_2O$	N	30	[205]
$[Cu^{I}Cu^{II}Mo^{V}(CN)_8]\cdot 8\,H_2O$	N	25	[210]
$Cs^{I}_2[Cu^{II}{}_7\{Mo^{IV}(CN)_8\}_4]\cdot 6\,H_2O$	N	23	[211]
$[\{Co^{II}(pmd)(H_2O)\}_2\{Co^{II}(H_2O)_2\}\{W^{V}(CN)_8\}_2(pmd)_2]\cdot 2\,H_2O$	N	40	[212]
$[Mn(tcne)_x]\cdot y\,CH_2Cl_2$	75	75	[225]
$[Mn(tEtopp)(tcne)]$[c]	25	25	[228]
$[Nd(dmf)_4(H_2O)_3(\mu\text{-}CN)Fe(CN)_5]\cdot H_2O$	N	N	[230]
$Ni[Fe(CN)_5NO]\cdot 5.3\,H_2O$[d]	N	N	[112,113]
$[Mo^{IV}(CN)_2\{(CN)Cu^{II}L\}_6](ClO_4)_8$[d]	N	N	[108]

[a] T_c(B) = Magnetic phase transition temperature before irradiation. [b] T_c(A) = Magnetic phase transition temperature after irradiation. N = None (lower than 5 K). [c] Photoinduced spin flop. [d] Photoinduced high-spin cluster.

8.1. Photoinduced Magnetization and Hysteresis in Prussian Blue Analogues

8.1.1. FeCo Prussian Blue

The first example of photomagnetism was reported for FeCo Prussian blue.[21,22,92,178–187] FeCo Prussian blue exhibits thermally induced metal-to-metal charge transfer between the Fe and Co ions (Figure 22),[92,182,188,189] which can be expressed as $\{Fe^{III}(t_{2g}{}^5e_g{}^0)\text{-}CN\text{-}Co^{II\text{-}HS}(t_{2g}{}^5e_g{}^2)\}\rightleftharpoons\{Fe^{II}(t_{2g}{}^6e_g{}^0)\text{-}CN\text{-}Co^{III\text{-}LS}(t_{2g}{}^6e_g{}^0)\}$. The transition temperature depends on the composition, and, in general, increases with decreasing Co/Fe ratio. For example, the transition temperatures of $Na_{0.60}[Co_{1.26}Fe(CN)_6]\cdot 3.9\,H_2O$, $Na_{0.53}[Co_{1.32}Fe(CN)_6]\cdot 4.4\,H_2O$, and $Na_{0.37}[Co_{1.37}Fe(CN)_6]\cdot 4.8\,H_2O$ are $T_c\uparrow = 300$ K and $T_c\downarrow = 260$ K, $T_c\uparrow = 270$ K and $T_c\downarrow = 230$ K, $T_c\uparrow = 220$ K and $T_c\downarrow = 180$ K, respectively.[92] It has recently been reported that only the Co ions surrounding the interstitial Cs ion are involved in the electron transfer in $Cs_{0.7}[Co_4\{Fe(CN)_6\}_{2.9}\square_{1.1}]\cdot 16\,H_2O$ ($\square$ represents the vacancy of the $\{Fe(CN)_6\}$ site), which suggests that the presence of the alkali ion is required for the electron transfer.[190] Furthermore, the smaller the Co/Fe ratio, the stronger the ligand field of the Co ions, which can explain the shift in the phase-transition temperature.[22] Pressure-induced electron transfer was recently reported in the related compound $K_{0.1}[Co_4\{Fe(CN)_6\}_{2.7}]\cdot 18\,H_2O$.[191]

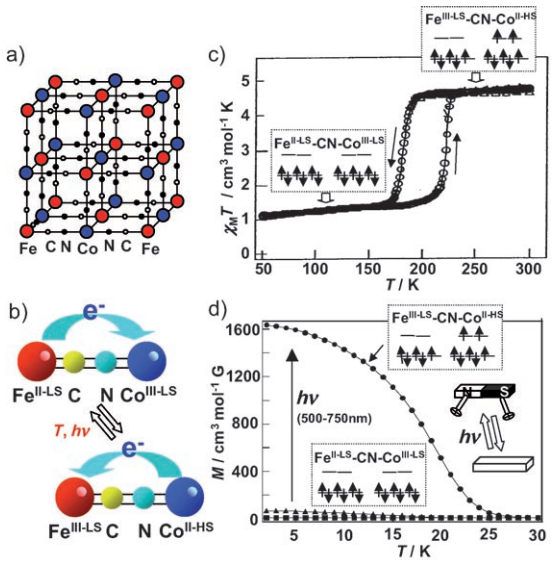

Figure 22. a) Structure of a FeCo Prussian blue analogue.[21] b) Thermal and photoinduced metal-to-metal charge transfer. c) Plot of $\chi_M T$ as a function of T.[189] d) Photoinduced magnetization.[21,93,178]

By exciting FeCo Prussian blue in the charge-transfer band of the transition from Fe^{II} to $Co^{III\text{-}LS}$, the metastable Fe^{III}-CN-$Co^{II\text{-}HS}$ state could be trapped at 5 K for several days. Figure 22 shows the field-cooled magnetization before and after irradiation of the $K_{0.4}[Co_{1.3}Fe(CN)_6]\cdot 4.5\,H_2O$.[21,178] The photoprocess can be expressed as $K_{0.4}[Co^{II\text{-}HS}{}_{1.3}Fe^{III}(CN)_6]\cdot 4.5\,H_2O \rightleftharpoons K_{0.4}[Co^{II\text{-}HS}{}_{0.3}\text{-}Co^{III\text{-}LS}Fe^{II}(CN)_6]\cdot 4.5\,H_2O$. The metastable state shows ferrimagnetic properties and a transition temperature of 26 K. Pejakovic showed that it exhibits spin-glasslike behavior.[192,193]

Metal-to-metal charge transfer is an entropy-driven process. As in the case of Co valence-tautomeric compounds, the spin multiplicity of the high-temperature phase with $Fe^{III}(t_{2g}{}^5e_g{}^0)$-CN-$Co^{II\text{-}HS}(t_{2g}{}^5e_g{}^2)$ structure (= $Fe^{III}Co^{II\text{-}HS}$ structure) is larger than that of the $Fe^{II}(t_{2g}{}^6e_g{}^0)$-CN-$Co^{III\text{-}LS}(t_{2g}{}^6e_g{}^0)$ structure (= $Fe^{II}Co^{III\text{-}LS}$ structure), that is, $\Delta S_{el} = S_{el}(Fe^{III}Co^{II\text{-}HS}) - S_{el}(Fe^{II}Co^{III\text{-}LS}) > 0$. Furthermore, the ligand–cobalt bond is longer in the high-temperature phase than in the low-temperature phase, which means that $\Delta S_{vib} = S_{vib}(Fe^{III}Co^{II\text{-}HS}) - S_{vib}(Fe^{II}Co^{III\text{-}LS})$ is positive. Hence, when the quantum-mechanical energy of the $Fe^{II}Co^{III\text{-}LS}$ state is slightly lower than the quantum-mechanical energy of the $Fe^{III}Co^{II\text{-}HS}$ state, a phase transition involving Fe-to-Co charge transfer can be observed upon warming, as, above a certain temperature, $Fe^{III}Co^{II\text{-}HS}$ should be the thermodynamically stable state. This is because the entropy of the $Fe^{III}Co^{II\text{-}HS}$ state is much larger than that of the $Fe^{II}Co^{III\text{-}LS}$ state ($\Delta S > 0$), and the entropy gain $T\Delta S$ compensates the energy loss.

8.1.2. FeMn Prussian Blue

FeMn Prussian blue exhibits a thermally induced phase transition (Figure 23).[194–200] The compound $Rb_x[Mn\{Fe(CN)_6\}_{(x+2)/3}]\cdot z\,H_2O$ ($x = 0.73$) shows a phase transition with a large thermal hysteresis loop with a width of 116 K ($T_{1/2}\downarrow = 147$ K, $T_{1/2}\uparrow = 263$ K) caused by the charge transfer from Mn^{II} to Fe^{III} and Jahn–Teller distortion of the Mn^{III} center produced.[198] The charge transfer can be expressed as $Fe^{III\text{-}LS}(t_{2g}{}^5e_g{}^0,\ S = 1/2)$-CN-$Mn^{II\text{-}HS}(t_{2g}{}^3e_g{}^2,\ S = 5/2) \rightleftharpoons Fe^{II}(b_{2g}{}^2e_g{}^4,\ S = 0)$-CN-$Mn^{III}(e_g{}^2b_{2g}{}^1a_{1g}{}^1,\ S = 2)$.[197] The compound $Rb_{0.98}[Mn_{1.01}Fe(CN)_6]\cdot 0.2\,H_2O$ also exhibits room-

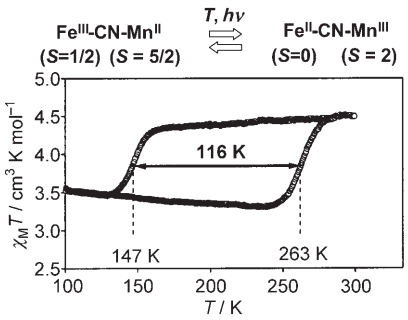

Figure 23. Plot of $\chi_M T$ as a function of T of a FeMn Prussian blue analogue.[196,198,201] Reprinted with permission from reference [198]. Copyright 2005, The American Chemical Society.

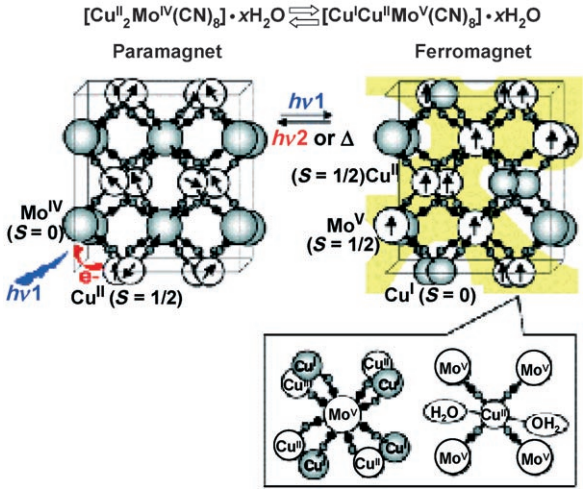

Figure 24. Photoinduced magnetic spin coupling in the solid state. The yellow shadow shows a possible route for the ferromagnetic spin alignment. The schematic structure is based on the crystal structure of $[Mn^{II}_2Mo^{IV}(CN)_8]\cdot 8H_2O$. The large circles are Mo ions, the medium-sized circles are Cu ions, the small black circles are carbon atoms, and the small gray circles are nitrogen atoms. Reprinted with permission from reference [210]. Copyright 2006, The American Chemical Society.

temperature hysteresis. When it is excited with light at 532 nm in the hysteresis loop at room temperature, a photoinduced phase transition from $Fe^{II}(b_{2g}{}^2e_g{}^4$, S = 0)-CN-$Mn^{III}(e_g{}^2b_{2g}{}^1a_{1g}{}^1$, S = 2) to $Fe^{III\text{-}LS}(t_{2g}{}^5e_g{}^0$, S = 1/2)-CN-$Mn^{II\text{-}HS}(t_{2g}{}^3e_g{}^2$, S = 5/2) is induced.[201] At low temperature it can be demagnetized by a single laser pulse.[196] Morgadonna et al. recently reported that the same charge transfer could be induced by X-ray irradiation.[202]

8.2. Photoinduced Magnetization and Hysteresis in Octacyanide Systems

Octacyanides are attracting increasing attention for the development of molecular magnets.[203] Some octacyanide-based magnets show phase transitions and photomagnetic properties. One example of these is the complex $Cs[\{Co^{II}$(3-cyanopyridine)$_2\}\{W^V(CN)_8\}]\cdot H_2O$,[204,205] which exhibits thermally induced charge transfer, $Cs[\{Co^{II}$(3-cyanopyridine)$_2\}\{W^V(CN)_8\}]\cdot H_2O \rightleftharpoons Cs[\{Co^{III}$(3-cyanopyridine)$_2\}\{W^{IV}(CN)_8\}]\cdot H_2O$, with a hysteresis width of 49 K. Excitation of the W^{IV}-to-Co^{III} charge-transfer band at around 800 nm leads to a metastable ferromagnetic state $Cs[\{Co^{II}$(3-cyanopyridine)$_2\}\{W^V(CN)_8\}]\cdot H_2O$ with $T_c = 30$ K. As in the case of the Co valence-tautomeric compounds, large changes in the ligand–metal bond lengths arising from the spin-crossover of the Co ions play an important role in the phase changes and the photomagnetism.

The complex $[Cu^{II}_2Mo^{IV}(CN)_8]\cdot 8H_2O$ also exhibits photomagnetic properties.[206–210] Figure 24 shows the photoinduced charge transfer from Mo^{IV} to Cu^{II} to form the metastable state $[Cu^ICu^{II}Mo^V(CN)_8]\cdot 8H_2O$, which is ferromagnetic with $T_c =$ 25 K. The related compound $Cs^I_2[Cu^{II}_7\{Mo^{IV}(CN)_8\}_4]\cdot 6H_2O$ also shows photoinduced charge transfer between Mo^{IV} and Cu^{II}.[211] The change can be expressed as $Cs^I_2[Cu^{II}_7\{Mo^{IV}(CN)_8\}_4]\cdot 6H_2O \rightleftharpoons Cs^I_2[Cu^I_4Cu^{II}_3\{Mo^V(CN)_8\}_4]\cdot 6H_2O$, and the T_c after irradiation is 23 K (Figure 25a).

Ohkoshi et al. observed photomagnetic effects in $[\{Co^{II}$(pmd)$(H_2O)\}_2\{Co^{II}(H_2O)_2\}\{W^V(CN)_8\}_2(pmd)_2]\cdot 2H_2O$ (pmd = pyrimidine). The critical temperature after irradiation ($\lambda =$ 840 nm) is 40 K. The photoprocess is expressed as $\{Co^{II\text{-}HS}$-$(S{=}3/2)\}\{Co^{III\text{-}LS}(S{=}0)\}_2$-NC-$\{W^{IV}(S{=}0)\}_2 \rightleftharpoons \{Co^{II\text{-}HS}(S{=}3/2)\}_3$-NC-$\{W^V(S{=}1/2)\}_2$ (Figure 25b).[212]

8.3. Electrochemical Control of the Magnetic Properties of Prussian Blue Analogues

The magnetic properties of Prussian blue analogues can be electrochemically controlled on the basis of their zeolitic properties. Prussian blue is an electrochromic compound,[213] and, in particular, FeFe Prussian blue ($[Fe^{III}_4\{Fe^{II}(CN)_6\}_3]\cdot 6H_2O$) exhibits reversible oxidation and reduction [Eqs. (1) and (2)].

$$[Fe^{III}_4\{Fe^{II}(CN)_6\}_3] + 4K^+ + 4e^- \rightleftharpoons K_4[Fe^{II}_4\{Fe^{II}(CN)_6\}_3] \quad (1)$$

$$[Fe^{III}_4\{Fe^{II}(CN)_6\}_3] + 3Cl^- - 3e^- \rightleftharpoons [Fe^{III}_4\{Fe^{III}(CN)_6\}_3](Cl)_3 \quad (2)$$

The redox reaction involves the uptake and release of ions. Also, the change in the oxidation state involves a distinct color change, and this aspect has been thoroughly studied. Changes in the oxidation state involve changes also in other physical properties, and in particular the magnetic properties can be modified by electrochemical redox reactions. Indeed, the critical temperature of Prussian blue successively increases with oxidation, because diamagnetic Fe^{II} changes to paramagnetic Fe^{III}, through which the magnetic interaction is enhanced.[51] Similarly, the critical temperature decreases upon reduction, which changes the magnetic properties from ferromagnetic to paramagnetic.

Similar ferromagnetic-to-paramagnetic interconversion has been observed in NiFe Prussian blue analogues, and a shift in the critical temperature at around room temperature was observed in CrCr analogues (Figure 26).[214,215] By combining electrochemical methods with the photomagnetic behavior, three-state switching can be realized.[178] In FeCo Prussian blue, these three states are Fe^{II}-CN-$Co^{II\text{-}HS}$, Fe^{III}-CN-$Co^{II\text{-}HS}$, and Fe^{II}-CN-$Co^{III\text{-}LS}$.[178]

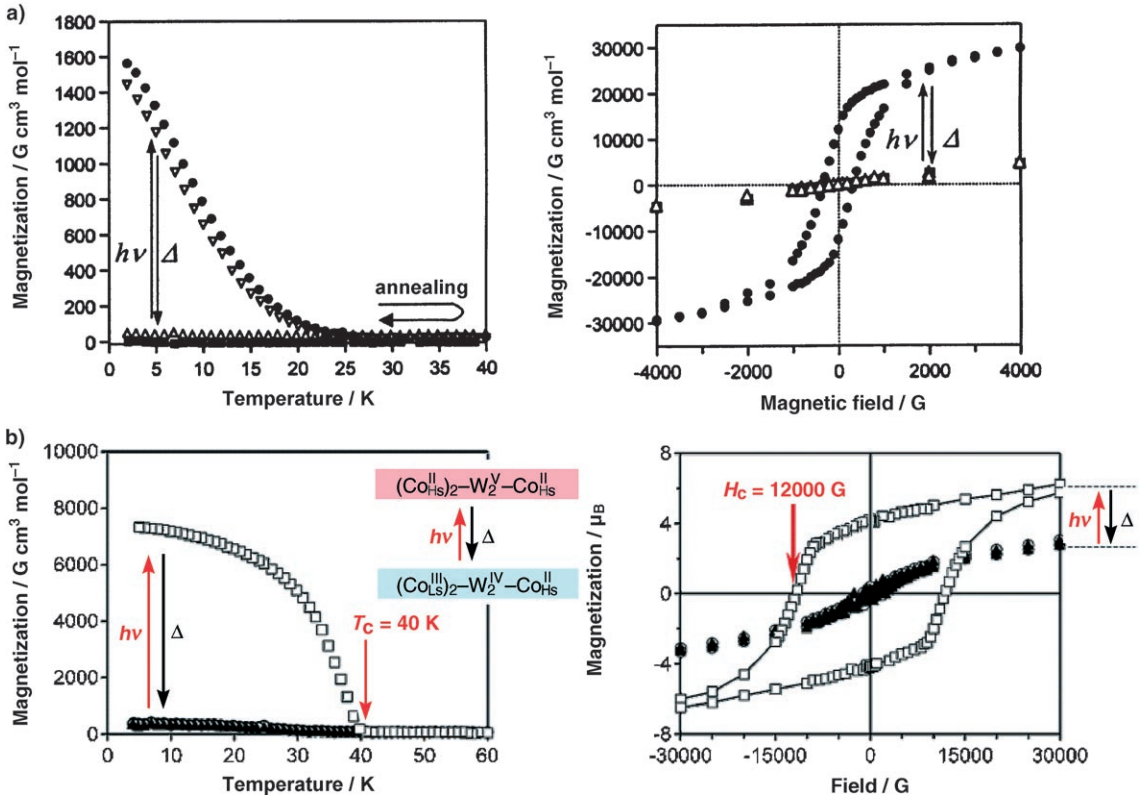

Figure 25. a) Left: Magnetization versus *T* curves for $Cs^{I}_{2}[Cu^{II}_{7}\{Mo^{IV}(CN)_8\}_4]\cdot 6H_2O$ in a magnetic field of 10 G before irradiation (■), after irradiation (●), and after thermal treatment at 200 K (△), as well as remanent magnetiztaion after irradiation (▽); right: magnetic hysteresis loops at 2 K before irradiation (■), and after irradiation (●), and after thermal treatment at 200 K (△). Reprinted with permission from reference [211]. Copyright 2005, The American Chemical Society. b) Field-cooled magnetization curves at 10 G (left) and magnetic hysteresis loops at 2 K (right) for $[\{Co(pmd)(H_2O)\}_2\{Co(H_2O)_2\}\{W(CN)_8\}_2(pmd)_2]\cdot 2H_2O$ before irradiation (▲), after irradiation (□), and after thermal treatment at 150 K (○). Reprinted with permission from reference [212]. Copyright 2006, The American Chemical Society.

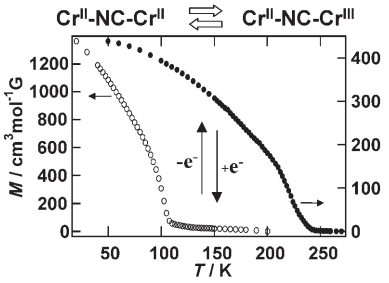

Figure 26. Electrochemical control of the magnetic properties of a CrCr analogue of Prussian blue. ○: Cr^{II}-NC-Cr^{II} state; ●: Cr^{II}-NC-Cr^{III} state. Reprinted with permission from reference [214]. Copyright 1996, American Association for the Advancement of Science.

8.4. Chemical Control of the Magnetic Properties of Prussian Blue Analogues

Chemical control of the magnetic properties has also been reported. For example, solvent exchange causes reversible variations in color for $[Co^{II}_{1.5}Cr^{III}(CN)_6]\cdot 7.5H_2O$,[216] because the coordination geometry of the Co^{II} ions changes as a result of adsorption and desorption of water ligands. These changes also induce a shift in the critical temperature from 25 to 18 K. Also, the mixed compound $[(Co^{II}_{0.41}Mn^{II}_{0.59})\{Cr^{III}(CN)_6\}_{2/3}]\cdot z H_2O$ exhibits humidity-induced changes in its magnetic behavior (Figure 27).[217] Cation-exchange-induced phase transitions were also observed in FeCo analogues.[188] In all these phenomena, the zeolitic properties play an important role.

8.5. Pressure Dependence of the Magnetic Properties of Prussian Blue Analogues

The CrFe analogue $K_{0.4}[Fe_4\{Cr(CN)_6\}_{2.8}]\square_{1.2}\cdot 16H_2O$ (□ = number of $\{Cr(CN)_6\}^{3-}$ vacancies) exhibits pressure-induced linkage isomerization of the cyanide ligand,[218] which rotates by 180° (Figure 28a), whereupon the Fe^{II} changes from a high- to a low-spin form. As a result, the value of T_c changes from 19 K at ambient pressure to 13 K at 1200 MPa.

8.6. Spin Crossover in CrFe Prussian Blue

Thermally induced spin crossover of the form $Fe^{II\text{-}HS} \rightleftharpoons Fe^{II\text{-}LS}$ has been observed in the CrFe analogue $Cs^{I}[\{Fe^{II\text{-}HS}\text{-}Cr^{III}(CN)_6\}_{0.94}\{Fe^{II\text{-}LS}Cr^{III}(NC)_6\}_{0.06}]\cdot 1.3H_2O$.[219] The transition

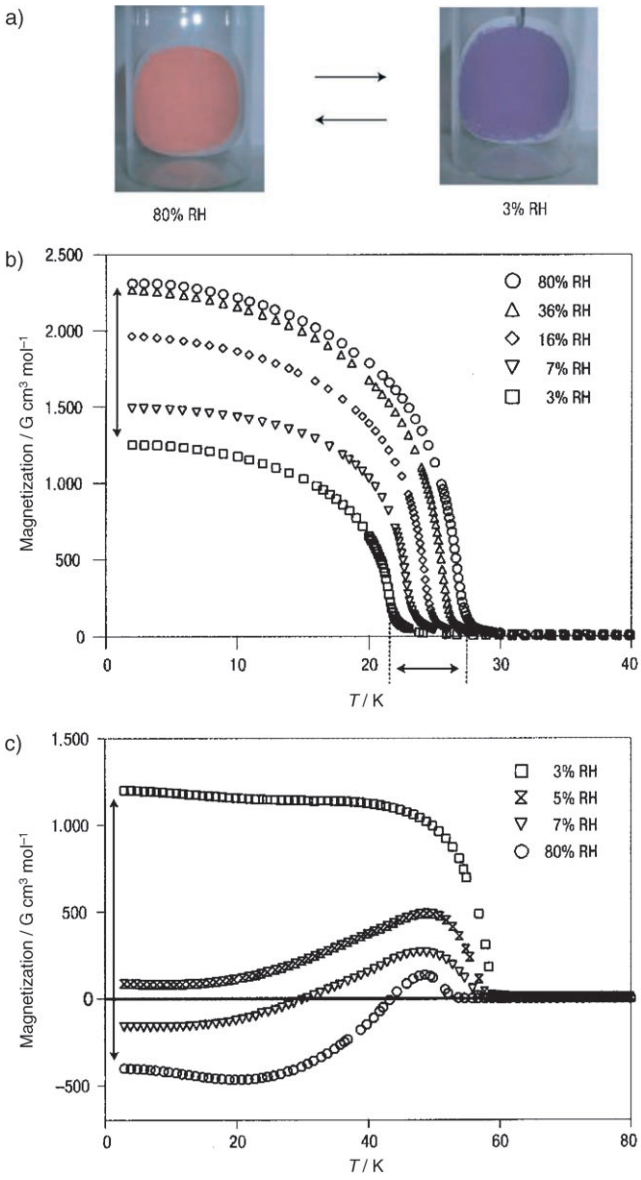

Figure 27. a) Photographs of the material $[(Co^{II}_{x}Mn^{II}_{1-x})\{Cr^{III}(CN)_6\}_{2/3}]\cdot z\,H_2O$ with $x=1$ at 80% RH and 3% RH (RH = relative humidity).[217] b) Magnetization versus T curves of the material with $x=1$ at 3, 7, 16, 36, and 80% RH ($H_0=10$ Oe). c) Magnetization versus T curves of the material with $x=0.41$ at 3, 5, 7, and 80% RH ($H_0=10$ Oe). Reprinted with permission from reference [217]. Copyright 2004, Nature.

temperatures are 211 K ($T_{1/2}\downarrow$) and 238 K ($T_{1/2}\uparrow$) (Figure 28b). The spin transition can be expressed as $Cs^{I}[\{Fe^{II\text{-}HS}Cr^{III}(CN)_6\}_{0.94}\{Fe^{II\text{-}LS}Cr^{III}(NC)_6\}_{0.06}]\cdot 1.3\,H_2O \rightleftharpoons Cs^{I}[\{Fe^{II\text{-}HS}_{0.12}Fe^{II\text{-}LS}_{0.88}Cr^{III}(CN)_6\}_{0.94}\{Fe^{II\text{-}LS}Cr^{III}(NC)_6\}_{0.06}]\cdot 1.3\,H_2O$.[219] The low-temperature phase is ferromagnetic and has a magnetic-ordering temperature of 9 K.

Another interesting property of CrFe Prussian blue analogues is their photoinduced magnetization.[220] The complex $[\{Fe^{II\text{-}HS}_{x}Mn^{II\text{-}HS}_{1-x}\}_{1.5}\{Cr^{III}(CN)_6\}]$, in which the ferromagnetic compound $[Fe^{II\text{-}HS}_{1.5}\{Cr^{III}(CN)_6\}]$ and the ferrimagnetic compound $[Mn^{II\text{-}HS}_{1.5}\{Cr^{III}(CN)_6\}]$ are mixed in the ratio $x=0.4$, exhibits photoinduced magnetic-pole inversion, a new type of photomagnetic effect.[221,222]

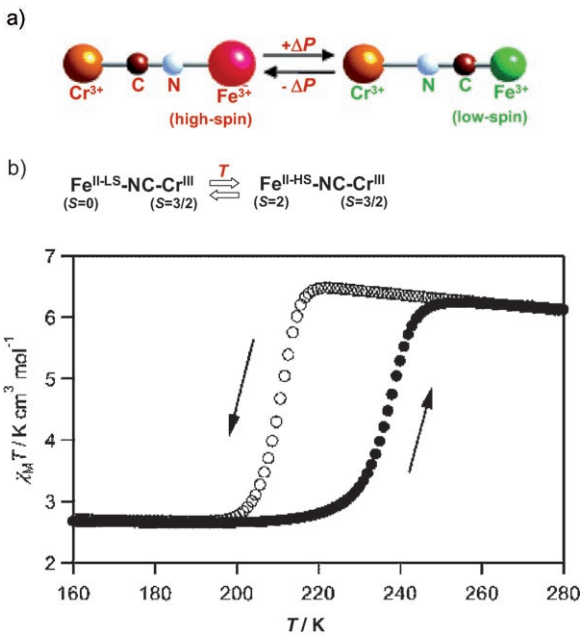

Figure 28. a) Pressure-induced control of exchange coupling owing to the CN flip in $K_{0.4}[Fe_4\{Cr(CN)_6\}_{2.8}]\square_{1.2}\cdot 16\,H_2O$. Reprinted with permission from reference [218]. Copyright 2005, The American Chemical Society. b) Temperature dependence of $\chi_M T$ value of $Cs^{I}[\{Fe^{II\text{-}HS}Cr^{III}(CN)_6\}_{0.94}\{Fe^{II\text{-}LS}Cr^{III}(NC)_6\}_{0.06}]\cdot 1.3\,H_2O$ in an external magnetic field of 5000 G, measured in cooling (○) and warming (●) modes. Reprinted with permission from reference [219]. Copyright 2005, The American Chemical Society.

8.7. Multibistability in Prussian Blue Analogues

Changes in the electronic properties induced by external stimuli lead also to changes in various physical properties. Hence, tunable molecular compounds are always multifunctional. In this way, for example, changes in dielectric properties were monitored in the hysteresis loop of FeMn Prussian blue,[223] and it was found that three physical properties—the dielectric, magnetic, and optical behavior—exhibit bistability at the temperature of the hysteresis loop. Similarly, bistability of the conducting, magnetic, and optical properties have been observed in FeCo analogues.[224]

8.8. Photoinduced Magnetization in tcne-Bridged Molecular Magnets

Besides CN-bridged systems, other compounds also show switchable magnetic properties. The most important examples are tcne-bridged molecular magnets (tcne = tetracyanoethylene). In particular, $[Mn(tcne)_x]\cdot y\,CH_2Cl_2$ ($x=2$, $y=0.8$) exhibits photoinduced magnetization.[225] The critical temperature is not changed by irradiation, but the frequency-dependent magnetic susceptibility is substantially increased after irradiation (Figure 29a). It is thought that the local structure can be modified by irradiation, which in turn modifies the magnetic behavior. However, in contrast to FeCo analogues, neither charge-transfer nor spin transitions

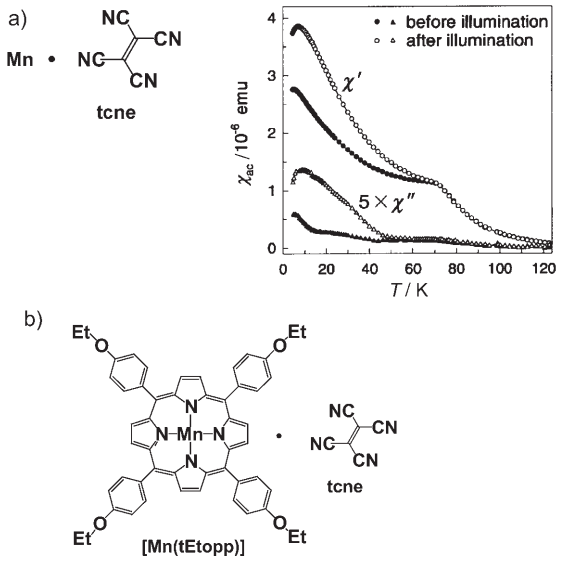

Figure 29. a) Photoinduced magnetization of [Mn(tcne)]. Reprinted with permission from reference [225]. Copyright 2002, The American Physical Society. b) Chemical structure of [Mn(tEtopp)(tcne)].[228]

are involved in the photoprocess. Hence, the value of T_c and the saturation magnetization are not affected.

Another typical molecule-based magnet that has been studied extensively is tcne–Mn porphyrin.[226,227] [Mn(tEtopp)(tcne)] (tEtopp = *meso*-tetrakis(4-ethoxyphenyl)-porphyrin) exhibits a UV-light-induced spin flop (Figure 29b),[228] corresponding to transformation from an antiferromagnetic into a parallel spin alignment.

8.9. Photoinduced Magnetization in CN-Bridged Molecular Clusters

The photomagnetic properties of the trinuclear (Cu-Mo-Cu) compound $[\{Cu^{II}(bpy)_2\}_2\{Mo^{IV}(CN)_8\}]\cdot 5H_2O\cdot CH_3OH$,[209] as well as hexanuclear clusters $[\{Mn(bpy)_2\}_4\{Mo(CN)_8\}_2]\cdot 14H_2O$ and $[\{Mn(bpy)_2\}_4\{W(CN)_8\}_2]\cdot 9H_2O$,[229] have been reported.

The dinuclear 3d–4f compound $[Nd(dmf)_4(H_2O)_3(\mu\text{-}CN)Fe(CN)_5]\cdot H_2O$ with a $Fe^{III\text{-}LS}(t_{2g}^5e_g^0,\ S=1/2)$-CN-$Nd^{III}$-($S$=3/2) structure also shows photoinduced magnetization effects.[230] Neither charge-transfer nor spin transitions can be observed in this system. Hence, the change in the magnetization is thought to be caused by structural changes induced by light. Similar photoeffects were observed in the related compound $[Nd(dmf)_4(H_2O)_3(\mu\text{-}CN)Co(CN)_5]\cdot H_2O$ with a $Co^{III\text{-}LS}(t_{2g}^6e_g^0,\ S=0)$-CN-$Nd^{III}$($S$=3/2) structure.[231] The relaxation temperatures of their photoinduced metastable states were 50 K and 40 K, respectively.

8.10. Switchable Magnetic Properties of opba- and dto-Bridged Molecular Magnets

Besides cyanide, oxalates and related species are also used as bridges in molecular magnets, for example, dto (dto = 1,2-dithiooxalate) and opba (opba = *ortho*-phenylenebis(oxamate)). It has recently been reported that some of these compounds show photo- and thermally induced changes in their magnetization.

A typical example is the compound $[NBu_4]_2[Mn_2\{Cu(opba)\}_3]\cdot 6DMSO\cdot H_2O$.[232] EPR studies of this MnCu compound with illumination in situ at 510.5 and 578.2 nm show that the magnetic order is affected by light as a result of photoinduced changes in the spin correlations. However, the changes in the magnetic properties could not be detected by SQUID magnetometer measurements.

Another example of thermally induced charge transfer is the mixed-valence complex $[(n\text{-}C_3H_7)_4N][Fe^{II}Fe^{III}(dto)_3]$ (Figure 30).[233–235] This Fe complex exhibits a particular type

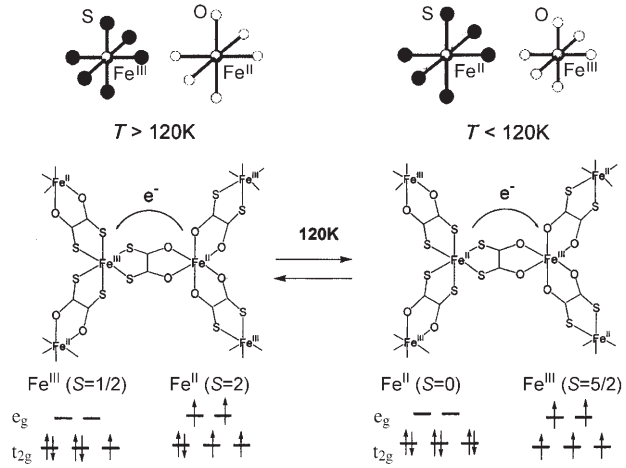

Figure 30. Thermally induced charge transfer in the mixed-valence complex $[(n\text{-}C_3H_7)_4N][Fe^{II}Fe^{III}(dto)_3]$ and the relationship between electron transfer and metal–ligand bond lengths.[233–236] Reprinted with permission from reference [233]. Copyright 2001, Elsevier.

of first-order phase transition in which spin crossover is coupled with charge transfer, which can be expressed as $Fe^{III\text{-}LS}$-dto-$Fe^{II\text{-}HS} \rightleftharpoons Fe^{II\text{-}LS}$-dto-$Fe^{III\text{-}HS}$. Magnetization measurements and ^{57}Fe Mössbauer spectra show that the phase transition takes place at around 120 K with a hysteresis of 15 K. The phase transition is a spin-entropy-driven process. The spin entropy in the $Fe^{III\text{-}LS}$-dto-$Fe^{II\text{-}HS}$ state is $R\ln(2\times5)$ and that in the $Fe^{II\text{-}LS}$-dto-$Fe^{III\text{-}HS}$ state is $R\ln(1\times6)$ (R = gas constant), corresponding to a difference in spin entropy ΔS of $4.25\,J\,K^{-1}\,mol^{-1}$. Heat-capacity measurements show that the entropy gain at the phase transition is $9.20\,J\,K^{-1}\,mol^{-1}$.[233,236] Hence, the entropy change originating from the lattice vibration should be $4.95\,J\,K^{-1}\,mol^{-1}$, which is much smaller than that in a spin-crossover transition.[235] Furthermore, this compound shows a ferromagnetic transition. Field-cooled magnetization measurements show that the magnetic phase-transition temperature is 6.5 K.[233,237] It is thought that valence delocalization between $Fe^{II\text{-}LS}$ and $Fe^{III\text{-}HS}$ induces ferromagnetic ordering, as in the case of the ferromagnetism in Prussian blue.[238]

8.11. Control of Magnetic Properties by Guest Molecules in a Metal–Organic Open Framework

Figure 31 shows the crystal structure of the complex $[Cu_3(ptmtc)_2(py)_6(CH_3CH_2OH)_2(H_2O)]$ (ptmtc = tris(2,3,5,6-tetrachloro-4-carboxyphenyl)methyl radical), in which large pores can be seen. The open metal–organic framework exhibits reversible solvent-induced structural changes, which involve changes also in the magnetic properties. Thus, guest molecules can be used to control the magnetic properties of the compound.[239]

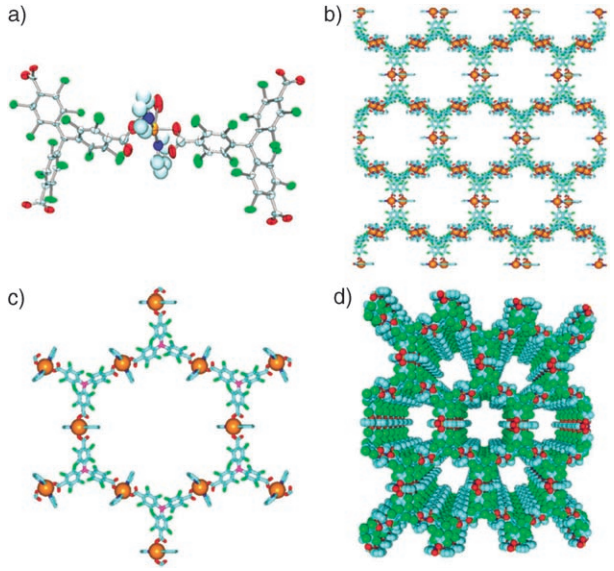

Figure 31. Crystal structure of $[Cu_3(ptmtc)_2(py)_6(CH_3CH_2OH)_2(H_2O)]$. a) ORTEP representation of the copper(II) tricarboxylate building block. b) Honeycomb arrangement of layers in an ABAB disposition along the *ab* plane. c) Hexagonal pores with carbon atoms (violet) located at the vertices and Cu^{II} ions (orange) located at the sides of the hexagon. d) View along the [001] direction showing the distribution of the nanopores in the open framework. Cu orange, C light blue, O red, Cl green, and N dark blue. Reprinted with permission from reference [239]. Copyright 2003, Nature.

8.12. Composite Materials

The combination of a two-dimensional molecular magnet and a photochromic compound yields a new type of molecular photomagnet. Upon irradiation of $(SP)[Fe^{II}Fe^{III}(dto)_3]$ (SP = spiropyran) with UV light (337 nm), a structural change in the spiropyran from the closed to the open one was induced. The structural change induced a change in the critical temperature and in the coercive field of the composite magnets.[240] Similarly, a change in the hysteresis loop that accompanies the photoisomerization of the SP was observed in $(SP)[Mn^{II}Cr^{III}(ox)_3]\cdot H_2O$ (ox = oxalate), which is a ferromagnet with $T_c = 5.5$ K.[241,242] Furthermore, the magnetic properties of an organic–inorganic hybrid system consisting of layered perovskite-type copper halides and photochromic diarylethenes, [2,2′-dimethyl-3,3′-(perfluorocyclopentene-1,2′-diyl)bis-(benzo-[*b*]thiophene-6-ammonium)][$CuCl_4$], can be modified by using a photochromic reaction of diarylethene.[243]

Another type of molecular photomagnet is a combination of a molecule-based magnet and a vesicle or a Langmuir–Blodgett (LB) film.[244–246] Anisotropic photoinduced magnetization has been observed in hybrid films composed of DDAB (dioctadecyldimethylammonium bromide), single nanosheets of clay (montmorillonite), and FeCo Prussian blue.[246] The magnetic easy axis lies along the plane of the film surface and the magnetic hard axis lies perpendicular to the surface.

9. Spin Crossover

Some d^n ($n = 4$–7) first-row transition-metal ions in octahedral environments exhibit a spin crossover between the low-spin and the high-spin states. Spin transitions were first observed by Cambi and Szego in 1931,[247] and since then many spin-transition compounds have been reported. This phenomenon has attracted much attention, not only from the viewpoint of basic science, but also for its practical applications, because such bistable compounds could be used for future memory and switching devices. The number of papers published so far is quite huge, so only representative examples can presented herein; several very useful review articles and books have been published recently.[7–9,28–32] As the control of spin-crossover behavior is an important subject, our main focus herein is on the development of spin-crossover complexes with large hysteresis, room-temperature spin transitions, multistep transitions in molecular clusters, and the tuning of properties through irradiation or guest molecules.

9.1. Spin-Crossover Complexes Exhibiting Hysteresis Loops

9.1.1. Large Hysteresis Loop

An important objective in the development of spin-crossover complexes is the preparation of compounds that display hysteresis loops. Hysteresis is only observed when cooperative interactions are operative.[30] Hence, compounds with a polymeric structure formed by hydrogen bonds, π–π interactions, and coordinate bonds have been prepared.

One example is *cis*-bis(thiocyanato)bis[*N*-(2′-pyridylmethylene)-4-(phenylethynyl)-anilino]iron(II) (=[Fe(pm-pea)$(NCS)_2$]), an Fe^{II} compound that features π–π interactions and shows a large hysteresis.[248] As shown in Figure 32, the transition temperatures are $T_{1/2}\downarrow = 194$ K and $T_{1/2}\uparrow = 231$ K, which corresponds to a hysteresis width of almost 40 K. The π–π interaction between the phenyl rings plays an important role in inducing the large hysteresis loop and also the cooperativity. Furthermore, doping Mn and Ni ions into this Fe^{II} compound increase the thermal hysteresis even more. The hysteresis widths of $[Fe_{0.75}Zn_{0.25}$(pm-pea)$(NCS)_2]$ and $[Fe_{0.8}Ni_{0.2}$(pm-pea)$(NCS)_2]$ are 90 and 92 K, respectively.[249,250]

The inclusion compound $[Fe(dpp)_2(NCS)_2]\cdot$py (dpp = dipyrido[3,2-*a*:2′3′-*c*]phenazine) shows spin-crossover behavior with a large hysteresis ($\Delta T_c = 40$ K).[251] The cause of the strong cooperativity in this system is the π–π interactions

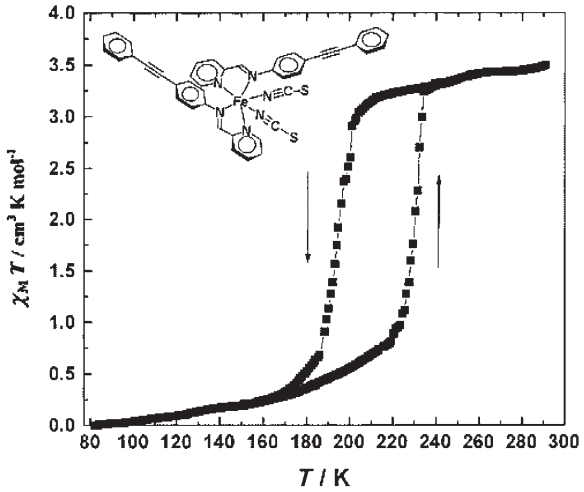

Figure 32. $\chi_M T$ versus T plots for [Fe(pm-pea)(NCS)$_2$] in both cooling and warming modes. Reprinted with permission from reference [248]. Copyright 1997, The American Chemical Society.

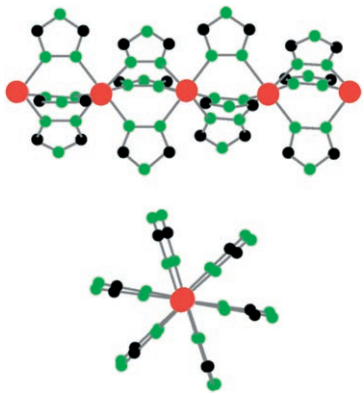

Figure 33. Structure of a polymeric chain {Fe(4-Rtrz)$_3$} in the low-spin state of the spin-crossover compounds [{Fe(4-Rtrz)$_3$}]A$_2$·nH$_2$O (4-Rtrz = 4-R-1,2,4-triazole; R = H or NH$_2$; A = anion), viewed both perpendicular to (top) and along (bottom) the chain direction (Fe, red; N, green; C, black). Reprinted with permission from reference [257]. Copyright 1998, American Association for the Advancement of Science.

between the ligands and the extended aromatic ring structure. Similar π–π interaction is responsible for the large thermal hysteresis of [Fe(qsal)$_2$](NCSe) (Hqsal = *N*-(8-quinolyl)salicylaldimine).[252] This Fe^{III} spin-crossover complex follows a two-step transition; the hysteresis width of the second step is approximately 70 K.

Another example that displays hysteresis is the Fe^{II} compound [Fe(paptH)$_2$](NO$_3$)$_2$ (paptH = 2-(2-pyridylamino)-4-(2-pyridyl)thiazole).[253] The hysteresis width is about 34 K with $T_{1/2}\downarrow = 229$ K and $T_{1/2}\uparrow = 263$ K.

A very large hysteresis was reported for the Fe^{II} complex [Fe(2-pic)$_3$]Cl$_2$·H$_2$O (2-pic = 2-picolylamine) in 1977.[254] The hysteresis width is 91 K with $T_{1/2}\downarrow = 199$ K and $T_{1/2}\uparrow = 290$ K. Sorai et al recently reinvestigated this system and concluded that the large thermal hysteresis is an apparent one caused by the existence of the low-spin metastable phase.[255]

9.1.2. Room-Temperature Hysteresis

Room-temperature hysteresis is observed in some Fe^{II} spin-crossover complexes. The Fe^{II} compound [Fe(Htrz)$_3$](ClO$_4$)$_2$ (Htrz = 1,2,4-1*H*-triazole) shows an abrupt transition with a hysteresis loop of 17 K ($T_{1/2}\downarrow = 296$ K and $T_{1/2}\uparrow = 313$ K) at just above room temperature when a drop of water is added.

When the Fe^{II} compound [Fe(Htrz)$_3$](ClO$_4$)$_2$ is mixed with [Fe(4-NH$_2$-trz)$_3$](ClO$_4$)$_2$ (4-NH$_2$-trz = 4-amino-1,2,4-triazole), the transition temperature shifts to lower temperature with increasing proportion of [Fe(4-NH$_2$-trz)$_3$]. When the mixing ratio is 0.05 (i.e., [Fe(Htrz)$_3$]$_{3-3x}$[Fe(4-NH$_2$-trz)$_3$]$_{3x}$(ClO$_4$)$_2$·nH$_2$O ($x = 0.05$); Figure 33), thermal hysteresis is observed at room temperature ($T_{1/2}\downarrow = 288$ K and $T_{1/2}\uparrow = 304$ K). At 294 K, the compound shows two different colors depending on the history of the sample.[256] Similarly, when the counteranion ClO$_4^-$ in [Fe(4-NH$_2$-trz)$_3$](ClO$_4$)$_2$ is replaced by a mixture of NO$_3$ and BF$_4$ with a mixing ratio of 0.85:0.15, the compound exhibits a room-temperature hysteresis of about 60 K (Figure 34).[257] The related compound [Fe(hyptrz)$_3$](4-chloro-3-nitrophenylsulfonate)$_2$·2H$_2$O (hyptrz = 4-(3′-hydroxypropyl)-1,2,4-triazole) exhibits a spin transition with a wide thermal hysteresis of about 50 K, although the hysteresis is observed below room temperature.[258]

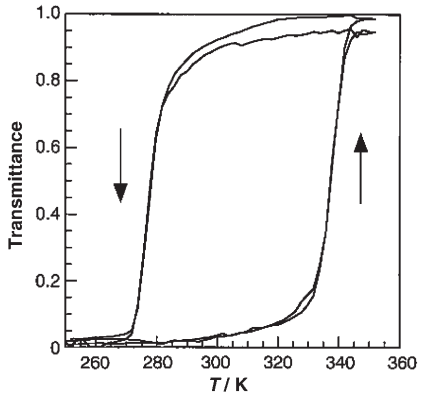

Figure 34. Thermal hysteresis loop detected optically through the transmittance at 520 nm of [Fe(4-NH$_2$-trz)$_3$](NO$_3$)$_{1.7}$(BF$_4$)$_{0.3}$ preencapsulated in a polymer. The hysteresis loop is reproducible over several tens of thermal cycles. Reprinted with permission from reference [257]. Copyright 1998, American Association for the Advancement of Science.

Another compound that shows room-temperature thermal hysteresis is [Fe(pyz){Pt(CN)$_4$}], which is obtained by dehydration of [Fe(pyz){Pt(CN)$_4$}]·nH$_2$O ($n = 2$–3)[259] at 430 K. As shown in Figure 35, the hysteresis loop is around 24 K.[260] Furthermore, the Fe^{III} complex Li[Fe^{III}(5-Br-thsa)$_2$]·H$_2$O, exhibits large hysteresis loop of 39 K at around room temperature ($T_{1/2}\downarrow = 294$ K and $T_{1/2}\uparrow = 333$ K).[261]

9.1.3. Reverse Spin Transitions with Large Room-Temperature Hysteresis

The Co^{II} complex [Co(C$_{16}$-tpy)$_2$](BF$_4$)$_2$ (C$_{16}$-tpy = 4′-hexadecyloxy-2,2′:6′,2″-terpyridine), which contains tpy ligands with long alkyl chains, shows large hysteresis with a change

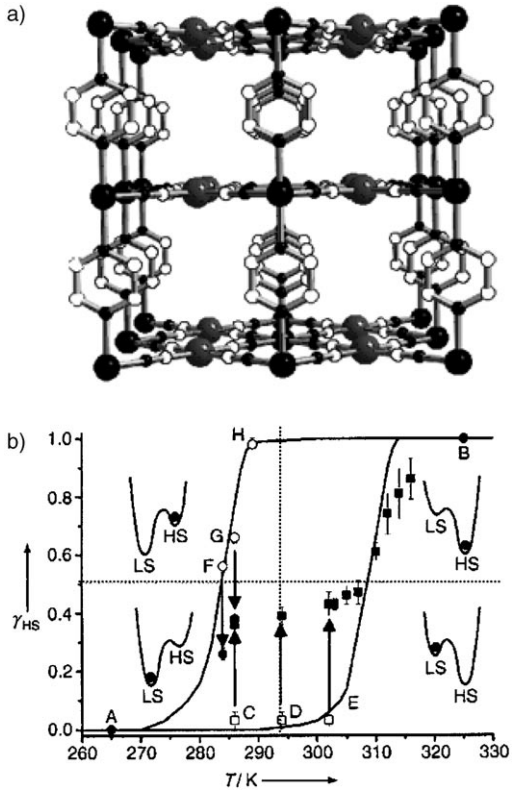

Figure 35. a) Structure of $[Fe(pyz)\{Pt(CN)_4\}]$.[259,260] b) Proportion of HS iron(II) ions before (□, ○) and after (■, ●) irradiation with 10 laser pulses on points A–H of the hysteresis loop of $[Fe(pyz)\{Pt(CN)_4\}]$. Points obtained by heating after irradiation at point E are also presented. Schematic diagrams of the free energy with minima corresponding to the LS and HS states at their respective temperatures are shown in each part of the graph separated by the dotted lines.[260] Reprinted from reference [260].

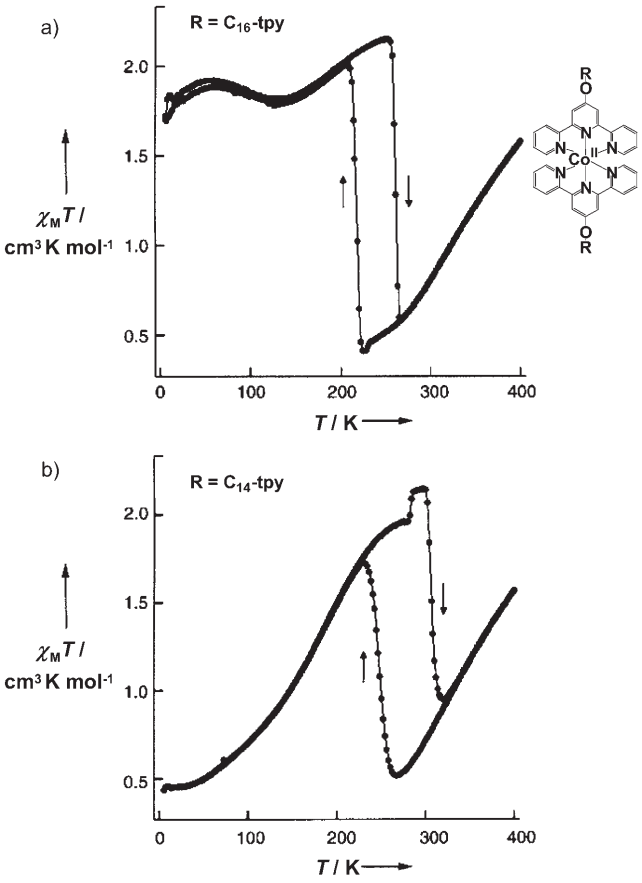

Figure 36. a) $\chi_m T$ versus T plots for $[Co(C_{16}\text{-tpy})_2](BF_4)_2$ and molecular structure of $[Co(R\text{-tpy})_2]^{2+}$ ($R = C_{16}$ or C_{14}). b) $\chi_m T$ versus T plots for $[Co(C_{14}\text{-tpy})_2](BF_4)_2$. Reprinted from reference [44].

between an $S = 1/2$ and an $S = 3/2$ spin state.[44] The spin crossover is thermally induced just below room temperature with a hysteresis width of 43 K ($T_{1/2}\downarrow = 217$ K and $T_{1/2}\uparrow = 260$ K; Figure 36). An important characteristic is that the LS-to-HS transition is induced in cooling mode and the reverse transition is induced in warming mode. In general, the HS state is usually the high-temperature phase and the LS state is usually the low-temperature phase. In this case, the opposite transition is observed, known as a "reverse spin transition". $[Co(C_{14}\text{-tpy})_2](BF_4)_2$ (C_{14}-tpy = 4′-tetradecyloxy-2,2′:6′,2″-terpyridine) also exhibited a reverse spin transition at room temperature with a very large hysteresis width ($\Delta T =$ 56 K, $T_{1/2}\downarrow = 250$ K and $T_{1/2}\uparrow = 306$ K). It is thought that the reverse spin transition is induced by a structural phase transition in which the long alkyl chain plays an important role.

9.2. Photoinduced Phase Transition in Spin Crossover Complexes

9.2.1. Light-Induced Excited Spin-State Trapping

An important property of some spin-crossover complexes is the photoinduced spin transition that is known as "light-induced excited spin-state trapping" (LIESST) (Figure 37).

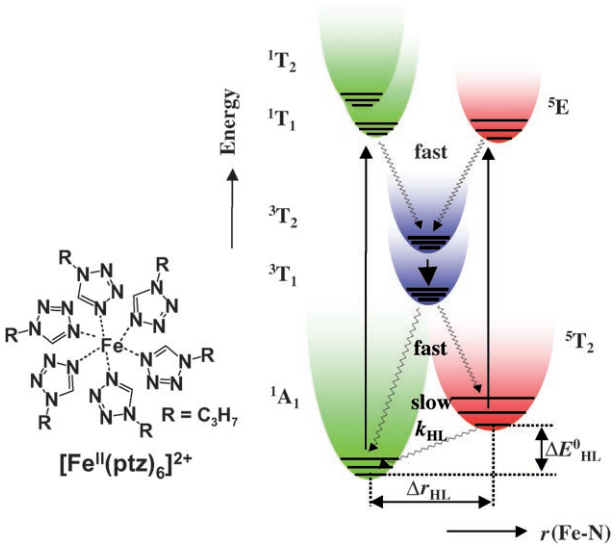

Figure 37. Schematic illustration of LIESST and reverse LIESST of a d^6 complex in the spin-crossover range[7] and the chemical structure of $[Fe(ptz)_6]^{2+}$.

The LIESST effect was discovered by Decurtins et al.,[7,49] and since then many Fe^{II} LIESST complexes that show photo-

induced LS-to-HS transitions have been reported. Furthermore, Hauser found that the reverse spin transition could be induced by irradiation with red light (reverse LIESST effect).[262] More recently, the first Fe^{III} complex that displays LIESST effects was reported.[50] So far, no LIESST compounds with metals other than Fe^{II} and Fe^{III} have been reported. The structure of the photoinduced HS state has been found by X-ray single-crystal analysis and Raman scattering to be different from that of the thermally accessible HS state.[263,264] In other words, by irradiation with light, a new phase can be created in some spin-crossover complexes that is similar in structure to the HS state at high temperature, but not identical.

9.2.2. Photoinduced Phase Transitions in Spin-Crossover Complexes

The LIESST phenomenon is only observed at quite low temperatures.[7,265] Hence, a technique to achieve photoinduced phase transitions has recently been developed to control the spin state at high temperatures. Koshihara et al. reported in 1992 that phase transitions can be induced in poly(diacetylene) films.[266] This material shows a phase transition between the A and the B phases, which are different in color, and a hysteresis loop can be observed. When this polymer is excited by light in the hysteresis loop, a phase transition between the A and the B phase can be induced. This process is known as a photoinduced phase transition.

Application of this technique to molecular magnetic materials could be used to induce phase transitions involving changes in magnetic properties. Indeed, several compounds show such photoinduced magnetization effects. One example is $[Fe(pyz)\{Pt(CN)_4\}]$, which was excited by applying a one-shot pulse of laser irradiation.[260] As shown in Figure 35, the stable state at around 305 K in warming mode is the HS state. However, owing to cooperative effects, the LS state can be trapped without transforming into the stable HS state. Thus, excitation of the compound at this temperature induces a phase transition from the metastable LS state to the stable HS state. This spin transition can be induced by using a pulsed Nd:YAG laser (8-ns pulses, $\lambda = 532$ nm).

Similarly, the reverse transition could be induced by using light with the same wavelength. In this case, the HS state is trapped at around 285 K in cooling mode without being transformed into the stable LS state. When the compound was irradiated with pulsed laser light, the HS-to-LS transition was induced. Thus, this compound exhibits bidirectional light-induced spin transition at around room temperature.

Before this work, Freysza et al. reported that a single laser pulse induces a spin-state transition in $[Fe(pm\text{-}bia)_2(NCS)_2]$ (pm-bia = *N*-2′-pyridylmethylene-4-aminobiphenyl) within the hysteresis loop.[267] Moreover, Liu et al. reported a similar photoinduced spin transition for $[FeL(CN)_2]\cdot H_2O$ (L = macrocyclic Schiff base with N_3O_2 donor set) in the hysteresis.[268] Only the LS-to-HS transition was observed in these two systems.

This technique is a powerful tool for switching magnetic properties at high temperature. Photoinduced phase transitions were also observed in FeMn Prussian blue,[201] in TTTA molecules,[165,166] and in FeCo Prussian blue.[269,270]

9.2.3. Ligand-Driven Spin Transitions

Another method of controlling spin transitions at relatively high temperatures is known as "ligand-driven spin transition".[271,272] Figure 38 shows as an example the Fe^{II} complex $[Fe(trans\text{-}stpy)_4(NCBPh_3)_2]$ (*trans*-stpy = *trans*-1-phenyl-2-(4-pyridyl)ethene), which exhibits a spin conversion at around 190 K, whereas the *cis* form $[Fe(cis\text{-}stpy)_4(NCBPh_3)_2]$ is in the HS state at all temperatures. Irradiation of the compound induced photoisomerization of the stpy ligand, which modifies the ligand field of the Fe^{II} complex and results in spin crossover of the Fe^{II} ions.[273] A similar ligand-driven spin transition was also reported for Fe^{III} spin-crossover complexes.[274]

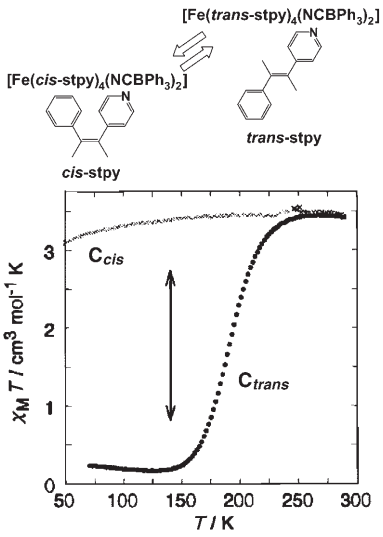

Figure 38. Temperature dependence of $\chi_M T$ for the C_{trans} and C_{cis} forms of $[Fe(stpy)_4(NCBPh_3)_2]$. At 140 K, photoinduced $C_{cis} \rightleftharpoons C_{trans}$ interconversion is expected to result in HS–LS crossover of the Fe^{II} center. Reprinted with permission from reference [273]. Copyright 1996, The American Chemical Society.

9.3. Control of Spin Crossover by Guest Molecules in a Metal–Organic Open Framework

Switching induced by guest molecules has been observed in the hysteresis loop of the spin-crossover coordination polymer $[Fe(pmd)(H_2O)\{Ag(CN)_2\}_2]\cdot H_2O$ (**1Ag**)$\rightleftharpoons$$[Fe(pmd)(H_2O)\{Ag(CN)_2\}_2]$ (**2Ag**) and $[Fe(pmd)(H_2O)\{Au(CN)_2\}_2]\cdot H_2O$ (**1Au**)$\rightleftharpoons$$[Fe(pmd)(H_2O)\{Au(CN)_2\}_2]$ (**2Au**) (pmd = pyrimidine)[31,275] As shown in Figure 39, removal of the water molecules from the crystal changes its magnetic properties. Rietveld analysis shows that structural transformation of the three interpenetrating nets into a single three-dimensional net occurs.

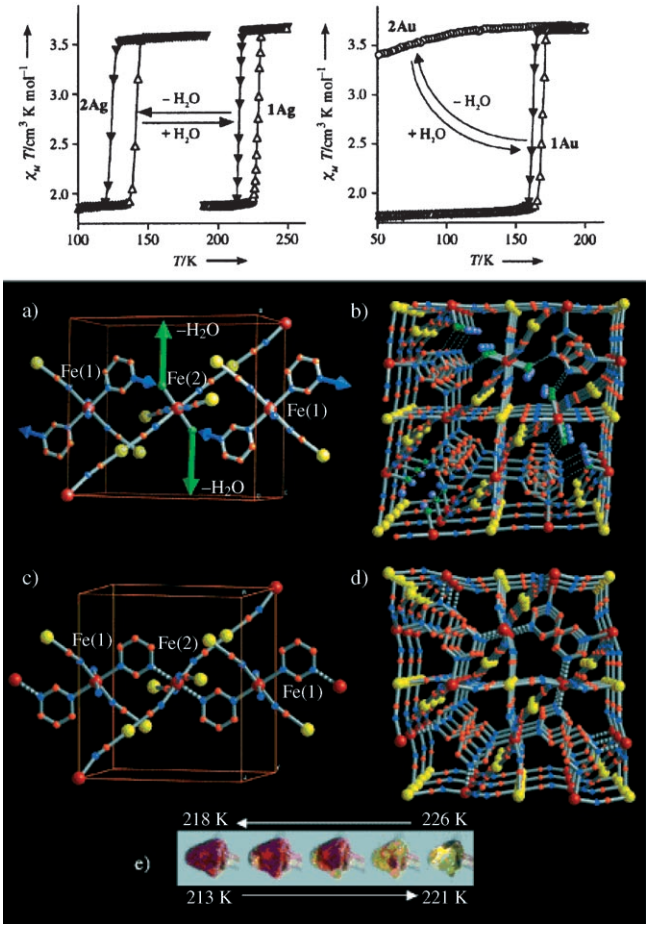

Figure 39. Top: Temperature dependence of $\chi_m T$.[275] Bottom: Unit cell of **1Ag** showing fragments of three networks. a) The arrows on the noncoordinated nitrogen atoms (blue) and coordinated water molecules (green) indicate dynamic events that take place during the topochemical solid-state reaction. b) Perspective view along [001] of the three nets showing the N(pmd)···H_2O hydrogen-bond system. c) Unit cell of **2Au** showing chains defined by the bridging pmd ligand (striped bonds represent the new coordination bonds generated after dehydration). d) Perspective view of the new 3D network **2Au**. e) Photographs showing the color change of a single crystal of **1Ag** around the critical region (yellow and deep red colors correspond to the high- and low-spin states, respectively). Reprinted from reference [275].

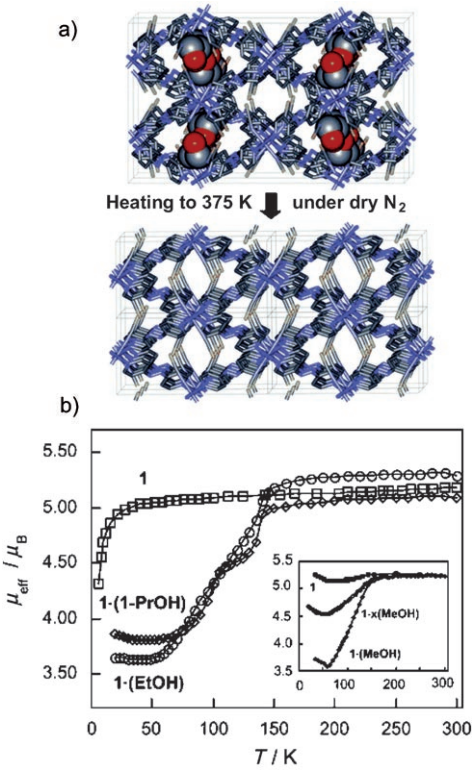

Figure 40. a) Crystal structures of $[Fe_2(azpy)_4(NCS)_4]\cdot(EtOH)$ at 150 and 375 K. Framework atoms are represented as sticks and the atoms of the ethanol guests are shown as spheres.[276] b) Magnetic properties of $[Fe_2(azpy)_4(NCS)_4]\cdot x(guest)$. The spin-crossover behavior is strongly affected by guest molecules. The inset shows the effect of partial and complete removal of methanol from $[Fe_2(azpy)_4(NCS)_4]\cdot(MeOH)$. Reprinted with permission from reference [276]. Copyright 2002, American Association for the Advancement of Science.

Guest-dependent spin-crossover was also observed in the nanoporous metal–organic framework $[Fe_2(azpy)_4(NCS)_4]\cdot$(guest) (azpy = *trans*-4,4′-azopyridine).[276] The spin transition is affected by changes in the local geometry of the iron(II) centers upon guest uptake and release. $[Fe_2(azpy)_4(NCS)_4]$ does not exhibit spin-crossover without guest molecules, but does after the uptake of guest molecules (Figure 40).

9.4. Control of Spin Crossover by the Modification of Ligands with Alkyl Chains

A further possibility to control spin-crossover behavior is the modification of ligands with alkyl chains.[277–281] Galyametdinov et al. reported the first example of the coexistence of a thermal spin transition and liquid-crystal properties with an Fe^{III} complex with an *N*-alkyloxysalicylidenyl-*N*′-ethyl-*N*-ethylenediamine ligand.[277] A spin transition triggered by a phase transition has also been reported in self-assembled Fe^{II} complexes.[278,279] Bodenthin claims that the phase change induces mechanical strain around the coordination sphere of the Fe^{II} ion, which causes a transition from LS to HS (Figure 41).[279] More recently, dendrimer Fe^{II} complexes [(G*n*-trz)Fe] (G*n*-trz: trz = triazole; *n* = generation number 0–2) with spin-crossover behavior have been synthesized (Figure 42).[281] The spin-crossover temperature decreased ($T_c = 335 \rightarrow 315 \rightarrow 300$ K) with increasing generation number of the dendritic unit ($n = 0 \rightarrow 1 \rightarrow 2$).

9.5. Multistep Transition in Spin-Crossover Clusters

The development of molecular clusters in which more than one metal ion is incorporated is an interesting subject, because the electronic, magnetic, and elastic interactions may lead to unusual behavior of the spin transitions.

The dinuclear Fe^{II} complex $[\{Fe^{II}(bt)(NCS)_2\}(bpym)\{Fe^{II}(bt)(NCS)_2\}]$ (bt = 2,2′-bithiazoline; bpym = 2,2′-bipyrimidine) exhibits a two-step spin transition,[282] which can be expressed as HS-HS⇌HS-LS⇌LS-LS. It is believed that

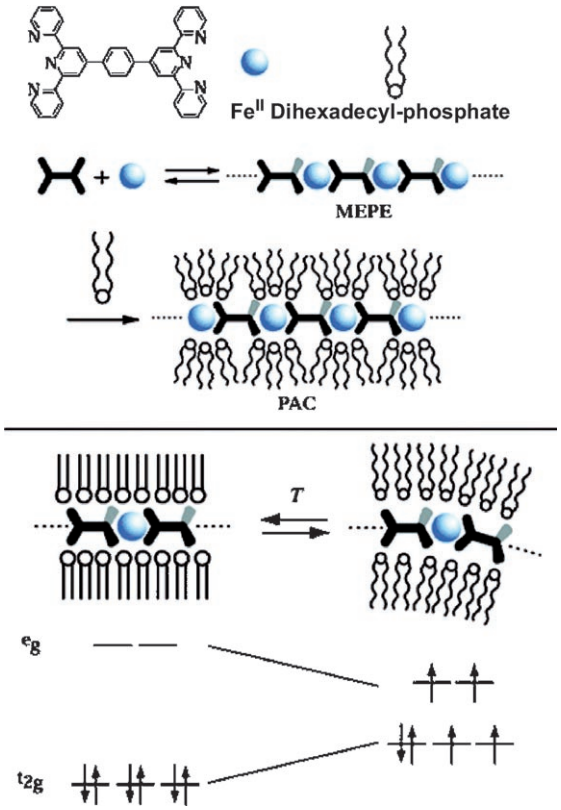

Figure 41. Top: Self-assembly of the ditopic bis(terpyridine) ligand and iron acetate in aqueous solution results in the formation of a supramolecular metallopolyelectrolyte (MEPE). The subsequent self-assembly of MEPE and dihexadecyl phosphate affords the polyelectrolyte amphiphile complex (PAC).[279] Bottom: Melting of the alkyl chains in the amphiphilic mesophase induces a spin transition from a diamagnetic LS state to a paramagnetic HS state. Reprinted with permission from reference [279]. Copyright 2005, The American Chemical Society.

antiferromagnetic elastic interactions between the Fe^{II} ions play an important role in the induction of this phenomenon. Furthermore, because of the presence of antiferromagnetic interactions, the ground state of the $[\{Fe^{II\text{-}HS}(bt)(NCS)_2\}(bpym)\{Fe^{II\text{-}HS}(bt)(NCS)_2\}]$ species is $S=0$. This dinuclear Fe^{II} complex is an unusual compound in which spin-crossover and magnetic interactions are combined.

Furthermore, the tetranuclear Fe^{II} complex $[Fe_4L_4](ClO_4)_8$ (L = 4,6-bis(2′,2″-bipyrid-6′-yl)-2-phenylpyrimidine; Figure 43) with a [2×2] grid structure shows successive spin transitions of the form HS-HS-HS-LS⇌HS-HS-LS-LS⇌HS-LS-LS-LS.[283] These transitions could be induced by changing the temperature, by irradiation with light, or by the application of pressure. More recently, a two-step transition was reported for the square Fe^{II} complex $[Fe^{II}_4(\mu\text{-}CN)_4(bpy)_4(tpa)_2](PF_6)_4$.[284] As shown in Figure 43, one of the Fe ions that is coordinated by tpa exhibits a spin transition at around 160 K, and the remaining one starts to show a spin transition at around 300 K upon warming.

Many other interesting phenomena have been reported recently, especially, the development of multifunctional materials that combine spin crossover with conductivity or

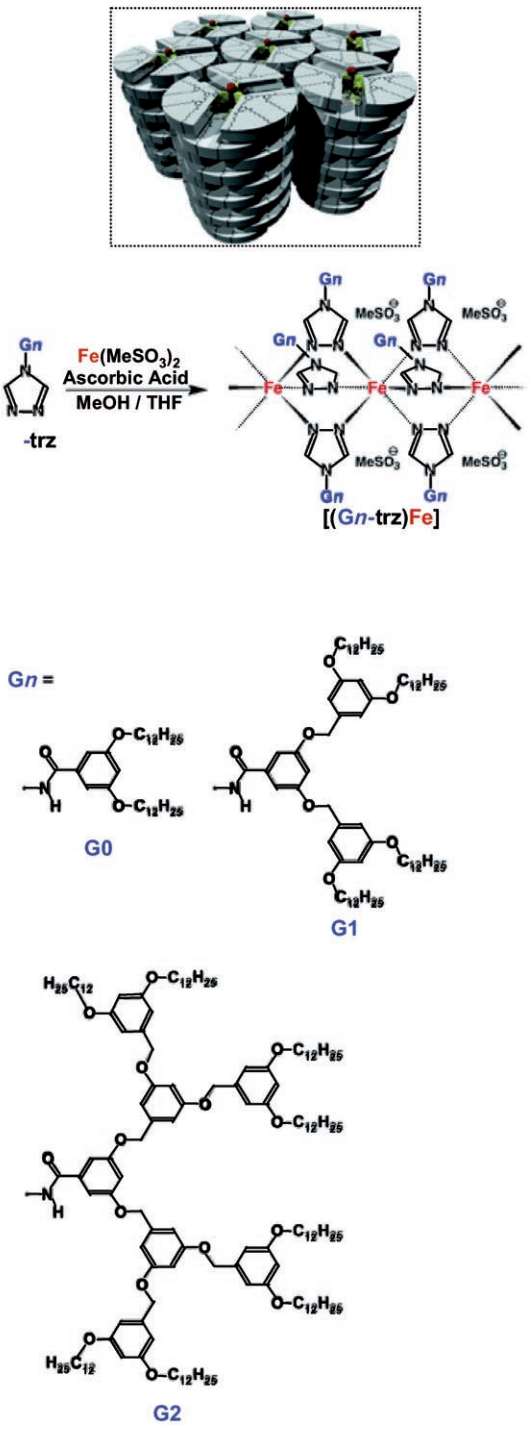

Figure 42. Synthesis of [(G*n*-trz)Fe] (*n* = 0–2). Inset: Structure of spin-crossover dendrimer. Reprinted with permission from reference [281]. Copyright 2005, The American Chemical Society.

dielectric properties.[285,286] A review article on this topic was published recently.[9]

10. Summary and Outlook

We have described recent advances in switchable molecular compounds. Photoirradiation, electrochemical redox

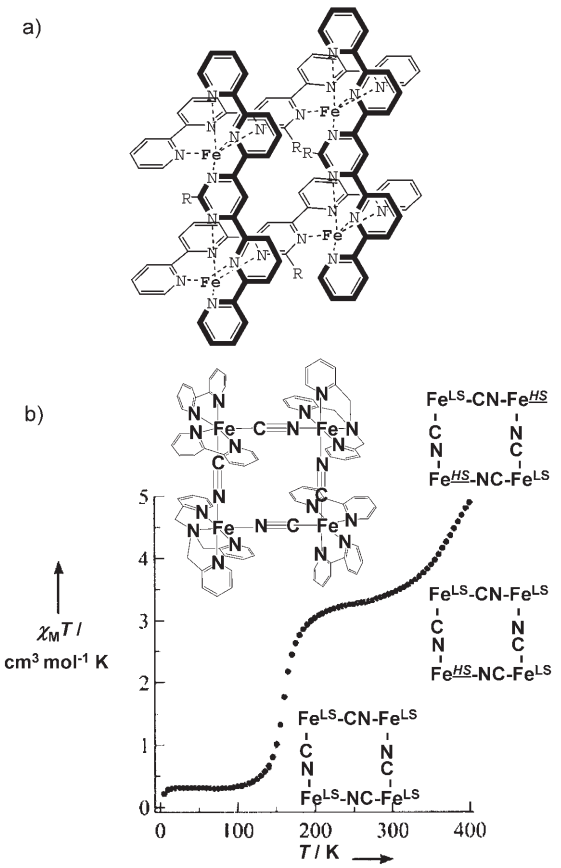

Figure 43. a) Molecular structure of $[Fe_4L_4](ClO_4)_8$.[283] b) Molecular structure of $[Fe^{II}{}_4(\mu\text{-}CN)_4(bpy)_4(tpa)_2](PF_6)_4$ and $\chi_M T$ versus T plot for $[Fe^{II}{}_4(\mu\text{-}CN)_4(bpy)_4(tpa)_2](PF_6)_4$. Reprinted from reference [284].

reactions, the uptake and release of ions and guest molecules, and external pressures can now be used to control the magnetic properties of various materials. For this purpose, ligand fields, intermolecular interactions (e.g. π–π interactions and hydrogen bonds), molecular structure (e.g. porous networks), and the energy of the frontier orbitals can be appropriately adjusted and new compounds with dynamic properties can be synthesized; however, some discoveries still seem to have come about by accident.

The structural changes involved in the switching phenomena play an important role in many cases and range from changes in the ligand–metal bond length and Jahn–Teller distortion to planar-to-tetrahedral interconversion. These changes contribute to changes in the entropy term, which might enable the induction of entropy-driven phase transitions. Moreover, relaxation from a metastable state to the ground state might be effectively prevented by large structural changes, as is the case in spin-crossover complexes. For a compound to exhibit switching phenomena, it must have spin states that are close in energy.

The design of the switchable molecular magnetic materials is becoming more and more important. In particular, the control of magnetic properties by light will be an important target in the future. Unfortunately, most phototunable magnetic materials work only below liquid-nitrogen temperature, and it will be important to find a way of being able to operate at room temperature. One may think that the trapping of the metastable state at room temperature is not easy in molecular compounds. However, photochromic molecules exhibit bistability even at room temperature. Diarylethenes in particular exhibit reversible photoisomerization over many cycles,[287] so a room-temperature photomagnet could be possible. Indeed, a Cu complex has been developed whose metastable state could be trapped at around room temperature,[108] and ligand-driven spin-crossover has also been observed at around room temperature.[272]

Photoinduced phase transition is another useful technique for controlling magnetic properties at room temperature. An important aspect of photoinduced phase transitions is that the photoinduced change can only be observed when the light intensity exceeds a threshold value. A weak point of photocontrol systems that include photochromic compounds is the possible destruction of memory caused by irradiation with light from the surroundings, which could be overcome in the case of photoinduced phase transitions. Hence, the study of photoinduced phase changes as well as the development of large thermal hysteresis widths are important subjects for the future.

It would also be interesting to design new compounds in which photoswitching properties and single-molecule (or single-chain) magnetic properties are coupled.[127] In the case of bulk magnets, the memory area cannot be decreased to smaller than several nanometers. In the case of single-molecule magnets, the size can be smaller than a few nanometers.

The preparation of molecular clusters that exhibit abrupt transitions or hysteresis loops is another important subject. Single-molecule magnets exhibit hysteresis in M–H plots, and it would be interesting to be able to develop molecular magnetic compounds that display hysteresis at the single cluster level in M–T plots.

Electrical control of magnetic properties is another important subject in this field. The phenomenon of current-induced magnetic-pole reversal is known in the field of spin electronics,[288] but similar effects have not been reported for molecular compounds. Hence, it is important to try to combine magnetic and conducting properties in a molecular compound. Furthermore, the combination or coexistence of photomagnetic compounds and superconducting materials might be interesting, because magnetic and superconducting properties are incompatible with each other.

Besides the preparation of new compounds, techniques for assembling switchable molecular magnets and accessing the molecules at the single molecular level would also be important areas for study. Many groups have synthesized new molecules for molecular-scale devices, but there have only been a few studies devoted to the assembly and accessing of functional molecules at the nanoscale.[289]

Abbreviations

bdta	1,3,2-benzodithiazolyl
bpy	2,2′-bipyridine
5-Br-thsa	5-bromosalicylaldehydethiosemicarbazone

bt	2,2′-bithiazoline
CA	*p*-chloranil
cat-N-bq	2-(2-hydroxy-3,5-di-*tert*-butylphenylimino)-4,6-di-*tert*-butylcyclohexa-3,5-dienone
cat-N-sq	dianionic semiquinonate analogue of cat-N-bq
CBDTA	cyano-functionalized benzodithiazolyl
Cl_4cat	tetrachlorocatecholate
Cl_4sq	tetrachlorosemiquinonate
cth	*dl*-5,7,7,12,14,14-hexamethyl-1,4,8,11-tetraazacyclotetradecane
3,5-dbcat	3,5-di-*tert*-butyl-1,2-catecholate
3,6-dbcat	3,6-di-*tert*-butyl-1,2-catecholate
dbcat	3,5-dbcat or 3,6-dbcat
3,5-dbsq	3,5-di-*tert*-butyl-1,2-semiquinonate
3,6-dbsq	3,6-di-*tert*-butyl-1,2-semiquinonate
dbsq	3,5-dbsq or 3,6-dbsq
dbq	3,5-dbcat, 3,5-dbsq, 3,6-dbcat, or 3,6-dbsq
dhbq	2,5-dihydroxy-1,4-benzoquinone
dmf	*N*,*N*-dimethylformamide
dpa	2,2′-dipyridylamine
dpp	dipyrido[3,2-*a*:2′3′-*c*]phenazine
dto	1,2-dithiooxalate
Htrz	1,2,4-1*H*-triazole
hyptrz	4-(3′-hydroxypropyl)-1,2,4-triazole
mmb	1-methyl-2-(methylthiomethyl)-1*H*-benzimidazole
mnt	maleonitriledithiolate
4-NH_2-trz	4-amino-1,2,4-triazole
npbifc	dineopentylbisferrocene
opba	*ortho*-phenylenebis(oxamate)
ox	oxalate
paptH	2-(2-pyridylamino)-4-(2-pyridyl)thiazole
pda	*para*-phenylenediamine
PDTA	1,3,2-dithiazolo[4,5-*b*]pyrazin-2-yl
phen	phenanthroline
phencat	9,10-phenanthrenediolate
phensq	9,10-phenanthrenesemiquinonate
phendiox	phencat or phensq
2-pic	2-picolylamine
pmd	pyrimidine
pm-pea	*N*-(2′-pyridylmethylene)-4-(phenylethynyl)aniline
ptz	1-propyltetrazole
py	pyridine
$Py(Bn)_2$	*N*,*N*-bis(benzyl)-*N*-[(2-pyridyl)methyl]-amine
py_2O	2,2′-bis(pyridyl) ether
pyz	pyrazine
RBnPy	1-(4′-R-benzyl)pyridinium
R′BnPyNH_2	1-(4′-R′-benzyl)-4-aminopyridinium
SP	spiropyran
tcne	tetracyanoethylene
tcnq	tetracyanoquinodimethane
TDP-DTA	1,2,5-thiadiazolo[3,4-*b*]-1,3,2-dithiazolo-[3,4-*b*]pyrazin-2-yl
tEtopp	*meso*-tetrakis(4-ethoxyphenyl)porphyrin
tmeda	*N*,*N*,*N*′,*N*′-tetramethylethylenediamine
tmpda	*N*,*N*,*N*′,*N*′-tetramethylpropylenediamine
tmphen	3,4,7,8-tetramethyl-1,10-phenanthroline
tpa	tris(2-pyridylmethyl)amine
tpy	2,2′:6′,2″-terpyridine
trans-stpy	*trans*-1-phenyl-2-(4-pyridyl)ethene
trz	triazole
TTF	tetrathiafulvalene
TTTA	1,3,5-trithia-2,4,6-triazapentalenyl

We thank Prof. A. Fujishima (KAST), Prof. K. Hashimoto (The University of Tokyo), Prof. T. Iyoda (Tokyo Institute of Technology), and all of our co-workers for valuable suggestions. This work was partly supported by a Grant-in-Aid for Scientific Research on Priority Areas (417) from the Ministry of Education, Science, Sport, and Culture of Japan.

Received: June 2, 2006

[1] J. M. Manriquez, G. T. Yee, R. S. McLean, A. J. Epstein, J. S. Miller, *Science* **1991**, *252*, 1415 – 1417.
[2] S. Ferlay, T. Mallah, R. Ouahes, P. Veillet, M. Verdaguer, *Nature* **1995**, *378*, 701 – 703.
[3] M. Kinoshita, P. Turek, M. Tamura, K. Nozawa, D. Shiomi, Y. Nakazawa, M. Ishikawa, M. Takahashi, K. Awaga, T. Inabe, Y. Maruyama, *Chem. Lett.* **1991**, 1225 – 1228.
[4] R. Sessoli, D. Gatteschi, A. Caneschi, M. A. Novak, *Nature* **1993**, *365*, 141 – 143.
[5] D. Gatteschi, R. Sessoli, *Angew. Chem.* **2003**, *115*, 278 – 309; *Angew. Chem. Int. Ed.* **2003**, *42*, 268 – 297.
[6] A. Caneschi, D. Gatteschi, N. Lalioti, C. Sangregorio, R. Sessoli, G. Venturi, A. Vindigni, A. Rettori, M. G. Pini, M. A. Novak, *Angew. Chem.* **2001**, *113*, 1810 – 1813; *Angew. Chem. Int. Ed.* **2001**, *40*, 1760 – 1763.
[7] P. Gütlich, A. Hauser, H. Spiering, *Angew. Chem.* **1994**, *106*, 2109 – 2141; *Angew. Chem. Int. Ed. Engl.* **1994**, *33*, 2024 – 2054.
[8] P. Gütlich, Y. Garcia, T. Woike, *Coord. Chem. Rev.* **2001**, *219–221*, 839 – 879.
[9] J. A. Real, A. B. Gaspar, M. C. Munoz, *Dalton Trans.* **2005**, 2062 – 2079.
[10] C. G. Pierpont, *Coord. Chem. Rev.* **2001**, *216–217*, 99 – 125.
[11] D. A. Shultz, *Comments Inorg. Chem.* **2002**, *23*, 1 – 21.
[12] A. Dei, D. Gatteschi, C. Sangregorio, L. Sorace, *Acc. Chem. Res.* **2004**, *37*, 827 – 835.
[13] K. Hashimoto, S. Ohkoshi, *Philos. Trans. R. Soc. London Ser. A* **1999**, *357*, 2977 – 3003.
[14] A. J. Epstein, *MRS Bull.* **2003**, *28*, 492 – 499.
[15] O. Sato, *J. Photochem. Photobiol. C* **2004**, *5*, 203 – 223.
[16] C. G. Pierpont, R. M. Buchanan, *Coord. Chem. Rev.* **1981**, *38*, 45 – 87.
[17] P. Gütlich, A. Dei, *Angew. Chem.* **1997**, *109*, 2852 – 2857; *Angew. Chem. Int. Ed. Engl.* **1997**, *36*, 2734 – 2736.
[18] C. G. Pierpont, *Coord. Chem. Rev.* **2001**, *219–221*, 415 – 433.
[19] C. G. Pierpont, A. S. Attia, *Collect. Czech. Chem. Commun.* **2001**, *66*, 33 – 51.
[20] E. Evangelio, D. Ruiz-Molina, *Eur. J. Inorg. Chem.* **2005**, 2957 – 2971.
[21] O. Sato, T. Iyoda, A. Fujishima, K. Hashimoto, *Science* **1996**, *272*, 704 – 705.
[22] M. Verdaguer, *Science* **1996**, *272*, 698 – 699.
[23] S. Ohkoshi, K. Hashimoto, *J. Photochem. Photobiol. C* **2001**, *2*, 71 – 88.
[24] D. A. Pejaković, J. L. Manson, C. Kitamura, J. S. Miller, A. J. Epstein, *Mol. Cryst. Liq. Cryst.* **2002**, *374*, 289 – 302.

[25] A. Dei, *Angew. Chem.* **2005**, *117*, 1184 – 1187; *Angew. Chem. Int. Ed.* **2005**, *44*, 1160 – 1163.
[26] P. Gütlich, *Struct. Bonding (Berlin)* **1981**, *44*, 83 – 195.
[27] E. Konig, G. Ritter, S. K. Kulshreshtha, *Chem. Rev.* **1985**, *85*, 219 – 234.
[28] O. Kahn, *Molecular Magnetism*, VCH, New York, **1993**.
[29] P. Gütlich, Y. Garcia, H. A. Goodwin, *Chem. Soc. Rev.* **2000**, *29*, 419 – 427.
[30] J. A. Real, A. B. Gaspar, V. Niel, M. C. Munoz, *Coord. Chem. Rev.* **2003**, *236*, 121 – 141.
[31] T. Glaser, *Angew. Chem.* **2003**, *115*, 5846 – 5848; *Angew. Chem. Int. Ed.* **2003**, *42*, 5668 – 5670.
[32] *Topics In Current Chemistry, Spin Crossover in Transition Metal Compounds I–III*, *Vol. 233–235* (Ed.: P. Gütlich, H. A. Goodwin), Springer, Berlin, **2004**.
[33] R. M. Buchanan, C. G. Pierpont, *J. Am. Chem. Soc.* **1980**, *102*, 4951 – 4957.
[34] D. M. Adams, A. Dei, A. L. Rheingold, D. N. Hendrickson, *J. Am. Chem. Soc.* **1993**, *115*, 8221 – 8229.
[35] O.-S. Jung, D. H. Jo, Y.-A. Li, B. J. Conklin, C. G. Pierpont, *Inorg. Chem.* **1997**, *36*, 19 – 24.
[36] O. Cador, A. Dei, C. Sangregorio, *Chem. Commun.* **2004**, 652 – 653.
[37] A. Caneschi, A. Dei, F. Fabrizi de Biani, P. Gütlich, V. Ksenofontov, G. Levchenko, A. Hoefer, F. Renz, *Chem. Eur. J.* **2001**, *7*, 3926 – 3930.
[38] S. H. Bodnara, A. Caneschi, A. Dei, D. A. Shultz, L. Soraceb, *Chem. Commun.* **2001**, 2150 – 2151.
[39] A. Caneschi, A. Cornia, A. Dei, *Inorg. Chem.* **1998**, *37*, 3419 – 3421.
[40] O. Cador, F. Chabre, A. Dei, C. Sangregorio, J. V. Slageren, M. G. F. Vaz, *Inorg. Chem.* **2003**, *42*, 6432 – 6440.
[41] J. Tao, H. Maruyama, O. Sato, *J. Am. Chem. Soc.* **2006**, *128*, 1790 – 1791.
[42] E. Evangelio, D. R. Molina, *Eur. J. Inorg. Chem.* **2005**, 2957 – 2971.
[43] D. A. Shultz, *Magnetism: Molecules to Materials II* (Eds.: J. S. Miller, M. Drillon), Wiley-VCH, Weinheim, **2001**, pp. 281 – 306.
[44] S. Hayami, Y. Shigeyoshi, M. Akita, K. Inoue, K. Kato, K. Osaka, M. Takata, R. Kawajiri, T. Mitani, Y. Maeda, *Angew. Chem.* **2005**, *117*, 4977 – 4981; *Angew. Chem. Int. Ed.* **2005**, *44*, 4899 – 4903.
[45] D. M. Adams, B. Li, J. D. Simon, D. N. Hendrickson, *Angew. Chem.* **1995**, *107*, 1580 – 1582; *Angew. Chem. Int. Ed. Engl.* **1995**, *34*, 1481 – 1483.
[46] D. M. Adams, D. N. Hendrickson, *J. Am. Chem. Soc.* **1996**, *118*, 11515 – 11528.
[47] A. Bencini, A. Caneschi, C. Carbonera, A. Dei, D. Gatteschi, R. Righinib, C. Sangregorio, J. V. Slageren, *J. Mol. Struct.* **2003**, *656*, 141 – 154.
[48] P. L. Gentili, L. Bussotti, R. Righini, A. Beni, L. Bogani, A. Dei, *Chem. Phys.* **2005**, *314*, 9 – 17.
[49] S. Decurtins, P. Gütlich, C. P. Kohler, H. Spiering, A. Hauser, *Chem. Phys. Lett.* **1984**, *105*, 1 – 4.
[50] S. Hayami, Z.-Z. Gu, M. Shiro, Y. Einaga, A. Fujishima, O. Sato, *J. Am. Chem. Soc.* **2000**, *122*, 7126 – 7127.
[51] O. Sato, S. Hayami, Y. Einaga, Z.-Z. Gu, *Bull. Chem. Soc. Jpn.* **2003**, *76*, 443 – 470.
[52] O. Sato, S. Hayami, Z.-Z. Gu, K. Seki, R. Nakajima, A. Fujishima, *Chem. Lett.* **2001**, 874 – 875.
[53] O. Sato, S. Hayami, Z.-Z. Gu, K. Takahashi, R. Nakajima, A. Fujishima, *Chem. Phys. Lett.* **2002**, *355*, 169 – 174.
[54] O. Sato, S. Hayami, Z.-Z. Gu, K. Takahashi, R. Nakajima, K. Seki, A. Fujishima, *J. Photochem. Photobiol. A* **2002**, *149*, 111 – 114.
[55] O. Sato, S. Hayami, Z.-Z. Gu, K. Takahashi, R. Nakajima, A. Fujishima, *Phase Transitions* **2002**, *75*, 779 – 785.
[56] F. Varret, M. Nogues, A. Goujon, *Magn. Mol. Mater.* **2001**, 257 – 295.
[57] A. Cui, K. Takahashi, A. Fujishima, O. Sato, *J. Photochem. Photobiol. A* **2004**, *161*, 243 – 246.
[58] A. Cui, K. Takahashi, A. Fujishima, O. Sato, *J. Photochem. Photobiol. A* **2004**, *167*, 69 – 73.
[59] T. Yokoyama, K. Okamoto, K. Nagai, T. Ohta, S. Hayami, Z.-Z. Gu, R. Nakajima, O. Sato, *Chem. Phys. Lett.* **2001**, *345*, 272 – 276.
[60] C. Carbonera, A. Dei, J. F. Letard, C. Sangregorio, L. Sorace, *Angew. Chem.* **2004**, *116*, 3198 – 3200; *Angew. Chem. Int. Ed.* **2004**, *43*, 3136 – 3138.
[61] O.-S. Jung, C. G. Pierpont, *J. Am. Chem. Soc.* **1994**, *116*, 2229 – 2230.
[62] G. A. Abakumov, V. I. Nevodchikov, *Dokl. Akad. Nauk SSSR* **1982**, *266*, 1407 – 1410.
[63] C. W. Lange, M. Foldeaki, V. I. Nevodchikov, V. K. Cherkasov, G. A. Abakumov, C. G. Pierpont, *J. Am. Chem. Soc.* **1992**, *114*, 4220 – 4222.
[64] C. G. Pierpont, *Proc. Indiana Acad. Sci.* **2002**, *114*, 247 – 254.
[65] D. Ruiz, J. Yoo, I. A. Guzei, A. L. Rheingold, D. N. Hendrickson, *Chem. Commun.* **1998**, 2089 – 2090.
[66] D. Ruiz-Molina, J. Veciana, K. Wurst, D. N. Hendrickson, C. Rovira, *Inorg. Chem.* **2000**, *39*, 617 – 619.
[67] D. Ruiz-Molina, K. Wurst, D. N. Hendrickson, C. Rovira, J. Veciana, *Adv. Funct. Mater.* **2002**, *12*, 347 – 351.
[68] M. W. Lynch, D. N. Hendrickson, B. J. Fitzgerald, C. G. Pierpont, *J. Am. Chem. Soc.* **1981**, *103*, 3961 – 3963.
[69] A. S. Attia, O.-S. Jung, C. G. Pierpont, *Inorg. Chim. Acta* **1994**, *226*, 91 – 98.
[70] A. S. Attia, C. G. Pierpont, *Inorg. Chem.* **1995**, *34*, 1172 – 1179.
[71] A. S. Attia, C. G. Pierpont, *Inorg. Chem.* **1997**, *36*, 6184 – 6187.
[72] A. S. Attia, C. G. Pierpont, *Inorg. Chem.* **1998**, *37*, 3051 – 3056.
[73] A. Caneschi, A. Dei, *Angew. Chem.* **1998**, *110*, 3220 – 3222; *Angew. Chem. Int. Ed.* **1998**, *37*, 3005 – 3007.
[74] N. Shaikh, S. Goswami, A. Panja, H.-L. Sun, F. Pan, S. Gao, P. Banerjee, *Inorg. Chem.* **2005**, *44*, 9714 – 9722.
[75] G. Speier, Z. Tyeklar, P. Toth, E. Speier, S. Tisza, A. Rockenbauer, A. M. Whalen, N. Alkire, C. G. Pierpont, *Inorg. Chem.* **2001**, *40*, 5653 – 5659.
[76] J. Rall, M. Wanner, M. Albrecht, F. M. Hornung, W. Kaim, *Chem. Eur. J.* **1999**, *5*, 2802 – 2809.
[77] W. Kaim, M. Wanner, A. Knodler, S. Zalis, *Inorg. Chim. Acta* **2002**, *337*, 163 – 172.
[78] S. Ye, B. Sarkar, M. Niemeyer, W. Kaim, *Eur. J. Inorg. Chem.* **2005**, 4735 – 4738.
[79] M. S. Dooley, M. A. McGuirl, D. E. Brown, P. N. Turowski, W. S. McIntire, P. F. Knowles, *Nature* **1991**, *349*, 262 – 264.
[80] N. Shaikh, S. Goswami, A. Panja, X.-Y. Wang, S. Gao, R. J. Butcher, P. Banerjee, *Inorg. Chem.* **2004**, *43*, 5908 – 5918.
[81] I. Ratera, D. Ruiz-Molina, F. Renz, J. Ensling, K. Wurst, C. Rovira, P. Gütlich, J. Veciana, *J. Am. Chem. Soc.* **2003**, *125*, 1462 – 1463.
[82] D. Dolphin, T. Niem, R. H. Felton, I. Fujita, *J. Am. Chem. Soc.* **1975**, *97*, 5288 – 5290.
[83] J. Seth, V. Palaniappan, D. F. Bocian, *Inorg. Chem.* **1995**, *34*, 2201 – 2206.
[84] Y. Shimazaki, F. Tani, K. Fukui, Y. Naruta, O. Yamauchi, *J. Am. Chem. Soc.* **2003**, *125*, 10512 – 10513.
[85] H. Ohtsu, K. Tanaka, *Angew. Chem.* **2004**, *116*, 6461 – 6463; *Angew. Chem. Int. Ed.* **2004**, *43*, 6301 – 6303.
[86] H. Ohtsu, K. Tanaka, *Chem. Eur. J.* **2005**, *11*, 3420 – 3426.
[87] G. A. Abakumov, V. I. Nevodchikov, V. K. Cherkasov, *Dokl. Akad. Nauk SSSR* **1984**, *278*, 641 – 645.
[88] G. A. Abakumov, G. A. Razuvaev, V. I. Nevodchikov, V. K. Cherkasov, *J. Organomet. Chem.* **1988**, *341*, 485 – 494.

[89] M. Mitsumi, H. Goto, S. Umebayashi, Y. Ozawa, M. Kobayashi, T. Yokoyama, H. Tanaka, S.-I. Kuroda, K. Toriumi, *Angew. Chem.* **2005**, *117*, 4236 – 4240; *Angew. Chem. Int. Ed.* **2005**, *44*, 4164 – 4168.
[90] C. P. Berlinguette, A. Dragulescu-Andrasi, A. Sieber, J. R. Galan-Mascaros, H.-U. Güdel, C. Achim, K. R. Dunbar, *J. Am. Chem. Soc.* **2004**, *126*, 6222 – 6223.
[91] C. P. Berlinguette, A. Dragulescu-Andrasi, A. Sieber, H.-U. Güdel, C. Achim, K. R. Dunbar, *J. Am. Chem. Soc.* **2005**, *127*, 6766 – 6779.
[92] N. Shimamoto, S. Ohkoshi, O. Sato, K. Hashimoto, *Inorg. Chem.* **2002**, *41*, 678 – 684.
[93] O. Sato, *Acc. Chem. Res.* **2003**, *36*, 692 – 700.
[94] Y. Umezono, W. Fujita, K. Awaga, *J. Am. Chem. Soc.* **2006**, *128*, 1084 – 1085.
[95] J. B. Torrance, J. E. Vazquez, J. J. Mayerle, V. Y. Lee, *Phys. Rev. Lett.* **1981**, *46*, 253 – 257.
[96] J. B. Torrance, A. Girlando, J. J. Mayerle, J. I. Crowley, V. Y. Lee, P. Batail, S. J. LaPlaca, *Phys. Rev. Lett.* **1981**, *47*, 1747 – 1750.
[97] S. Aoki, T. Nakayama, A. Miura, *Phys. Rev. B* **1993**, *48*, 626 – 629.
[98] P. García, S. Dahaoui, P. Fertey, E. Wenger, C. Lecomte, *Phys. Rev. B* **2005**, *72*, 104115.
[99] S. Koshihara, Y. Takahashi, H. Sakai, Y. Tokura, T. Luty, *J. Phys. Chem. B* **1999**, *103*, 2592 – 2600.
[100] H. Okamoto, Y. Ishige, S. Tanaka, H. Kishida, S. Iwai, Y. Tokura, *Phys. Rev. B* **2004**, *70*, 165202.
[101] E. Collet, M. B.-L. Cointe, H. Cailleau, *J. Phys. Soc. Jpn.* **2006**, *75*, 011002.
[102] T. Mitani, G. Saito, Y. Tokura, T. Koda, *Phys. Rev. Lett.* **1984**, *53*, 842 – 845.
[103] S. Horiuchi, Y. Okimoto, R. Kumai, Y. Tokura, *Science* **2003**, *299*, 229 – 232.
[104] T. Mochida, K. Takazawa, M. Takahashi, M. Takeda, Y. Nishio, M. Sato, K. Kajita, H. Mori, M. M. Matsushita, T. Sugawara, *J. Phys. Soc. Jpn.* **2005**, *74*, 2214 – 2216.
[105] T. Mochida, S. Yamazaki, S. Suzuki, S. Shimizu, H. Mori, *Bull. Chem. Soc. Jpn.* **2003**, *76*, 2321 – 2328.
[106] S. Nishida, Y. Morita, K. Fukui, K. Sato, D. Shiomi, T. Takui, K. Nakasuji, *Angew. Chem.* **2005**, *117*, 7443 – 7446; *Angew. Chem. Int. Ed.* **2005**, *44*, 7277 – 7280.
[107] J. Zhang, M. M. Matsushita, X. X. Kong, J. Abe, T. Iyoda, *J. Am. Chem. Soc.* **2001**, *123*, 12105 – 12106.
[108] J. M. Herrera, V. Marvaud, M. Verdaguer, J. Marrot, M. Kalisz, C. Mathoniere, *Angew. Chem.* **2004**, *116*, 5584 – 5587; *Angew. Chem. Int. Ed.* **2004**, *43*, 5468 – 5471.
[109] U. Hauser, V. Oestreich, H. D. Rohrweck, *Z. Phys. A* **1977**, *280*, 17 – 25.
[110] T. Woike, W. Krasser, P. S. Bechthold, S. Haussuhl, *Phys. Rev. Lett.* **1984**, *53*, 1767 – 1770.
[111] M. D. Carducci, M. R. Pressprich, P. Coppens, *J. Am. Chem. Soc.* **1997**, *119*, 2669 – 2678.
[112] Z.-Z. Gu, O. Sato, T. Iyoda, K. Hashimoto, A. Fujishima, *J. Phys. Chem.* **1996**, *100*, 18289 – 18291.
[113] Z.-Z. Gu, O. Sato, T. Iyoda, K. Hashimoto, A. Fujishima, *Chem. Mater.* **1997**, *9*, 1092 – 1097.
[114] K. Itoh, *Chem. Phys. Lett.* **1967**, *1*, 235 – 238.
[115] E. Wasserman, R. W. Murray, W. A. Yager, A. M. Trozzolo, G. Smolinsky, *J. Am. Chem. Soc.* **1967**, *89*, 5076 – 5078.
[116] T. Takui, K. Itoh, *Chem. Phys. Lett.* **1973**, *19*, 120 – 124.
[117] T. Sugawara, S. Bandow, K. Kimura, H. Iwamura, K. Itoh, *J. Am. Chem. Soc.* **1984**, *106*, 6449 – 6450.
[118] T. Sugawara, S. Bandow, K. Kimura, H. Iwamura, K. Itoh, *J. Am. Chem. Soc.* **1986**, *108*, 368 – 371.
[119] Y. Teki, T. Takui, K. Itoh, H. Iwamura, K. Kobayashi, *J. Am. Chem. Soc.* **1986**, *108*, 2147 – 2156.
[120] H. Iwamura, *Pure. Appl. Chem.* **1986**, *58*, 187 – 196.
[121] H. Iwamura, N. Koga, *Acc. Chem. Res.* **1993**, *26*, 346 – 351.
[122] Y. Teki, T. Takui, K. Itoh, *J. Am. Chem. Soc.* **1983**, *105*, 3722 – 3723.
[123] N. Koga, S. Karasawa, *Bull. Chem. Soc. Jpn.* **2005**, *78*, 1384 – 1400.
[124] Y. Sano, M. Tanaka, N. Koga, K. Matsuda, H. Iwamura, P. Rabu, M. Drillon, *J. Am. Chem. Soc.* **1997**, *119*, 8246 – 8252.
[125] S. Karasawa, M. Tanaka, N. Koga, H. Iwamura, *Chem. Commun.* **1997**, 1359 – 1360.
[126] S. Karasawa, H. Kumada, N. Koga, H. Iwamura, *J. Am. Chem. Soc.* **2001**, *123*, 9685 – 9686.
[127] S. Karasawa, G. Zhou, H. Morikawa, N. Koga, *J. Am. Chem. Soc.* **2003**, *125*, 13676 – 13677.
[128] S. Karasawa, Y. Sano, T. Akita, N. Koga, T. Itoh, H. Iwamura, P. Rabu, M. Drillon, *J. Am. Chem. Soc.* **1998**, *120*, 10080 – 10087.
[129] S. Nakatsuji, *Chem. Soc. Rev.* **2004**, *33*, 348 – 353.
[130] K. Tanaka, F. Toda, *J. Chem. Soc. Perkin Trans. 1* **2000**, 873 – 874.
[131] L. Xu, T. Sugiyama, H. Huang, Z. Song, J. Meng, T. Matsuura, *Chem. Commun.* **2002**, 2328 – 2329.
[132] T. Hayashi, K. Maeda, *Bull. Chem. Soc. Jpn.* **1960**, *33*, 565 – 566.
[133] B. M. Monroe, G. C. Weed, *Chem. Rev.* **1993**, *93*, 435 – 448.
[134] M. Kawano, T. Sano, J. Abe, Y. Ohashi, *J. Am. Chem. Soc.* **1999**, *121*, 8106 – 8107.
[135] H. Kurata, T. Tanaka, M. Oda, *Chem. Lett.* **1999**, 749 – 750.
[136] H. Kurata, Y. Takehara, T. Kawase, M. Oda, *Chem. Lett.* **2003**, *32*, 538 – 539.
[137] K. Hamachi, K. Matsuda, T. Itoh, H. Iwamura, *Bull. Chem. Soc. Jpn.* **1998**, *71*, 2937 – 2943.
[138] K. Matsuda, M. Irie, *J. Photochem. Photobiol. C* **2004**, *5*, 169 – 182.
[139] K. Matsuda, M. Irie, *J. Am. Chem. Soc.* **2000**, *122*, 7195 – 7201.
[140] K. Matsuda, M. Irie, *J. Am. Chem. Soc.* **2000**, *122*, 8309 – 8310.
[141] K. Matsuda, M. Irie, *J. Am. Chem. Soc.* **2001**, *123*, 9896 – 9897.
[142] K. Matsuda, M. Irie, *Chem. Eur. J.* **2001**, *7*, 3466 – 3473.
[143] K. Matsuda, M. Matsuo, S. Mizoguti, K. Higashiguchi, M. Irie, *J. Phys. Chem. B* **2002**, *106*, 11218 – 11225.
[144] N. Tanifuji, M. Irie, K. Matsuda, *J. Am. Chem. Soc.* **2005**, *127*, 13344 – 13353.
[145] I. Ratera, D. R. Molina, J. V. Gancedo, K. Wurst, N. Daro, J.-F. Létard, C. Rovira, J. Veciana, *Angew. Chem.* **2001**, *113*, 933 – 936; *Angew. Chem. Int. Ed.* **2001**, *40*, 919 – 922.
[146] A. Ito, Y. Nakano, M. Urabe, T. Kato, K. Tanaka, *J. Am. Chem. Soc.* **2006**, *128*, 2948 – 2953.
[147] C. Corvaja, M. Maggini, M. Prato, G. Scorrano, M. Venzin, *J. Am. Chem. Soc.* **1995**, *117*, 8857 – 8858.
[148] K. Ishii, J. Fujisawa, Y. Ohba, S. Yamauchi, *J. Am. Chem. Soc.* **1996**, *118*, 13079 – 13080.
[149] N. Mizuochi, Y. Ohba, S. Yamauchi, *J. Phys. Chem. A* **1999**, *103*, 7749 – 7752.
[150] Y. Teki, *Polyhedron* **2005**, *24*, 2299 – 2308.
[151] Y. Teki, S. Miyamoto, K. Iimura, M. Nakatsuji, Y. Miura, *J. Am. Chem. Soc.* **2000**, *122*, 984 – 985.
[152] K. Itoh, *Pure. Appl. Chem.* **1978**, 1251 – 1259.
[153] Y. Teki, S. Nakajima, *Chem. Lett.* **2004**, *33*, 1500 – 1501.
[154] Y. Teki, S. Miyamoto, M. Nakatsuji, Y. Miura, *J. Am. Chem. Soc.* **2001**, *123*, 294 – 305.
[155] R. G. Kepler, *J. Chem. Phys.* **1963**, *39*, 3528 – 3532.
[156] G. T. Pott, F. V. Bruggen, J. Kommandeur, *J. Chem. Phys.* **1967**, *47*, 408 – 413.
[157] J. G. Vegter, T. Hibma, J. Kommandeur, *Chem. Phys. Lett.* **1969**, *3*, 427 – 429.
[158] W. Fujita, K. Awaga, *Science* **1999**, *286*, 261 – 263.
[159] J. L. Brusso, O. P. Clements, R. C. Haddon, M. E. Itkis, A. A. Leitch, R. T. Oakley, R. W. Reed, J. F. Richardson, *J. Am. Chem. Soc.* **2004**, *126*, 8256 – 8265.

[160] J. L. Brusso, O. P. Clements, R. C. Haddon, M. E. Itkis, A. A. Leitch, R. T. Oakley, R. W. Reed, J. F. Richardson, *J. Am. Chem. Soc.* **2004**, *126*, 14692 – 14693.
[161] T. M. Barclay, A. W. Cordes, N. A. George, R. C. Haddon, M. E. Itkis, M. S. Mashuta, R. T. Oakley, G. W. Patenaude, R. W. Reed, J. F. Richardson, H. Zhang, *J. Am. Chem. Soc.* **1998**, *120*, 352 – 360.
[162] A. Alberola, R. J. Collis, S. M. Humphrey, R. J. Less, J. M. Rawson, *Inorg. Chem.* **2006**, *45*, 1903 – 1905.
[163] W. Fujita, K. Awaga, Y. Nakazawa, K. Saito, M. Sorai, *Chem. Phys. Lett.* **2002**, *352*, 348 – 352.
[164] K. Awaga, T. Tanaka, T. Shirai, M. Fujimori, Y. Suzuki, H. Yoshikawa, W. Fujita, *Bull. Chem. Soc. Jpn.* **2006**, *79*, 25 – 34.
[165] H. Matsuzaki, W. Fujita, K. Awaga, H. Okamoto, *Phys. Rev. Lett.* **2003**, *91*, 7403 – 7406.
[166] J. Takeda, M. Imae, O. Hanada, S. Kurita, M. Furuya, K. Ohno, T. Kodaira, *Chem. Phys. Lett.* **2003**, *378*, 456 – 462.
[167] J. Xie, X. Ren, Y. Song, W. Zhang, W. Liu, C. He, Q. Meng, *Chem. Commun.* **2002**, 2346 – 2347.
[168] X. Ren, Q. Meng, Y. Song, C. Lu, C. Hu, *Inorg. Chem.* **2002**, *41*, 5686 – 5692.
[169] C. Ni, D. Dang, Y. Li, S. Gao, Z. Ni, Z. Tian, Q. Meng, *J. Solid State Chem.* **2005**, *178*, 100 – 105.
[170] C. Ni, Y. Li, D. Dang, Z. Ni, Z. Tian, Z. Yuan, Q. Meng, *Inorg. Chem. Commun.* **2005**, *8*, 105 – 108.
[171] X. M. Ren, S. Nishihara, T. Akutagawa, S. Noro, T. Nakamura, *Inorg. Chem.* **2006**, *45*, 2229 – 2234.
[172] M. E. Itkis, X. Chi, A. W. Cordes, R. C. Haddon, *Science* **2002**, *296*, 1443 – 1445.
[173] S. K. Pal, M. E. Itkis, F. S. Tham, R. W. Reed, R. T. Oakley, R. C. Haddon, *Science* **2005**, *309*, 281 – 284.
[174] R. M. Bozorth, H. J. Williams, D. E. Walsh, *Phys. Rev.* **1956**, *103*, 572 – 578.
[175] A. N. Holden, B. T. Matthias, P. W. Anderson, H. W. Lewis, *Phys. Rev.* **1956**, *102*, 1463 – 1463.
[176] S. H. Holmes, G. S. Girolami, *J. Am. Chem. Soc.* **1999**, *121*, 5593 – 5594.
[177] O. Hatlevik, W. E. Buschmann, J. Zhang, J. L. Manson, J. S. Miller, *Adv. Mater.* **1999**, *11*, 914 – 918.
[178] O. Sato, Y. Einaga, T. Iyoda, A. Fujishima, K. Hashimoto, *J. Electrochem. Soc.* **1997**, *144*, L11 – L13.
[179] O. Sato, Y. Einaga, T. Iyoda, A. Fujishima, K. Hashimoto, *Inorg. Chem.* **1999**, *38*, 4405 – 4412.
[180] A. Bleuzen, C. Lomenech, V. Escax, F. Villain, F. Varret, C. Cartier dit Moulin, M. Verdaguer, *J. Am. Chem. Soc.* **2000**, *122*, 6648 – 6652.
[181] C. Cartier dit Moulin, F. Villain, A. Bleuzen, M.-A. Arrio, P. Sainctavit, C. Lomenech, V. Escax, F. Baudelet, E. Dartyge, J.-J. Gallet, M. Verdaguer, *J. Am. Chem. Soc.* **2000**, *122*, 6653 – 6658.
[182] V. Escax, A. Bleuzen, C. Cartier dit Moulin, F. Villain, A. Goujon, F. Varret, M. Verdaguer, *J. Am. Chem. Soc.* **2001**, *123*, 12536 – 12543.
[183] F. Varret, H. Constant-Machado, J. L. Dormann, A. Goujon, J. Jeftic, M. Nogues, A. Bousseksou, S. Klokishner, A. Dorbecq, M. Verdaguer, *Hyperfine Interact.* **1998**, *113*, 37 – 46.
[184] A. Goujon, O. Roubeau, F. Varret, A. Dolbecq, A. Bleuzen, M. Verdaguer, *Eur. Phys. J. B* **2000**, *14*, 115 – 124.
[185] A. Goujon, F. Varret, V. Escax, A. Bleuzen, M. Verdaguer, *Polyhedron* **2001**, *20*, 1339 – 1345.
[186] A. Goujon, F. Varret, V. Escax, A. Bleuzen, M. Verdaguer, *Polyhedron* **2001**, *20*, 1347 – 1354.
[187] D. A. Pejakovic, J. L. Manson, J. S. Miller, A. J. Epstein, *J. Appl. Phys.* **2000**, *87*, 6028 – 6030.
[188] O. Sato, Y. Einaga, T. Iyoda, A. Fujishima, K. Hashimoto, *J. Phys. Chem.* **1997**, *101*, 3903 – 3905.
[189] N. Shimamoto, S. Ohkoshi, O. Sato, K. Hashimoto, *Mol. Cryst. Liq. Cryst.* **2000**, *344*, 95 – 100.
[190] A. Bleuzen, V. Escax, A. Ferrier, F. Villain, M. Verdaguer, P. Munsch, J.-P. Iti, *Angew. Chem.* **2004**, *116*, 3814 – 3817; *Angew. Chem. Int. Ed.* **2004**, *43*, 3728 – 3731.
[191] V. Ksenofontov, G. Levchenko, S. Reiman, P. Gütlich, A. Bleuzen, V. Escax, M. Verdaguer, *Phys. Rev. B* **2003**, *68*, 024415.
[192] D. A. Pejakovic, J. L. Manson, J. S. Miller, A. J. Epstein, *J. Appl. Phys.* **2000**, *88*, 4457 – 4457.
[193] D. A. Pejaković, J. L. Manson, J. S. Miller, A. J. Epstein, *Phys. Rev. Lett.* **2000**, *85*, 1994 – 1997.
[194] S. Ohkoshi, H. Tokoro, K. Hashimoto, *Coord. Chem. Rev.* **2005**, *249*, 1830 – 1840.
[195] S. Ohkoshi, H. Tokoro, M. Utsunomiya, M. Mizuno, M. Abe, K. Hashimoto, *J. Phys. Chem. B* **2002**, *106*, 2423 – 2425.
[196] H. Tokoro, S. Ohkoshi, K. Hashimoto, *Appl. Phys. Lett.* **2003**, *82*, 1245 – 1247.
[197] H. Tokoro, S. Ohkoshi, T. Matsuda, K. Hashimoto, *Inorg. Chem.* **2004**, *43*, 5231 – 5236.
[198] S. Ohkoshi, T. Matsuda, H. Tokoro, K. Hashimoto, *Chem. Mater.* **2005**, *17*, 81 – 84.
[199] K. Kato, Y. Moritomo, M. Takata, M. Sakata, M. Umekawa, N. Hamada, S. Ohkoshi, H. Tokoro, K. Hashimoto, *Phys. Rev. Lett.* **2003**, *91*, 255502.
[200] Y. Moritomo, M. Hanawa, Y. Ohishi, K. Kato, M. Takata, A. Kuriki, E. Nishibor, M. Sakata, S. Ohkoshi, H. Tokoro, K. Hashimoto, *Phys. Rev. B* **2003**, *68*, 4106 – 4112.
[201] H. Tokoro, T. Matsuda, K. Hashimoto, S. Ohkoshi, *J. Appl. Phys.* **2005**, *97*, 508 – 510.
[202] S. Margadonna, K. Prassides, A. N. Fitch, *Angew. Chem.* **2004**, *116*, 6476 – 6479; *Angew. Chem. Int. Ed.* **2004**, *43*, 6316 – 6319.
[203] P. Przychodzeń, T. Korzeniak, R. Podgajny, B. Sieklucka, *Coord. Chem. Rev.* **2006**, *250*, 2234 – 2260.
[204] Y. Arimoto, S. Ohkoshi, Z. J. Zhong, H. Seino, Y. Mizobe, K. Hashimoto, *Chem. Lett.* **2002**, 832 – 833.
[205] Y. Arimoto, S. Ohkoshi, Z. J. Zhang, H. Seino, Y. Mizobe, K. Hashimoto, *J. Am. Chem. Soc.* **2003**, *125*, 9240 – 9241.
[206] S. Ohkoshi, N. Machida, Y. Abe, Z. J. Zhong, K. Hashimoto, *Chem. Lett.* **2001**, 312 – 313.
[207] S. Ohkoshi, N. Machida, Z. J. Zhong, K. Hashimoto, *Synth. Met.* **2001**, *122*, 523 – 527.
[208] G. Rombaut, C. Mathonière, P. Guionneau, S. Golhen, L. Ouahab, M. Verelst, P. Lecante, *Inorg. Chim. Acta* **2001**, *326*, 27 – 36.
[209] G. Rombaut, M. Verelst, S. Golhen, L. Ouahab, C. Mathonière, O. Kahn, *Inorg. Chem.* **2001**, *40*, 1151 – 1159.
[210] S. Ohkoshi, H. Tokoro, T. Hozumi, Y. Zhang, K. Hashimoto, C. Mathonière, I. Bord, G. Rombaut, M. Verelst, C. Cartier dit Moulin, F. Villain, *J. Am. Chem. Soc.* **2006**, *128*, 270 – 277.
[211] T. Hozumi, K. Hashimoto, S. Ohkoshi, *J. Am. Chem. Soc.* **2005**, *127*, 3864 – 3869.
[212] S.-I. Ohkoshi, S. Ikeda, T. Hozumi, T. Kashiwagi, K. Hashimoto, *J. Am. Chem. Soc.* **2006**, *128*, 5320 – 5321.
[213] K. Itaya, I. Uchida, V. D. Neff, *Acc. Chem. Res.* **1986**, *19*, 162 – 168.
[214] O. Sato, T. Iyoda, A. Fujishima, K. Hashimoto, *Science* **1996**, *271*, 49 – 51.
[215] O. Sato, Z.-Z. Gu, H. Etoh, J. Ichiyanagi, T. Iyoda, A. Fujishima, K. Hashimoto, *Chem. Lett.* **1997**, 37 – 38.
[216] Y. Sato, S. Ohkoshi, K. Arai, M. Tozawa, K. Hashimoto, *J. Am. Chem. Soc.* **2003**, *125*, 14590 – 14595.
[217] S. Ohkoshi, K. Arai, Y. Sato, K. Hashimoto, *Nat. Mater.* **2004**, *3*, 857 – 861.
[218] E. Coronado, M. Gimenez-Lopez, G. Levchenko, F. Romero, V. Garcia-Baonza, A. Milner, M. Paz-Pasternak, *J. Am. Chem. Soc.* **2005**, *127*, 4580 – 4581.
[219] W. Kosaka, K. Nomura, K. Hashimoto, S. Ohkoshi, *J. Am. Chem. Soc.* **2005**, *127*, 8590 – 8591.

[220] S. Ohkoshi, Y. Einaga, A. Fujishima, K. Hashimoto, *J. Electroanal. Chem.* **1999**, *473*, 245 – 249.
[221] S. Ohkoshi, S. Yorozu, O. Sato, T. Iyoda, A. Fujishima, K. Hashimoto, *Appl. Phys. Lett.* **1997**, *70*, 1040 – 1042.
[222] S. Ohkoshi, K. Hashimoto, *J. Am. Chem. Soc.* **1999**, *121*, 10591 – 10597.
[223] S. Ohkoshi, T. Nuida, T. Matsuda, H. Tokoro, K. Hashimoto, *J. Mater. Chem.* **2005**, *15*, 3291 – 3295.
[224] O. Sato, T. Kawakami, M. Kimura, S. Hishiya, S. Kubo, Y. Einaga, *J. Am. Chem. Soc.* **2004**, *126*, 13176 – 13177.
[225] D. A. Pejaković, C. Kitamura, J. S. Miller, A. J. Epstein, *Phys. Rev. Lett.* **2002**, *88*, 057202.
[226] J. Zhang, J. Ensling, V. Ksenofontov, P. Gütlich, A. J. Epstein, J. S. Miller, *Angew. Chem.* **1998**, *110*, 676 – 679; *Angew. Chem. Int. Ed.* **1998**, *37*, 657 – 660.
[227] E. J. Brandon, C. Kollmar, J. S. Miller, *J. Am. Chem. Soc.* **1998**, *120*, 1822 – 1826.
[228] K. Nagai, T. Iyoda, A. Fujishima, K. Hashimoto, *Solid State Commun.* **1997**, *102*, 809 – 812.
[229] C. Mathonière, R. Podgajny, P. Guionneau, C. Labrugere, B. Sieklucka, *Chem. Mater.* **2005**, *17*, 442 – 449.
[230] G. Li, T. Akitsu, O. Sato, Y. Einaga, *J. Am. Chem. Soc.* **2003**, *125*, 12396 – 12397.
[231] G. Li, T. Akitsu, O. Sato, Y. Einaga, *J. Solid State Chem.* **2004**, *177*, 3835 – 3838.
[232] M. D. Sastry, M. K. Bhide, R. M. Kadam, S. A. Chavan, J. V. Yakhmi, O. Kahn, *Chem. Phys. Lett.* **1999**, *301*, 385 – 388.
[233] N. Kojima, W. Aoki, M. Itoi, Y. Ono, M. Seto, Y. Kobayashi, Y. Maeda, *Solid State Commun.* **2001**, *120*, 165 – 170.
[234] N. Kojima, W. Aoki, M. Seto, Y. Kobayashi, Y. Maeda, *Synth. Met.* **2001**, *121*, 1796 – 1797.
[235] M. Itoi, A. Taira, M. Enomoto, N. Matsushita, N. Kojima, Y. Kobayashi, K. Asai, K. Koyama, T. Nakano, Y. Uwatoko, J. Yamaura, *Solid State Commun.* **2004**, *130*, 415 – 420.
[236] T. Nakamoto, Y. Miyazaki, M. Itoi, Y. Ono, N. Kojima, M. Sorai, *Angew. Chem.* **2001**, *113*, 4852 – 4855; *Angew. Chem. Int. Ed.* **2001**, *40*, 4716 – 4719.
[237] M. Itoi, M. Enomoto, N. Kojima, *J. Magn. Magn. Mater.* **2004**, *272–276*, 1093 – 1094.
[238] B. Mayoh, P. Day, *J. Chem. Soc. Dalton Trans.* **1976**, 1483 – 1486.
[239] D. Maspoch, D. Ruiz-Molina, K. Domingo, M. Cavallini, F. Biscarini, J. Tejada, C. Rovira, J. Veciana, *Nat. Mater.* **2003**, *2*, 190 – 195.
[240] I. Kashima, M. Okubo, Y. Ono, M. Itoi, N. Kida, M. Hikita, M. Enomoto, N. Kojima, *Synth. Met.* **2005**, *153*, 473 – 476.
[241] S. Bénard, E. Rivière, P. Yu, K. Nakatani, F. Delouis, *Chem. Mater.* **2001**, *13*, 159 – 162.
[242] K. Nakatani, P. Yu, *Adv. Mater.* **2001**, *13*, 1411 – 1413.
[243] M. Okubo, M. Enomoto, N. Kojima, *Synth. Met.* **2005**, *152*, 461 – 464.
[244] Y. Einaga, *Bull. Chem. Soc. Jpn.* **2006**, *79*, 361 – 372.
[245] Y. Einaga, O. Sato, T. Iyoda, A. Fujishima, K. Hashimoto, *J. Am. Chem. Soc.* **1999**, *121*, 3745 – 3750.
[246] T. Yamamoto, Y. Umemura, O. Sato, Y. Einaga, *J. Am. Chem. Soc.* **2005**, *127*, 16065 – 16073.
[247] L. Cambi, L. Szego, *Ber. Dtsch. Chem. Ges.* **1931**, *64*, 2591 – 2598.
[248] J.-F. Létard, P. Guionneau, E. Codjovi, O. Lavastre, G. Bravic, D. Chasseau, O. Kahn, *J. Am. Chem. Soc.* **1997**, *119*, 10861 – 10862.
[249] J.-F. Létard, L. Capes, G. Chastanet, N. Moliner, S. Letard, J.-A. Real, O. Kahn, *Chem. Phys. Lett.* **1999**, *313*, 115 – 120.
[250] H. Daubric, C. Cantin, C. Thomas, J. Kliava, J.-F. Létard, O. Kahn, *Chem. Phys. Lett.* **1999**, *244*, 75 – 88.
[251] Z. J. Zhong, J.-Q. Tao, Z. Yu, C.-Y. Dun, Y.-J. Liu, X.-Z. You, *J. Chem. Soc. Dalton Trans.* **1998**, 327 – 328.
[252] S. Hayami, Z.-Z. Gu, Y. Einaga, A. Fujishima, O. Sato, *J. Am. Chem. Soc.* **2001**, *123*, 11644 – 11650.
[253] G. Ritter, E. König, W. Irler, H. A. Goodwin, *Inorg. Chem.* **1978**, *17*, 224 – 228.
[254] M. Sorai, J. Ensling, K. M. Hasselbach, P. Gütlich, *Chem. Phys.* **1977**, *20*, 197 – 208.
[255] T. Nakamoto, A. Bhattacharjee, M. Sorai, *Bull. Chem. Soc. Jpn.* **2004**, *77*, 921 – 932.
[256] J. Kröber, E. Codjovi, O. Kahn, F. Grolière, C. Jay, *J. Am. Chem. Soc.* **1993**, *115*, 9810 – 9811.
[257] O. Kahn, C. J. Martinez, *Science* **1998**, *279*, 44 – 48.
[258] Y. Garcia, J. Moscovici, A. Michalowicz, V. Ksenofontov, G. Levchenko, G. Bravic, D. Chasseau, P. Gütlich, *Chem. Eur. J.* **2002**, *8*, 4992 – 5000.
[259] V. Niel, J. M. Martinez-Agudo, M. C. Munoz, A. B. Gaspar, J. A. Real, *Inorg. Chem.* **2001**, *40*, 3838 – 3839.
[260] S. Bonhommeau, G. Molnar, A. Galet, A. Zwick, J. A. Real, J. J. McGarvey, A. Bousseksou, *Angew. Chem.* **2005**, *117*, 4137 – 4141; *Angew. Chem. Int. Ed.* **2005**, *44*, 4069 – 4073.
[261] S. Floquet, M. L. Boillot, E. Riviere, F. Varret, K. Boukheddaden, D. Morineau, P. Negrier, *New J. Chem.* **2003**, *27*, 341 – 348.
[262] A. Hauser, *Chem. Phys. Lett.* **1986**, *124*, 543 – 548.
[263] M. Marchivie, P. Guionneau, J. A. K. Howard, G. Chastanet, J.-F. Létard, A. E. Goeta, D. Chasseau, *J. Am. Chem. Soc.* **2002**, *124*, 194 – 195.
[264] T. Tayagaki, K. Tanaka, *Phys. Rev. Lett.* **2001**, *86*, 2886 – 2889.
[265] S. Hayami, Z.-Z. Gu, Y. Einaga, Y. Kobayashi, Y. Ishikawa, Y. Yamada, A. Fujishima, O. Sato, *Inorg. Chem.* **2001**, *40*, 3240 – 3242.
[266] S. Koshihara, Y. Tokura, K. Takeda, T. Koda, *Phys. Rev. Lett.* **1992**, *68*, 1148 – 1151.
[267] E. Freysza, S. Montanta, S. Letarda, J.-F. Létard, *Chem. Phys. Lett.* **2004**, *394*, 318 – 323.
[268] H.-W. Liu, A. Fujishima, O. Sato, *Appl. Phys. Lett.* **2005**, *86*, 122511.
[269] N. Shimamoto, S. Ohkoshi, O. Sato, K. Hashimoto, *Chem. Lett.* **2002**, 486 – 487.
[270] H. W. Liu, K. Matsuda, Z.-Z. Gu, K. Takahashi, A. L. Cui, R. Nakajima, A. Fujishima, O. Sato, *Phys. Rev. Lett.* **2003**, *90*, 167403.
[271] M. L. Boillot, J. Zarembowitch, A. Sour, *Top. Curr. Chem.* **2004**, *234*, 261 – 276.
[272] M. L. Boillot, S. Chantraine, J. Zarembowitch, J. Y. Lallemand, J. Prunet, *New J. Chem.* **1999**, *23*, 179 – 183.
[273] M.-L. Boillot, C. Roux, J.-P. Audiere, A. Dausse, J. Zarembowitch, *Inorg. Chem.* **1996**, *35*, 3975 – 3980.
[274] A. Sour, M.-L. Boillot, E. Riviere, P. Lesot, *Eur. J. Inorg. Chem.* **1999**, 2117 – 2119.
[275] V. Niel, A. L. Thompson, M. C. Munoz, A. Galet, A. E. Goeta, J. A. Real, *Angew. Chem.* **2003**, *115*, 3890 – 3893; *Angew. Chem. Int. Ed.* **2003**, *42*, 3760 – 3763.
[276] G. J. Halder, C. J. Kepert, B. Moubaraki, K. S. Murray, J. D. Cashion, *Science* **2002**, *298*, 1762 – 1765.
[277] Y. Galyametdinov, V. Ksenofontov, A. Prosvirin, I. Ovchinnikov, G. Ivanova, P. Gütlich, W. Haase, *Angew. Chem.* **2001**, *113*, 4399 – 4401; *Angew. Chem. Int. Ed.* **2001**, *40*, 4269 – 4271.
[278] T. Fujigaya, D.-L. Jiang, T. Aida, *J. Am. Chem. Soc.* **2003**, *125*, 14690 – 14691.
[279] Y. Bodenthin, U. Pietsch, H. Möhwald, D. G. Kurth, *J. Am. Chem. Soc.* **2005**, *127*, 3110 – 3114.
[280] D. L. Reger, J. R. Gardinier, W. R. Gemmill, M. D. Smith, A. M. Shahin, G. J. Long, L. Rebbouh, F. Grandjean, *J. Am. Chem. Soc.* **2005**, *127*, 2303 – 2316.
[281] T. Fujigaya, D.-L. Jiang, T. Aida, *J. Am. Chem. Soc.* **2005**, *127*, 5484 – 5489.
[282] J. F. Létard, J. A. Real, N. Moliner, *J. Am. Chem. Soc.* **1999**, *121*, 10630 – 10631.

[283] E. Breuning, M. Ruben, J. M. Lehn, F. Renz, Y. Garcia, V. Ksenofontov, P. Gütlich, E. Wegelius, K. Rissanen, *Angew. Chem.* **2000**, *112*, 2563 – 2566; *Angew. Chem. Int. Ed.* **2000**, *39*, 2504 – 2507.
[284] M. Nihei, M. Ui, M. Yokota, L. Han, A. Maeda, H. Kishida, H. Okamoto, H. Oshio, *Angew. Chem.* **2005**, *117*, 6642 – 6645; *Angew. Chem. Int. Ed.* **2005**, *44*, 6484 – 6487.
[285] S. Dorbes, L. Valade, J. A. Real, C. Faulmann, *Chem. Commun.* **2005**, 69 – 70.
[286] S. Bonhommeau, T. Guillon, L. M. L. Daku, P. Demont, J. S. Costa, J.-F. Létard, G. Molnár, A. Bousseksou, *Angew. Chem.* **2006**, *118*, 1655 – 1659; *Angew. Chem. Int. Ed.* **2006**, *45*, 1625 – 1629.
[287] M. Irie, *Chem. Rev.* **2000**, *100*, 1685 – 1716.
[288] E. B. Myers, D. C. Ralph, J. A. Katine, R. N. Louie, R. A. Buhrman, *Science* **1999**, *285*, 867 – 870.
[289] M. Irie, T. Fukaminato, T. Sasaki, N. Tamai, T. Kawai, *Nature* **2002**, *420*, 759 – 760.

